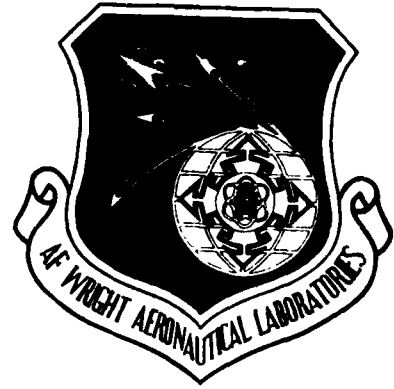


MICROCOPY RESOLUTION TEST CHART
NATIONAL BUREAU OF STANDARDS-1963-A

2

AFWAL-TR-85-2054



AD-A163 052

ALTITUDE IGNITION/LEAN DECEL STUDY

D. Andreadis

United Technologies Corporation
Pratt & Whitney
Engineering Division
P.O. Box 2691, West Palm Beach, Florida 33402

DTIC
ELECTE
JAN 13 1986
S D D

November 1985

Final Report for Period August 1983 — January 1985

Approved for Public Release: Distribution Unlimited

Aero Propulsion Laboratory
Air Force Wright Aeronautical Laboratories
Air Force Systems Command
Wright-Patterson AFB, Ohio 45433

DTIC FILE COPY

86 1 13 024

NOTICE

When Government drawings, specifications, or other data are used for any purpose other than in connection with a definitely related Government procurement operation, the United States Government thereby incurs no responsibility nor any obligation whatsoever; and the fact that the government may have formulated, furnished, or in any way supplied the said drawings, specifications, or other data, is not to be regarded by implication or otherwise as in any manner licensing the holder or any other person or corporation, or conveying any rights or permission to manufacture use, or sell any patented invention that may in any way be related thereto.

This report has been reviewed by the Office of Public Affairs (ASD/PA) and is releasable to the National Technical Information Service (NTIS). At NTIS, it will be available to the general public, including foreign nations.

This technical report has been reviewed and is approved for publication.


KENNETH N. HOPKINS
Project Engineer
Components Branch
Turbine Engine Division
Aero Propulsion Laboratory
FOR THE COMMANDER


MICHAEL E. STEFKOVICH, Major, USAF
Chief, Components Branch
Turbine Engine Division
Aero Propulsion Laboratory


H. I. BUSH
Director
Turbine Engine Division
Aero Propulsion Laboratory

If your address has changed, if you wish to be removed from our mailing list, or if the addressee is no longer employed by your organization please notify AFWAL/POTC, W-PAFB, OH 45433 to help us maintain a current mailing list.

Copies of this report should not be returned unless return is required by security considerations, contractual obligations, or notice on a specific document.

UNCLASSIFIED

SECURITY CLASSIFICATION OF THIS PAGE

REPORT DOCUMENTATION PAGE

1a. REPORT SECURITY CLASSIFICATION UNCLASSIFIED		1b. PROCUREMENT INSTRUMENT IDENTIFICATION NUMBER AT63052	
2a. SECURITY CLASSIFICATION AUTHORITY		3. DISTRIBUTION/AVAILABILITY OF REPORT Approved for Public Release; Distribution Unlimited	
2b. DECLASSIFICATION/DOWNGRADING SCHEDULE			
4. PERFORMING ORGANIZATION REPORT NUMBER(S) FR-18710		5. MONITORING ORGANIZATION REPORT NUMBER(S) AFWAL-TR-85-2054	
6a. NAME OF PERFORMING ORGANIZATION United Technologies Corporation Pratt & Whitney	6b. OFFICE SYMBOL <i>(If applicable)</i>	7a. NAME OF MONITORING ORGANIZATION Air Force Wright Aeronautical Laboratories Aero Propulsion Laboratory (AFWAL/POTC)	
6c. ADDRESS (City, State and ZIP Code) Government Products Division P.O. Box 2691, West Palm Beach, FL 33402		7b. ADDRESS (City, State and ZIP Code) Wright-Patterson AFB, OH 45433	
8a. NAME OF FUNDING/SPONSORING ORGANIZATION Aero Propulsion Laboratory	8b. OFFICE SYMBOL <i>(If applicable)</i> AFWAL/POTC	9. PROCUREMENT INSTRUMENT IDENTIFICATION NUMBER F33615-83-C-2329	
8c. ADDRESS (City, State and ZIP Code) Wright-Patterson AFB, OH 45433		10. SOURCE OF FUNDING NOS.	
		PROGRAM ELEMENT NO. 62203F	PROJECT NO. 3066
		TASK NO. 05	WORK UNIT NO. 71
11. TITLE (Include Security Classification) Altitude Ignition / Lean Decel Study			
12. PERSONAL AUTHOR(S) Dean Andreadis (Pratt & Whitney)			
13a. TYPE OF REPORT Final Report	13b. TIME COVERED FROM 8/83 TO 1/85	14. DATE OF REPORT (Yr., Mo., Day) November 1985	15. PAGE COUNT 89
16. SUPPLEMENTARY NOTATION			
17. COSATI CODES		18. SUBJECT TERMS (Continue on reverse if necessary and identify by block number)	
FIELD	GROUP	SUB. GR.	Ignition; Lean Deceleration Blowout; Characteristic Times; Fuel Evaporation; Chemical Reaction; Spark Kernel Quenching; Hot Flow Residence Engine Data <i>time</i>
21	02		
21	01		
19. ABSTRACT (Continue on reverse if necessary and identify by block number)			
<p>The objective of this study was to develop analytical tasks consisting of new or improved models for predicting altitude ignition and lean deceleration blowout. The approach taken (in this study) was to describe the ignition and flame stabilization limits in terms of characteristic "time" models. Characteristic times associated with chemical kinetics, fuel evaporation and hot flow residence are quantified for ignition and lean deceleration blowout limits. These expressions were interrelated according to the criteria for successful ignition and flame stabilization. Statistical analysis was used to compare the various expressions and select the appropriate terms that formulate models which best fit the data for altitude ignition and lean deceleration blowout.</p> <p>The models linearly correlate variations in combustor pressure, inlet temperature, fuel-air ratio, fuel temperature, air velocity, pressure drop, combustor front end geometry and injector size using existing data from USAF, Navy, NASA and P&W sponsored programs on operability performance of military and commercial gas turbine combustors. These models have been based entirely on full scale engine test. <i>Keywords: Ignition; flame propagation</i></p>			
20. DISTRIBUTION/AVAILABILITY OF ABSTRACT UNCLASSIFIED/UNLIMITED X SAME AS RPT. <input type="checkbox"/> DTIC USERS <input type="checkbox"/>		21. ABSTRACT SECURITY CLASSIFICATION UNCLASSIFIED	
22a. NAME OF RESPONSIBLE INDIVIDUAL Kenneth N. Hopkins		22b. TELEPHONE NUMBER <i>(Include Area Code)</i> (513) 255-5974	22c. OFFICE SYMBOL AFWAL/POTC

SUMMARY

The purpose of this analytical study was to develop new or improved altitude ignition and lean deceleration blowout correlations which relate the operating limits of a combustion system to engine operating parameters. These correlations can then be universally applied to current or future aircraft gas turbine combustion systems for ignition and stability assessment.

The data base used in constructing the models consisted of the substantial body of experimental data acquired during recent USAF, Navy, NASA and P&W sponsored programs on operability performance of military and commercial, gas turbine engines including F100(3), PW1128 Development, F100-ILC Core, PW2037, JT9D-7R4 and TF30-P-414/414A.

The approach taken in this study was to consider the effects of the following physical processes in the combustor fundamental to ignition and flame stabilization: thermal and turbulent diffusion, chemical reaction, fuel evaporation and turbulent mixing. Since more than two physical processes are involved, the models for ignition and lean deceleration blowout were formulated based on the characteristic "time" rather than "rate" approach. The characteristic time model does not attempt to analyze the entire combustor flow field, but rather considers key regions of the flow field and defines expressions for the time required for spark kernel quenching, chemical reaction, fuel evaporation and hot flow residence.

The criteria for successful ignition and flame stabilization were defined as follows:

- The limiting case for ignition occurred when the time for quenching the spark kernel is on the order of the sum of the chemical reaction plus evaporation times and evaluated in the region near the igniter
- The flame stabilization was viewed as the competition between the hot flow residence time in the primary zone and the chemical reaction plus evaporation times evaluated in the shear-layer region between the hot recirculation zone and the free stream.

Table 1 presents the characteristic times which have been related and the combustor physical processes which were found to provide the best models for altitude ignition and lean deceleration blowout. The first column in Table 1 lists the performance parameter and the mode of engine operation which were evaluated. The second column lists the combustor limits which were determined in this study. The third column lists the combustor related parameters which were determined according to the geometric and operating characteristics of the individual combustors. The fourth column lists the governing physical process for the specific models which were developed in this study and the last column identifies the degree of the relationship based on the regression coefficient of determination.

The combustor physical processes (evaporation and chemical reaction) and operating parameter (spark kernel quench time) developed by Ballal and Lefebvre, Reference 1 for the phenomena of spark ignition were selected to predict altitude ignition performance. Since ignition and flame stabilization are similar phenomena, the combustor physical processes for the phenomena of flame stabilization were defined in the same manner as in the spark ignition with the exception that the parameters involved are evaluated according to the primary zone conditions. These physical processes and the combustor primary zone volumetric hot residence time were selected to predict altitude stability and lean deceleration blowout limit.

TABLE 1.

ALTITUDE IGNITION AND LEAN DECELERATIONS MODELS

<i>Performance Parameter</i>	<i>Combustor Limit</i>	<i>Combustor Operating Parameter</i>	<i>Governing Physical Process</i>	<i>Model Rating</i>
1. Altitude Ignition				
a. Windmill	Ignition Stability	Spark Kernel Quenching Volumetric Hot Residence*	Fuel Evaporation Chemical Reaction and Fuel Evaporation	Very Good Good
b. Spooldown	Ignition Stability	Spark Kernel Quenching Volumetric Hot Residence	Fuel Evaporation Chemical Reaction and Fuel Evaporation	Good Very Good
2. Lean Deceleration Blowout	Stability	Volumetric Hot Residence	Chemical Reaction	Excellent

*Combustor Primary Zone Hot Residence Time

1485C

Although the evaporation time was found to be longer than the chemical reaction time for the phenomena of windmill and spooldown ignition, consideration of both physical processes provided a higher degree of correlation. However, the lean deceleration blowout limit is controlled by chemical reaction for the engine data used in this study.

In most cases, very good data correlations with near zero intercept have been obtained. Examination of the correlations provides good insight into the effect of combustor and engine parameters on altitude ignition and lean deceleration blowout performance. The accuracy of the ignition and flame stabilization models is limited by the inadequate knowledge of the mean drop size, drop size distribution, turbulence intensity, and equivalence ratio in the combustion zone and near the ignitor. Further improvements in the models will require measurements of drop size and turbulence intensity levels to better quantify these variables.

FOREWORD

Personnel of United Technologies Corporation, Pratt & Whitney Aircraft, Florida Operations, prepared this final report under contract F33615-83-C-2329. The program conducted under the sponsorship of the United States Air Force, Air Force Wright Aeronautical Laboratories, Air Force Systems Command, Wright-Patterson Air Force Base, Ohio; and the National Aeronautics and Space Administration. This report documents work conducted during the period from August 1983 to January 1985. Mr. K. N. Hopkins was the Air Force Project Engineer and Mr. D. Andreadis was the P&W Program Manager.

The author wishes to acknowledge the contributions of R. R. Kazmar, Technology Manager, A. I. Masters, Rockets and Technology Manager and C. E. Smith, Technical Specialist for their guidance and technical contributions and to C. W. Whipple for his efforts in data preparation. Also, from Pratt & Whitney Aircraft, East Hartford Operations: Messrs. W. S. Taylor, K. J. Kevin, D. Kirichok, P. A. Keller and B. C. Schlein for their guidance in gathering commercial engine data.

Accession For	
NTIS CRA&I	<input checked="" type="checkbox"/>
DTIC TAB	<input type="checkbox"/>
Unannounced	<input type="checkbox"/>
Justification	
By	
Distribution /	
Availability Codes	
Dist	Avail and/or Special
A-1	



TABLE OF CONTENTS

<i>Section</i>		<i>Page</i>
I	INTRODUCTION	1
II	DEVELOPMENT OF SPARK IGNITION AND FLAME STABILIZATION MODELS	3
	1. Definition of Parameters	3
	2. Literature Survey	7
	3. Spark Ignition Models	7
	4. Flame Stabilization Models	10
III	ALTITUDE IGNITION MODELS	13
	1. Windmill Ignition and Primary Zone Flame Stabilization	14
	2. Spooldown Ignition and Primary Zone Flame Stabilization	33
IV	LEAN DECELERATION BLOWOUT MODEL	49
V	CONCLUSIONS	63
	REFERENCES	65
	APPENDIX A — Literature Survey of Altitude Ignition and Lean Decel Program	67

LIST OF ILLUSTRATIONS

<i>Figure</i>		<i>Page</i>
1	Chemical Reaction Plus Evaporation Effects on Windmill Ignition Limit	15
2	Chemical Reaction Plus Evaporation Effects on Primary Zone Stability Limit During Windmill Ignition	16
3	Chemical Reaction Plus Evaporation Effects on Windmill Ignition Limit	18
4	Chemical Reaction Plus Evaporation Effects on Primary Zone Stability Limit During Windmill Ignition	19
5	Evaporation Effects on Windmill Ignition Limit	20
6	Chemical Reaction Effects on Windmill Ignition Limit	21
7	Evaporation Effects on Primary Zone Stability Limit During Windmill Ignition	22
8	Chemical Reaction Effects on Primary Zone Stability During Windmill Ignition	23
9	Effect of Flow Parameter on Spark Kernel Quench Time During Windmill Ignition	24
10	Effect of Flow Parameter on Volumetric Hot Residence Time During Windmill Ignition	25
11	Effect of Primary Zone Velocity on Spark Kernel Quench During Windmill Ignition	26
12	Effect of Primary Zone Velocity on Volumetric Hot Residence Time During Windmill Ignition	27
13	Effect of Root Mean Square Turbulent Velocity Effect on Windmill Ignition Limit	28
14	Effect of Combustor Pressure Drop on Windmill Ignition Limit	29
15	Effect of Root Mean Square Turbulent Velocity Effect on Stability Limit During Windmill Ignition	30
16	Effect of Combustor Pressure Drop Effect on Stability Limit During Windmill Ignition	31
17	Effect of Sauter Mean Diameter on Windmill Ignition Limit	32
18	Chemical Reaction Plus Evaporation Effects on Spooldown Ignition Limits	34

LIST OF ILLUSTRATIONS (Continued)

<i>Figure</i>		<i>Page</i>
19	Chemical Reaction Plus Evaporation Effects on Primary Zone Stability Limit During Spooldown Ignition	35
20	Evaporation Effect on Spooldown Ignition Limit	36
21	Chemical Reaction Effect on Spooldown Ignition Limit	37
22	Evaporation Effects on Primary Zone Stability Limit During Spooldown Ignition	38
23	Chemical Reaction Effects on Primary Zone Stability Limit During Spooldown Ignition	39
24	Effect of Flow Parameter on Spark Kernel Quench During Spooldown Ignition	40
25	Effect of Flow Parameter on Volumetric Hot Residence During Spooldown Ignition	41
26	Effect of Primary Zone Velocity on Spark Kernel Quench During Spooldown Ignition	42
27	<i>Effect of Primary Zone Velocity on Volumetric Hot Residence Time During Spooldown Ignition</i>	43
28	Effect of Root Mean Square Turbulent Velocity on Spooldown Ignition	44
29	Effect of Combustor Pressure Drop on Spooldown Ignition	45
30	Effect of Root Mean Square Turbulent Velocity on Primary Zone Stability Limit During Spooldown Ignition	46
31	Effect of Combustor Pressure Drop on Primary Zone Stability Limit During Spooldown Ignition	47
32	Effect of Sauter Mean Diameter on Spooldown Ignition	48
33	Identification of Lean Decel Blowout Points for F100-ILC Development Engine FX217-21	50
34	Chemical Reaction and Evaporation Effects on Lean Decel Blowout Limit	52
35	Chemical Reaction and Evaporation Effects on Lean Decel Blowout Limit	53
36	Evaporation Effect on Lean Decel Blowout Limit	54
37	Chemical Reaction Effects on Lean Decel Blowout Limit	55

LIST OF ILLUSTRATIONS (Continued)

<i>Figure</i>		<i>Page</i>
38	Chemical Reaction Effect on Lean Decel Blowout Limit	56
39	Effect of Pressure Drop on Chemical Reaction Time During Lean Decel Blowout	57
40	Chemical Reaction Versus Combustor Fuel Air Ratio Overall During Lean Decel Blowout	58
41	Effect of Fuel Flow to Burner Pressure Ratio on Volumetric Hot Residence Time During Lean Decel Blowout	59
42	Fuel Flow to Burner Pressure Ratio Versus Primary Zone Equivalence Ratio	60
43	Effect of Combustor Pressure on Fuel Air Ratio During Lean Decel Blowout	61
44	Effect of Combustor Total Inlet Temperature on Fuel Air Ratio Overall During Decel Blowout	62

LIST OF TABLES

<i>Table</i>		<i>Page</i>
1	Altitude Ignition and Lean Decelerations Models	iv
2	Altitude Ignition and Lean Decel Data	2

GLOSSARY OF TERMS

A	Pre-exponential factor in equation (18), msec kg/m ³
B	Mass transfer number Equation (4)
C ₁	Ratio of the mean surface area diameter to the Sauter mean diameter
C ₂	Ratio of the mean diameter to the Sauter mean diameter
C ₃	Ratio of the mean volume diameter to the Sauter mean diameter
C _{ci}	Constant in Equation (29)
C _{cs}	Constant in Equation (32)
C _{ei}	Constant in Equation (28)
C _{es}	Constant in Equation (31)
C _p	Specific heat at constant pressure, J/kg-K
d	Diameter, m
dq	Spark kernel quenching diameter, m Equation (5)
E	Activation energy, cal/mole
E _{min}	Minimum spark ignition energy, J
f	Fraction of Fuel Vaporized, Equation (4)
k	Thermal conductivity, J/m-s-K
l	Length, m
l _{co}	Effective CO quench length Equation (23)
M	Molar mass, kg/kgmol
N ₁ , N ₂	Constants in Equation (1)
N ₃	Constant in Equation (2)
N ₄	Constant in Equation (3)
P	Pressure, kPa
ΔP	Pressure differential, kPa
Pr	Prandtl number
R _u	Universal gas constant kJ/kg-mol-K
Re _D	Reynolds number based on initial mean drop size
RU	Ratio of fuel flow rate to burner pressure, $\frac{\text{lbm}}{\text{hr}} \frac{\text{lb}_f}{\text{in.}^2}$ — Figures 41 and 42
r ²	Statistical Coefficient of Determination
S _c	Schmidt number Equation (7)
S _L	Laminar flame speed, m/s Equation (10)
SMD	Sauter mean diameter of fuel spray, microns Equation (1 through 3)
S _T	Turbulent flame speed, m/s Equation (11)
T	Temperature, K
ΔT	Temperature rise due to combustion, K

t_p	Liquid film thickness (microns)
U	Velocity, m/s
u'	Root mean square of the fluctuating velocity, m/s Equation (9)
V	Volume, m^3
W	Mass flow rate, kg/s
W_{ap2}	$Wa\sqrt{T_3}/P_3$ Flow parameter, $(lbm/sec) \cdot R^{1/2}/(lbf/in.^2)$ — Figures 9 and 10
Z	$C_1 C_2^{0.5}/C_3^3$
α	Thermal diffusivity, m^2/s
β	Droplet evaporation coefficient, m^2/s Equation (6) (7)
ε	Constant in Equation (9)
η	Constant in Equation (11)
μ	Dynamic viscosity, kg/m-s
ν	Kinematic viscosity, m^2/s
ρ	Density, kg/m^3
σ	Deviation
σ_f	Surface tension, N/m Equation (1) (3)
τ_{eb}	Droplet evaporation time, msec Equations (16) (12)
τ_{EB}	Droplet evaporation time for flame stabilization, msec Equation (25)
τ_{hc}	Chemical reaction time, msec Equations (12) (18)
τ_{HC}	Chemical reaction time for flame stabilization, msec Equation (26)
τ_{el}	Turbulent mixing time for ignition, msec Equation (14) (12)
τ_{SL}	Turbulent mixing time for flame stabilization, msec Equations (21) (23)
τ_q	Characteristic time for spark quench, msec Equations (13) (15) (15A) (27)
τ_{ei}	Characteristic time for fuel evaporation (ignition), msec Equations (13) (17) (28)
τ_{ci}	Characteristic time for chemical reaction (ignition), msec Equations (13) (19) (29)
τ_{vhr}	Volumetric hot residence time in the primary zone, msec Equations (20) (22) (30) (33)
τ_{en}	Characteristic time for fuel evaporation (stability), msec Equations (20) (24) (31) (34)
τ_{cs}	Characteristic time for chemical reaction (stability), msec Equations (20) (32) (35)
ϕ	Equivalence ratio
Ω	Fraction of total fuel in form of vapor

Subscripts

a	Air
comb	Combustor
f	Fuel
g	Gas
i	Ignition
s	Stability
inj	Injected
ign	Plane of the ignitor
o	Reference value
ad	Adiabatic value
st	Stoichiometric value
pz	Primary zone
3	Combustor inlet value

Conversion Factors

	To Convert From:	To:	Multiply by:
Length	Centimeter (cm)	Inches (in.)	3.937 E-01
	Meter (m)	Feet (ft)	3.281
	Micron (μm)	Meters (m)	1.000 E-06
Mass	Kilogram (kg)	Pounds (lbm)	2.205
Force	Newton ($\text{kg}\cdot\text{m}/\text{s}^2$)	Pounds (lbf)	2.248 E-01
Pressure	Newton/square meter (N/m^2)	Atmosphere (atm)	9.869 E-06
	Kilopascal (kPa)	Pounds/square foot (lbf/ft^2)	2.089 E+01
Temperature	Degree Kelvin (K)	Degree Fahrenheit ($^{\circ}\text{F}$)	$t_{\text{F}} = 1.8 [t_{\text{K}} - 273.15] + 32$
	Degree Rankine ($^{\circ}\text{R}$)	Degree Fahrenheit ($^{\circ}\text{F}$)	$t_{\text{R}} = t_{\text{F}} + 459.67$
	Degree Kelvin (K)	Degree Rankine ($^{\circ}\text{R}$)	$t_{\text{K}} = t_{\text{R}}/1.8$
Volume	Cubic meter (m^3)	Cubic feet (ft^3)	3.531 E+01
Density	Kilogram/cubic meter (kg/m^3)	Pounds-mass/cubic feet (lbm/ft^3)	6.243 E-02
Surface Tension	Newton/meter (N/m)	Pounds-force/foot (lbf/ft)	6.852 E-02
Dynamic Viscosity	Kilogram/meter-second ($\text{kg}/\text{m}\cdot\text{s}$)	Pounds-force/foot-second ($\text{Lbf}/\text{ft}\cdot\text{s}$)	6.721 E-01
Kinematic viscosity	Squared meter/second (m^2/s)	Square-feet/second (ft^2/s)	1.076 E+01
Thermal conductivity	Joule/meter-second-Kelvin ($\text{J}/\text{m}\cdot\text{s}/\text{K}$)	Btu/hour-foot-degree Rankine ($\text{Btu}/\text{hr}\cdot\text{ft}\cdot^{\circ}\text{R}$)	5.780 E-01
Specific Heat	Joule/kilogram-Kelvin ($\text{J}/\text{kg}\cdot\text{K}$)	Btu/pounds-mass-degree Fahrenheit ($\text{Btu}/\text{lbm}\cdot^{\circ}\text{F}$)	2.388 E-04
Energy	Joule	British thermal units (Btu)	9.486 E-04
Velocity	Centimeter/second (cm/s)	Inches/second (m/s)	3.937 E-01
	Meter/second (m/s)	Feet/second (ft/s)	3.281

Physical Constants

Universal gas constant $R_u = 0.730 \text{ atm}\cdot\text{ft}^3/(\text{lb}\cdot\text{mol}) (^{\circ}\text{R})$
 $= 8.315 \text{ kJ}/(\text{kg}\cdot\text{mol}) (\text{K})$
 $= 1545 \text{ ft}\cdot\text{lbf} (\text{lb}\cdot\text{mol}) (^{\circ}\text{R})$
 $= 1.986 \text{ Btu}/(\text{lb}\cdot\text{mol}) (^{\circ}\text{R})$

SECTION I

INTRODUCTION

Two of the primary requirements of a gas turbine combustor design are to maintain combustion over a wide range of operating conditions (including the transient state of rapid deceleration) and to achieve rapid relighting and engine acceleration after flame-out at altitude. The modern military fighter and commercial engines are called upon to operate at very low inlet temperatures, pressures, and at primary zone fuel air ratios that on the average are well outside the limits of flamability for hydrocarbon air mixtures. Under these conditions, combustion may become unstable which results in a tendency for the flame to blow-out and not relight.

Present and future generations of gas turbine combustors are being designed for higher turbine inlet temperature and minimum smoke emission. This requires that a larger percentage of the air be routed to the combustor primary zone to obtain proper stoichiometry during high power operation. However, during altitude ignition and engine deceleration, the primary zone stoichiometry becomes excessively lean. This reduces combustion stability margin and leads to potential deceleration blowout and an inability to ignite at required altitude.

A number of experimental evaluations to determine altitude ignition and lean deceleration blowout limits have been sponsored by the Air Force, Navy, NASA and Pratt & Whitney over the past few years. These tests have provided a wealth of data. The data sources selected for this study are as shown in Table 2. The objective of the Altitude Ignition and Lean Decel Study has been to use this data base and to develop analytical tools consisting of new or improved models for predicting altitude ignition and lean decel performance. The models may then be used as the basis for: (1) serving as a design tool for new combustion systems; (2) permitting necessary design modifications to be made in the early stages of the combustor design; and (3) reducing the time and cost for testing new combustion systems in order to define ignition and stabilization limits.

The Altitude Ignition and Lean Decel Study was conducted in three tasks as listed below.

- Task I — An in-depth literature survey was made of existing ignition and stability theory emphasizing altitude ignition and lean deceleration blowout
- Task II — The available in-house and external engine test and rig test data were gathered to support the analytical effort. Emphasis was placed on engine data because it includes effects such as combustor inlet air flow distortion and control acceleration and deceleration schedules, both of which are difficult to duplicate in a rig
- Task III — The selection and development of the model which best fits the data for altitude ignition (windmill and spooldown modes) and the best correlation for lean deceleration blowout was made.

TABLE 2.

ALTITUDE IGNITION AND LEAN DECEL DATA

<i>Engine</i>	<i>Type of Data Gathered</i>
a. Military Engines	
F100(3) Engine P1068X-13	Altitude Ignition (Windmill and Spooldown)
F100(3) Engine FX219-21	Altitude Ignition (Spooldown)
PW1128 Development Engine FX225-19	Altitude Ignition (Windmill and Spooldown)
ILC Core Engine FX208-29	Altitude Ignition (Windmill)
TF30-P-414/414A Engine P-286-1 and 2	Altitude Ignition (Windmill)
F100-PW-200 Engine FX217-19	Lean Decel Blowout
F100 ILC Development Engine FX217-21	Lean Decel Blowout
b. Commercial Engines	
PW2037 Engine X-669-1/B747	Altitude Ignition (Windmill)
JT9D-7R4 Engine X-579-31	Altitude Ignition (Windmill)
JT9D-7R4 Engine X-491-2	Altitude Ignition (Windmill)
PW2037 Engine X-663-1	Lean Decel Blowout
PW2037 Engine X-664-7	Lean Decel Blowout

1486C

The development of altitude ignition and lean deceleration under Task III was conducted according to the following steps. First, relationships were established which associate characteristic times, with the physical processes in the combustor for ignition and stabilization. Second, these expressions were interrelated according to the criteria for successful ignition and stabilization. Third, statistical analysis was used to compare the various expressions and select the appropriate terms that formulate models which best fit the data for altitude ignition and lean deceleration blowout. These models have been based entirely on full-scale engine tests.

SECTION II

DEVELOPMENT OF SPARK IGNITION AND FLAME STABILIZATION MODELS

1. DEFINITION OF PARAMETERS

The success in adapting existing ignition and stability models to engine operating conditions was dependent in a large part to properly defining the various fuel and air properties, operating and design parameters which were employed. The definition of these parameters is presented in this section. In most cases the basis for defining the parameter was clear cut. In other cases the definition was obtained through a systematic evaluation of the effect of the parameters involved.

a. Fuel Properties

For the military and commercial engine data in this study, expressions were developed for the following fuel properties:

- Density
- Surface tension
- Absolute viscosity
- Vapor pressure
- Latent heat of vaporization
- Specific heat
- Mass transfer number.

The fuel properties were determined as a function of the fuel temperature. The fuel temperature was obtained from the data set plus an estimated temperature rise in the fuel system and injector. In addition, some fuel properties were evaluated as a function of 10 percent distillation temperature for spark ignition phenomena and 50 percent distillation temperature for flame stabilization phenomena.

b. Air and Gas Properties

The air and gas properties, such as density, absolute viscosity, specific heat, thermal diffusivity, thermal conductivity and Prandtl number were determined as a function of combustor inlet temperature or gas temperature in the primary zone.

c. Injector Velocity and Spray Angle

The injector velocity was evaluated by considering the fuel injector and swirler flow as one dimensional incompressible flow with axial and tangential components. Given the injector and swirler air flow rate, the effective and physical flow areas, combustor pressure and temperature, it is possible to determine the average axial component of the injected velocity and the spray angle of the injector. The axial velocity and the spray angle were used to calculate the tangential component, and the addition of these components provided on average injected velocity at the exit plane of the injector. Also, reference velocities were calculated at the plane of the ignitor and primary holes.

d. Sauter Mean Diameter

To calculate the droplet evaporation time for a particular combustor, the fuel spray droplet Sauter mean diameter (SMD) must be determined for the particular combustion system of interest. Unfortunately, droplet size measurements were not available. Instead, empirical correlation parameter were used to predict the SMD for each atomizing nozzle.

(1) Airblast Atomizing Nozzles

The F100(3), PW1128, and PW2037 engines employ airblast atomizing fuel nozzles. Rizkalla and Lefebvre's correlation parameter for this type of atomizer, Reference 30, was used to estimate the relative fuel spray droplet diameter.

$$\text{SMD} = \left[N_1 \left(\frac{\sigma_f}{\rho_a U_{inj}^{2.0}} \right)^{0.6} \left(\frac{\rho_f}{\rho_a} \right)^{0.25} \left(1 + \frac{W_f}{W_a} \right)^{0.85} t_p^{0.4} \right] + \left[N_2 \left(\frac{\mu_f^{2.0}}{\sigma_f \rho_f} \right)^{0.45} \left(1 + \frac{W_f}{W_a} \right)^{0.35} t_p^{0.35} \right] \quad (1)$$

where:

- N_1, N_2 = Constant (dependent on fuel nozzle design)
- ρ_a = Air density, (kg/m³)
- ρ_f = Fuel density, (kg/m³)
- σ_f = Surface tension, (N/m)
- μ_f = Dynamic viscosity, (kg/m-s)
- W_f = Fuel flow, (kg/s)
- W_a = Air flow, (kg/s)
- U_{inj} = Injected velocity, (m/s)
- t_p = Liquid film thickness (microns).

(2) Hybrid Atomizing Nozzles

The JT9D-7R4 combustor employs hybrid atomizing fuel nozzles. For this type of atomizer, a correlation parameter developed at Pratt & Whitney was used to predict the relative fuel spray droplet diameter.

$$\text{SMD} = [N_3 (W_f)^{0.215} [e^{(0.6332 \sqrt{T_f})^{0.18}}] / (\Delta P_f)^{0.442}] \quad (2)$$

where:

- N_3 = Constant (dependent on fuel nozzle design)
- W_f = Fuel flow (kg/s)
- T_f = Fuel temperature (°K)
- ΔP_f = Pressure drop in the fuel nozzle passage (kPa).

(3) Pressure Atomizing Nozzles

The TF30 combustor employs pressure atomizing fuel nozzles. Lefebvre correlation parameter for this type of atomizer (Reference 31) was used to estimate the relative fuel spray droplet diameter.

$$\text{SMD} = N_2 \sigma_f^{0.25} v_f^{0.25} W_f^{0.25} \Delta P_f^{-0.5} \rho_g^{0.25} \quad (3)$$

where:

- N_2 = Constant (dependent on fuel nozzle design)
- v_f = Kinematic viscosity, (m²/sec)
- ρ_g = Density of the gas, (kg/m³).

e. Effective Fuel Air Ratio and Gas Temperature in Primary Zone

The rate of fuel evaporation is not always sufficiently high to ensure that all of the fuel is fully vaporized within the primary zone. Thus, an iterative procedure was developed to determine the fraction of fuel vaporized or an "effective" fuel air ratio and the corresponding gas temperature within the combustion zone. The procedure starts with an initial guess effective fuel air ratio equal to the stoichiometric fuel air ratio and determines the corresponding gas temperature. The fraction of fuel vaporized is then calculated according to the following expression (Reference 31):

$$f_f = 8 \left(\frac{\rho_k}{\rho_f} \right) \left(\frac{k}{c_p} \right)_k \ln(1 + B) \left(\frac{V_{pz}}{W_{pz} \text{SMD}^{2.0}} \right) (1 + 0.22 \text{Re}_D^{0.5}) \quad (4)$$

where:

- f_f = Fraction of fuel vaporized within combustion zone
- k_g = Gaseous thermal conductivity, (J/m-s-K)
- c_{pg} = Gaseous specific heat, (J/kg-K)
- B = Mass transfer number based on 50 percent boiling temperature
- V_{pz} = Volume of the primary zone, m^3
- W_{pz} = Primary zone airflow, (kg/sec)
- SMD = Sauter mean diameter, microns
- Re_D = Droplet Reynolds number based on mean drop size

From the fraction of fuel vaporized, an effective fuel air ratio is calculated and compared to the initial effective fuel air ratio. If the calculated value of effective fuel air ratio is not equal to the initial value used to obtain the gas temperature, an iteration process is used to balance them. It should be noted that equation 4 allows the fraction of fuel vaporized to exceed unity which means that the fuel is fully vaporized within the recirculation zone. In these circumstances, the primary zone fuel air ratio is used to determine the gas temperature and properties in the primary zone.

f. Primary Zone Volume

The primary zone volume is required to evaluate the fraction of fuel vaporized and the volumetric hot residence time. The volume of the primary zone of an annular combustor formed by the spray angle of the fuel injector and the primary zone jets is calculated in the following manner. The volume is assumed to take the shape of a frustum of a right circular cone with the slant height at the spray angle, the lower base at the plane of the primary holes and the upper base at the exit of the injector plane. It uses the primary zone length as the vertical height of the frustum. While the radius of the lower and upper bases are represented by one half of the annulus height in the plane of the primary holes and the exit swirler radius of the injector, respectively.

g. Spark Kernel Quench Diameter

A definition of minimum ignition energy is required to evaluate the diameter of the spark kernel (dq). As suggested by Ballal and Lefebvre, Reference 1, minimum ignition energy is defined as the energy required to heat a spherical volume of air with diameter dq , up to the stoichiometric flame temperature, which results in the following equation:

$$dq = \left[\frac{E_{\min}}{\pi \cdot 6 \rho_a c_{p,a} \Delta T_{st}} \right]^{1/3} \quad (5)$$

where:

- E_{\min} = Minimum ignition energy, (J)
- $c_{p,a}$ = Specific heat of air, (J/kg-K)
- ΔT_{st} = Stoichiometric flame temperature rise, (K)

h. Evaporation Coefficient

To compute the droplet evaporation time in the spark ignition and flame stabilization models developed by Peters, Plee, and Mellor, Reference 2, it is necessary to determine the droplet evaporation coefficient which accounts for fuel properties influences and is corrected for convection according to the phenomena of interest.

For the ignition model

$$\beta_i = \frac{8k_g}{\rho_f c_{p,g}} \ln(1+B) (0.185 \text{ Re}_D^{0.6}) \quad (6)$$

where:

- k_g = Gaseous thermal conductivity (J/m-s-K)
- $c_{p,g}$ = Gaseous specific heat (J/kg-K)
- ρ_f = Fuel density at 10 percent boiling point kg/m³
- B = Transfer number based on the 10 percent boiling temperature
- Re_D = Droplet Reynolds number based on mean drop size.

For the stabilization model

$$\beta_s = \frac{8k_g}{\rho_f c_{p,g}} \ln(1+B) (1+0.276 \text{ Re}_D^{1/2} \text{ Sc}^{1.3}) \quad (7)$$

where:

- ρ_f = Fuel density at 50 percent boiling point, (kg/m³)
- B = Transfer number based on 50 percent boiling point temperature
- Sc = Gas phase Schmidt number.

i. Root Mean Square of the Fluctuating Velocity

Turbulence measurements were not available from the data presented in Section I. However, using the approach of Lefebvre, Reference 28, the root mean square of the fluctuating velocity, u' , was predicted from the pressure loss across the particular combustor and the inlet temperature and pressure. The pressure energy loss must appear as turbulence energy prior to dissipation as molecular motion. If the pressure loss is proportional to the turbulent kinetic energy. In equation form:

$$\Delta P \propto \frac{2}{3} \rho_a (u')^2 \quad (8)$$

Substituting the perfect gas law equation for the density and solving for u' equation (8) becomes:

$$u' = \varepsilon \left[1.5 R_u T_3 \left(\frac{\Delta P}{P} \right) / 100 \right]^{0.5} \quad (9)$$

where:

- ε = Constant of proportionality
- R_u = Universal gas constant 8315 (J/kg mole K)
- M_a = Molar mass of air, 29 (kg/kgmole)
- T_3 = Combustor inlet temperature (K)
- $\frac{\Delta P}{P}$ = Percent combustor pressure drop.

j. Laminar and Turbulent Flame Speeds

The laminar flame speed is calculated from a correlation developed by Pratt & Whitney. This correlation was calibrated against ethane and propane data, and includes the effects of pressure, inlet temperature and fuel air ratio.

$$S_L = S_{L_o} \left(\frac{T_3}{T_{3_o}} \right)^{1.4} \left(\frac{T_{ad} - T_3}{T_{ad_o} - T_{3_o}} \right)^{1.4} \exp(-2 \times 10^4 / T_{ad} + 2 \times 10^4 / T_{ad_o}) \quad (10)$$

where:

S_L = Laminar flame speed, (m/s)
 T_3 = Combustor inlet temperature (R)
 T_{ad} = Adiabatic flame temperature (R)
o = Reference conditions.

The turbulent flame speed is based on the Shchelkin's model which relates turbulence properties to the increase in specific surface area of the flame. This approach leads to a relationship of the form:

$$S_T = S_L \left[1 + \eta \left(\frac{u'}{S_L} \right)^2 \right]^{0.5} \quad (11)$$

where:

S_T = Turbulent flame speed, (m/s)

in which η is a constant of the order of unity.

2. LITERATURE SURVEY

An indepth literature survey was conducted of existing ignition and stability theory and correlations emphasizing altitude ignition and lean deceleration blowout. Titles, authors sources, and a brief description of literature reports applicable to this study are shown in Appendix A. A list of all available reports uncovered during the literature survey can be found in the Reference Section. The following models were considered in this study.

3. SPARK IGNITION MODELS

The spark ignition model developed by Peters and Mellor, Reference 2, states that for ignition to occur, the energy of the spark must heat an initial volume such that the heat release rate within that volume is greater than the loss rate. Heat generation is limited first by a droplet evaporation rate and then by a chemical reaction rate. The heat loss in a gas turbine combustor environment is due to turbulent diffusion; hence, it is controlled by a turbulent mixing time. The ignition limit is reached when τ_{sl} , the turbulent mixing time, equals the sum of τ_{eb} , the droplet evaporation time plus τ_{hc} , the chemical reaction time. In equation form:

$$\tau_{sl} = \tau_{hc} + \tau_{eb} \quad (12)$$

The spark ignition model by Ballal and Lefebvre, Reference 1, states that for ignition to occur, the passage of the spark must create a small, roughly spherical volume of air (spark kernel) whose temperature is sufficiently high to initiate evaporation and chemical reaction. If the rate

of heat release by combustion exceeds the rate of heat loss by thermal conduction and turbulent diffusion, then the kernel grows to a size capable of flame propagation. The ignition limit is reached when the time required for the fuel to evaporate (τ_{ei}) chemically react (τ_{ci}) is equal to or less than the time required for the cold mixture to quench (τ_q) the spark kernel by thermal conduction and turbulent diffusion. In equation form:

$$\tau_q = \tau_{ei} + \tau_{ci} \quad (13)$$

a. Evaluation of the Characteristic Times

(1) Turbulent Mixing, τ_{sl}

The turbulent mixing time, τ_{sl} , was defined as the ratio of the diameter of the spark kernel (d_q) to the mean flow velocity at the plane of the ignitor (U_{ign}). In equation form:

$$\tau_{sl} = d_q / U_{ign} \text{ (msec)} \quad (14)$$

(2) Spark Kernel Quench Time, τ_q

The spark kernel quench time, τ_q , was defined as the ratio of the heat capacity of the spark kernel divided by the average rate of heat loss from the kernel by thermal conduction and turbulent diffusion, i.e.,

For moderate turbulence

$$\tau_q = \frac{d_q^2}{8(\alpha + 0.08 u' d_q)} \text{ (msec)} \quad (15)$$

For high turbulence, this reduces to:

$$\tau_q = \frac{d_q}{0.64 u'} \text{ (msec)} \quad (15a)$$

where:

- d_q = Spark kernel diameter, (m)
- α = Thermal diffusivity, (m^2/s)
- u' = Root mean square of the fluctuating velocity, (m/s)

(3) Fuel Evaporation Times, τ_{eb} and τ_{ei}

Peters and Mellor computed the droplet evaporation time, τ_{eb} , from the "d² law" based upon the initial SMD of the spray. The droplet evaporation time was defined as the ratio of the square of the Sauter mean diameter divided by the droplet evaporation coefficient. Since the total amount of fuel being vaporized contributes to the ignition process, τ_{eb} was divided by the total number of drops in the spark kernel. Peters and Mellor noted that the equivalence ratio in the primary zone is proportional to the total drops in the spray. In equation form:

$$\tau_{eb} = (SMD)^2 / \beta_i \phi_{ign} \text{ (msec)} \quad (16)$$

where:

- SMD = Sauter mean diameter of the spray, (m)
 β_i = Droplet evaporation coefficient for spark ignition, (m²/s)
 ϕ_{ign} = Equivalence ratio near the ignitor.

Ballal and Lefebvre defined the evaporation time, τ_{ei} , as the difference between the fuel liquid evaporation time and the time to produce the vapor that already exists in the system. Fuel liquid evaporation time was obtained as the ratio of the mass of fuel contained within the spark kernel to the rate of fuel evaporation, while vaporization time was obtained as the ratio of the mass of vapor present to the rate of evaporation of the liquid drops in the spray. Therefore, evaporation time was calculated in the following manner:

For high turbulence conditions

$$\tau_{ei} = \frac{(\text{Pr}/2)(1 - \Omega) \rho_f (\text{SMD})^{1.5}}{Z \rho_a^{0.5} \mu_a^{0.5} u'^{0.5} \phi_{inj} \ln(1 + B_{st})} \text{ (msec)} \quad (17)$$

where:

- Pr = Prandtl number
 Ω = Fraction of total fuel in form of vapor
 ρ_f = Fuel density, (kg/m³)
SMD = Sauter mean diameter, (m)
 $Z = C_1 C_2^{0.5} / C_3^3$
 C_1 = Ratio of the mean surface area diameter to the Sauter mean diameter
 C_2 = Ratio of the mean diameter to the Sauter mean diameter
 C_3 = Ratio of the mean volume diameter to the Sauter mean diameter
 ρ_a = Air density (kg/m³)
 μ_a = Dynamic viscosity, (kg/m-sec)
 u' = Root mean square of the fluctuating velocity, (m/sec)
 B_{st} = Mass transfer number at stoichiometric temperature
 ϕ_{inj} = Injector equivalence ratio.

(4) Chemical Reaction Times, τ_{hc} and τ_{cl}

Peters and Mellor derived the chemical reaction time, τ_{hc} from the Arrhenius expression in terms of the rate of hydrocarbon oxidation.

$$\tau_{hc} = \frac{A \exp(E/RT_{st})}{\phi_{ign} \rho_g} \text{ (msec)} \quad (18)$$

where:

- A = Pre-exponential factor, 10⁻⁵ (msec-kg/m³)
E = Activation energy, 26,100 (cal/mole)
R = Universal gas constant, 1.986 (cal/mole-K)
 T_{st} = Stoichiometric adiabatic flame temperature, (K)
 ρ_g = Gas phase density, (kg/m³)
 ϕ_{ign} = Equivalence ratio near the igniter.

Ballal and Lefebvre described the chemical reaction time as a function of the laminar and turbulent flame speeds.

For high turbulence conditions:

$$\tau_{ci} = \frac{15.6\alpha}{u'(S_T - 0.63 u')} \text{ (msec)} \quad (19)$$

where:

$$\begin{aligned} \alpha &= \text{Thermal diffusivity, (m}^2/\text{s)} \\ u' &= \text{Root mean square of the fluctuating velocity, (m/s)} \\ S_T &= \text{Turbulent flame speed, (m/s).} \end{aligned}$$

4. FLAME STABILIZATION MODELS

In the present study, the flame stabilization process is viewed as occurring in the shear layer surrounding the combustor recirculation zone by way of turbulent mixing of fresh reactants and hot products and partially oxidized fuel. The stability limit is reached when the volumetric residence time, τ_{vhr} , of the hot turbulent eddies present in the shear-layer region is of the order of evaporation time, τ_{es} , plus chemical reaction time, τ_{cs} . In equation form:

$$\tau_{vhr} = \tau_{es} + \tau_{cs} \text{ (msec)} \quad (20)$$

Plee and Mellor considered the same approach and criteria with the exception that the volumetric hot residence time was replaced with the turbulent mixing time. Also, the turbulent mixing time was multiplied by the ratio of T_3/T_{st} . This accounts for the fluid mechanic acceleration across the shear layer due to the temperature gradient, and was included in the characteristic times of evaporation, τ_{EB} , and chemical reaction τ_{HC} so that the fluid mechanics and chemistry are uncoupled. In equation form:

$$\tau_{vL} = \tau_{EB} + \tau_{HC} \text{ (msec)} \quad (21)$$

a. Evaluation of the Characteristic Times

(1) Volumetric Hot Residence Time, τ_{vhr}

The volumetric hot residence time, τ_{vhr} , is defined as the ratio of the primary zone volume divided by the airflow through the primary zone times the gas density. In equation form:

$$\tau_{vhr} = V_{pz} \rho_g / W a_{pz} \text{ (msec)} \quad (22)$$

where:

$$\begin{aligned} V_{pz} &= \text{Volume of the primary zone, (m}^3\text{)} \\ \rho_g &= \text{Gas density, (kg/m}^3\text{)} \\ W a_{pz} &= \text{Air in the primary zone, (kg/sec).} \end{aligned}$$

(2) Turbulent Mixing Time, τ_{SL}

The turbulent mixing time, τ_{SL} , was characterized by an eddy decay time which was related to the macroscopic characteristic length for CO emissions, l_{CO} , and reference velocity in the primary zone, U_{pz} , introduced by Mellor and Washam to model emissions:

$$\tau_{SL} = \tau_{SL,CO} = l_{CO}/U_{pz} \text{ (msec)} \quad (23)$$

The characteristic length for CO emissions is defined by:

$$l_{CO} = [d_{comb}^4 + l_{pz}^4]^{1/4}$$

where:

l_{pz} = Axial distance from the discharge plane of the fuel injector to the center line of the primary holes

d_{comb} = Combustor diameter.

(3) Fuel Evaporation Times, τ_{es} and τ_{EB}

The droplet evaporation time, τ_{es} is defined as the ratio of the mass of fuel present to the average rate of fuel evaporation for a polydisperse spray. Thus according to Ballal and Lefebvre, the droplet evaporation time is given:

$$\tau_{es} = \frac{C_3^3 \rho_f c_{p,g} (SMD)^2 (1-\Omega)}{8C_1 k_g \phi_{pz} \ln(1+B) (1+0.25 C_2^{0.25} Re_D^{0.5})} \text{ (msec)} \quad (24)$$

where:

ρ_f = Fuel density at 50 percent distillation temperature, (kg/m³)

$c_{p,g}$ = Specific heat of gas, (J/kg-K)

SMD = Sauter mean diameter, (m)

Ω = Fraction of total fuel in form of vapor

C_1 = Ratio of the mean surface area diameter to the Sauter mean diameter

C_2 = Ratio of the mean diameter to the Sauter mean diameter

C_3 = Ratio of the mean volume diameter to the Sauter mean diameter

k_g = Thermal conductivity of gas, (J/m-s-K)

ϕ_{pz} = Equivalence ratio in the primary zone

B = Mass transfer number at 50 percent distillation temperature

Re_D = Droplet Reynolds number based on mean drop size.

Plee and Mellor computed the droplet evaporation time, τ_{EB} , using equation (16). However, the convection correction in the evaporation coefficient was modified according to equation (7), the equivalence ratio was removed and properties were evaluated at 50 percent distillation temperature for the phenomena of flame stabilization. This results in the following equation form:

$$\tau_{EB} = [(SMD)^2 \beta_s] \left(\frac{T_{st}}{T_1} \right) \text{ (msec)} \quad (25)$$

where:

- SMD = Sauter mean diameter, (microns)
- β_s = Evaporation coefficient for stability, (m²/s)
- T_{st} = Stoichiometric adiabatic flame temperature, (K)
- T_3 = Combustor inlet temperature, (K).

(4) Chemical Reaction Time, τ_{cs} and τ_{HC}

The chemical reaction time, τ_{cs} , considered in this study for the phenomena of flame stabilization is defined as in the spark ignition phenomena developed by Ballal and Lefebvre equation (19). Flame stabilization and ignition are similar phenomena. In both cases, a fuel and air mixture must be heated so that the fuel evaporates, mixes with the air and chemical reactions begin at the rate sufficient for establishing flame. The difference between ignition and flame stabilization is the energy source that utilizes combustion, hot recirculation gas for flame stabilization, and a spark ignition. Consequently, the formulation of the chemical reaction time for ignition is the same for the flame stabilization.

The chemical reaction time, τ_{HC} , developed by Plee and Mellor for the phenomena of flame stabilization is defined in the same manner as in the spark ignition phenomena with the exception of the pre-exponential factor is 10^{-4} , the activation energy is 21,000 cal/mole, the gas density term is removed and the equivalence ratio is evaluated as the primary zone equivalence ratio. In equation form:

$$\tau_{HC} = (A/\phi_{pz}) \exp(E/R_u T_u) \left(\frac{T_{st}}{T_3} \right) \text{ (msec)} \quad (26)$$

where:

- A = Pre-exponential factor, 10^{-4} (msec-kg/m³)
- E = Activation energy, 21,000, (cal/mole)
- ϕ_{pz} = Equivalence ratio in the primary zone
- R_u = Universal gas constant, 1.986, (cal/mole-K)
- T_{st} = Stoichiometric adiabatic flame temperature, (K)
- T_3 = Combustor inlet temperature, (K).

SECTION III

ALTITUDE IGNITION MODELS

Altitude ignition followed by engine acceleration has been one of the most significant combustor performance variables affected by the trend toward increased air flow in the primary zone. In recent years, analytical and experimental studies have been conducted to provide a useful theoretical foundation for relating ignition characteristics to combustor operating parameters. Some of these theories were presented in Section II, and were considered in the development of altitude ignition models for windmill and spool-down engine performance.

Altitude ignition models were developed using F100(3), PW1128 Development, F100-ILC Core, PW2037, JT9D-7R4 and TF30-P-414/414A engine data. Ignition operating conditions were determined by plotting the high pressure rotor speed and combustor pressure as a function of time. Ignition followed by engine acceleration was identified by the sudden increase in combustor pressure and verified by the increase in high pressure rotor speed. However, if no response occurred, the operating point was defined as no ignition. Also, blowout points were determined by the sudden decrease in combustor pressure or high pressure rotor speed during engine acceleration.

The process of altitude ignition is viewed to occur in the following manner. Upon attempting to relight an engine either by windmill or spool-down mode, the spark kernel must grow to a minimum spherical volume of sufficiently high temperature to initiate rapid evaporation, and sustain both chemical reaction and flame propagation while the primary zone operating conditions must be stable. Otherwise, ignition followed by engine acceleration will not occur.

Comparison of the degree of correlation of the ignition and flame stabilization models is presented in Section II. The characteristic times developed by Ballal and Lefebvre for the phenomena of spark ignition were selected to describe the physical processes in the combustor during windmill and spool-down ignition. The spark kernel ignition model includes the effects of thermal and turbulent diffusion, evaporation and chemical reaction time. The following expressions describe the characteristic times associated with each physical process:

Spark kernel quenching time:

$$\tau_{q_i} = \frac{d_q}{0.64 u'} \text{ (msec)} \quad (27)$$

Evaporation time:

$$\tau_{e_i} = \frac{C_{e_i}(\text{Pr}_r/2)(1-\Omega)\rho_f(\text{SMD})^{1.5}}{Z\rho_a^{0.5}\mu_a^{0.5}u'^{0.5}\phi_{inj}\ln(1+B_{st})} \text{ (msec)} \quad (28)$$

Chemical reaction time:

$$\tau_{c_i} = \frac{C_{c_i}(15.6\alpha)}{u'(S_T-0.63u')} \text{ (msec)} \quad (29)$$

Where the proportionality and the constant weighting factors, $C_{e_i} = C_{c_i} = 2.66$ and 1.0 for windmill and spool-down ignition, are necessary because characteristic times are simply order of magnitude estimates of the processes involved.

Since successful ignition must be followed by engine acceleration, the primary zone stability limit was also analyzed at the time of ignition. The flame stabilization and spark ignition are similar phenomena. Consequently the formulation of the physical processes for the flame stabilization model is very similar to the spark ignition model. The primary zone flame stabilization model considers the effects of volumetric flow residence, evaporation and chemical reaction. These physical processes are defined analytically as:

Volumetric hot residence time:

$$\tau_{vhr} = \frac{V_{pz} \rho_g}{W a_{pz}} \text{ (msec)} \quad (30)$$

Evaporation time:

$$\tau_{ev} = \frac{C_{ev} C_{s3}^3 \rho_f C_{p,k} (SMD)^2 (1-\Omega)}{8 C_1 k_g \phi_{pz} \ln(1+0.25 C_2^{0.25} Re_D^{0.5})} \text{ (msec)} \quad (31)$$

Chemical reaction time:

$$\tau_{cs} = \frac{C_{cs}(15.6\alpha)}{u' (S_T - 0.63 u')} \text{ (msec)} \quad (32)$$

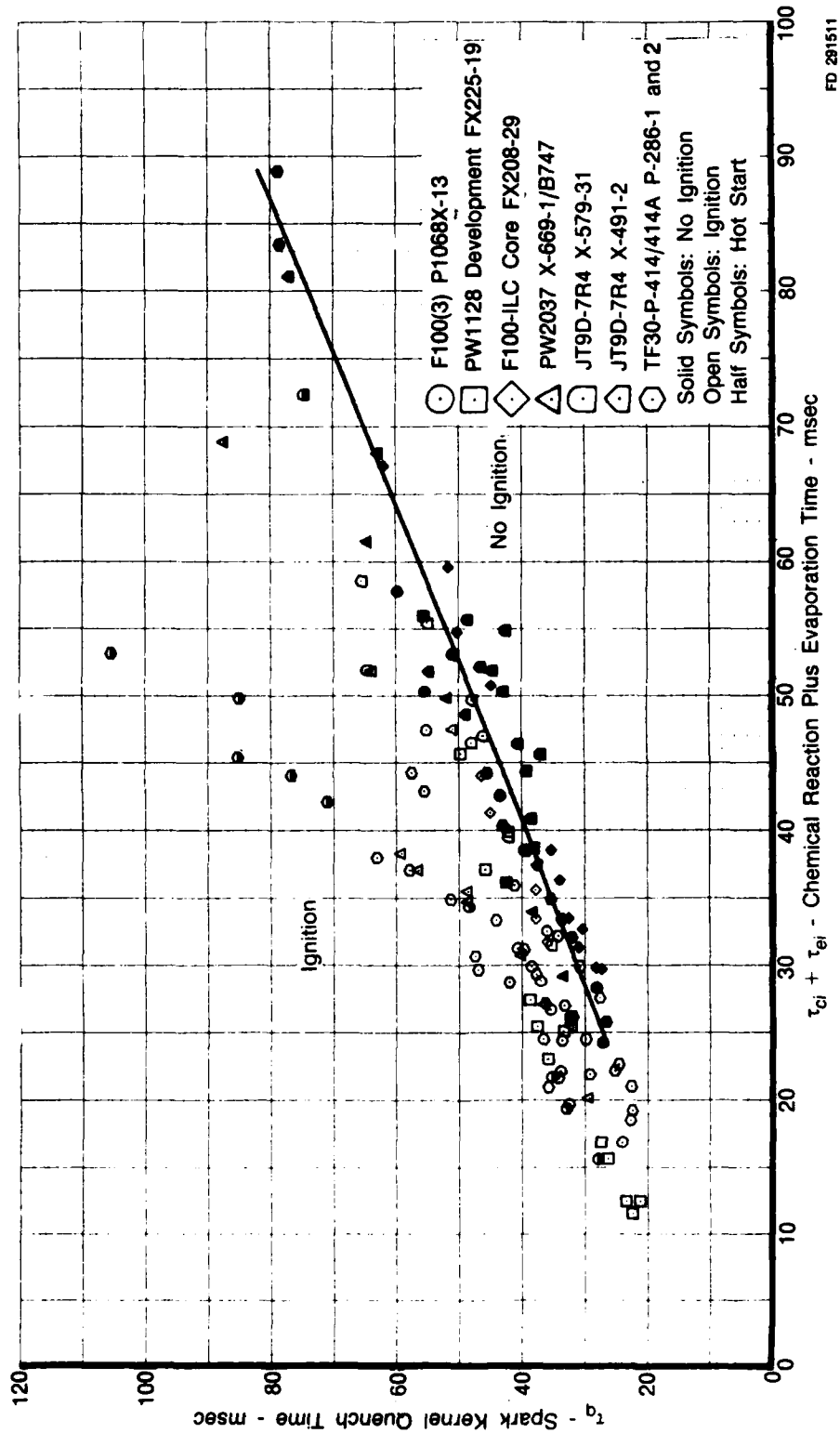
where, $C_{es} = C_{cs} = 1.66$ for windmill and spooldown.

1. WINDMILL IGNITION AND PRIMARY ZONE FLAME STABILIZATION

In the present study, windmill ignition limit data from seven engines F100(3), PW1128 Development, F100-ILC Core, PW2037, JT9D-7R4 and TF30-P-414/414A were analyzed. Linear correlation models of windmill ignition and primary zone stability limits were obtained as shown in Figures 1 and 2.

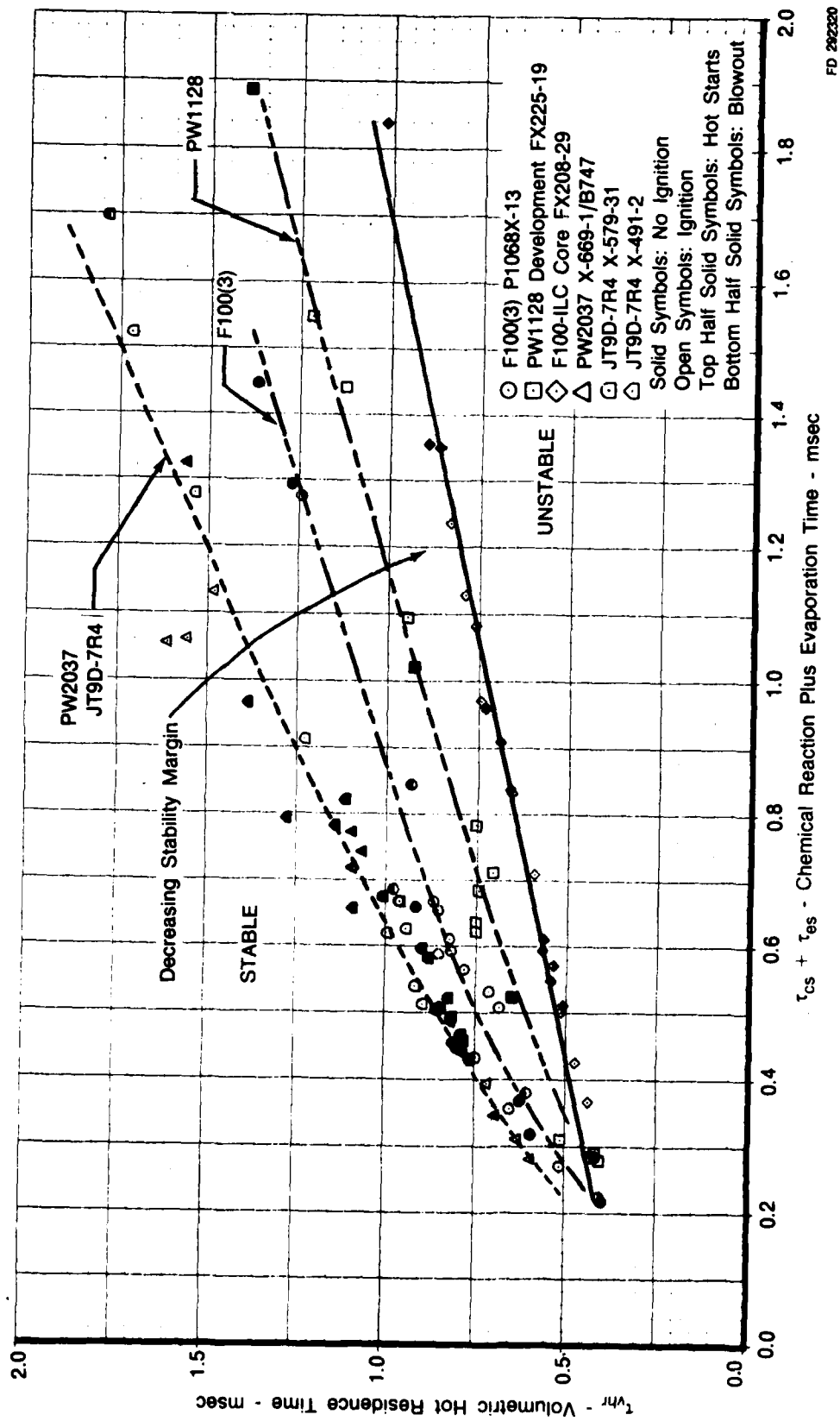
A good correlation model of the spark ignition limit was obtained by correlating the available spark kernel quench time τ_q as a function of the evaporation plus chemical reaction time $\tau_{ei} + \tau_{ci}$. The solid line in Figure 1 represents the spark ignition limit and separates the regions of ignition and no ignition. With increased evaporation plus chemical reaction time for specified spark quench time, the engine approaches the limit of no ignition, and as a result, longer spark quench time is required to establish successful ignition.

Figure 2 presents the relationship between volumetric hot residence time and the sum of evaporation plus chemical reaction for the phenomena of primary zone flame stabilization immediately after ignition. The solid line represents the primary zone stability limit and separates the regions of stable and unstable conditions. Current and advanced engines with increased primary zone air flow and/or reduced volume approach the limit of stability by decreasing volumetric hot residence time for a specified chemical plus evaporation time. To obtain successful ignition followed by engine acceleration, the combustor operating conditions must exist within the ignition and stable region.



FD 291511

Figure 1. — Chemical Reaction Plus Evaporation Effects on Windmill Ignition Limit



FD 282320

Figure 2. — Chemical Reaction Plus Evaporation Effects on Primary Zone Stability Limit During Windmill Ignition

The equations of the limit lines, coefficients of determination (0.920 and 0.950) and standard deviations (3.725 and 0.037) for ignition and stability are shown in Figures 3 and 4, respectively. The dotted lines represent the 95 percent confidence band. For any value of the evaporation plus chemical reaction, the interval about the Y axis between the dotted lines represents the true value of Y with 95 percent confidence band.

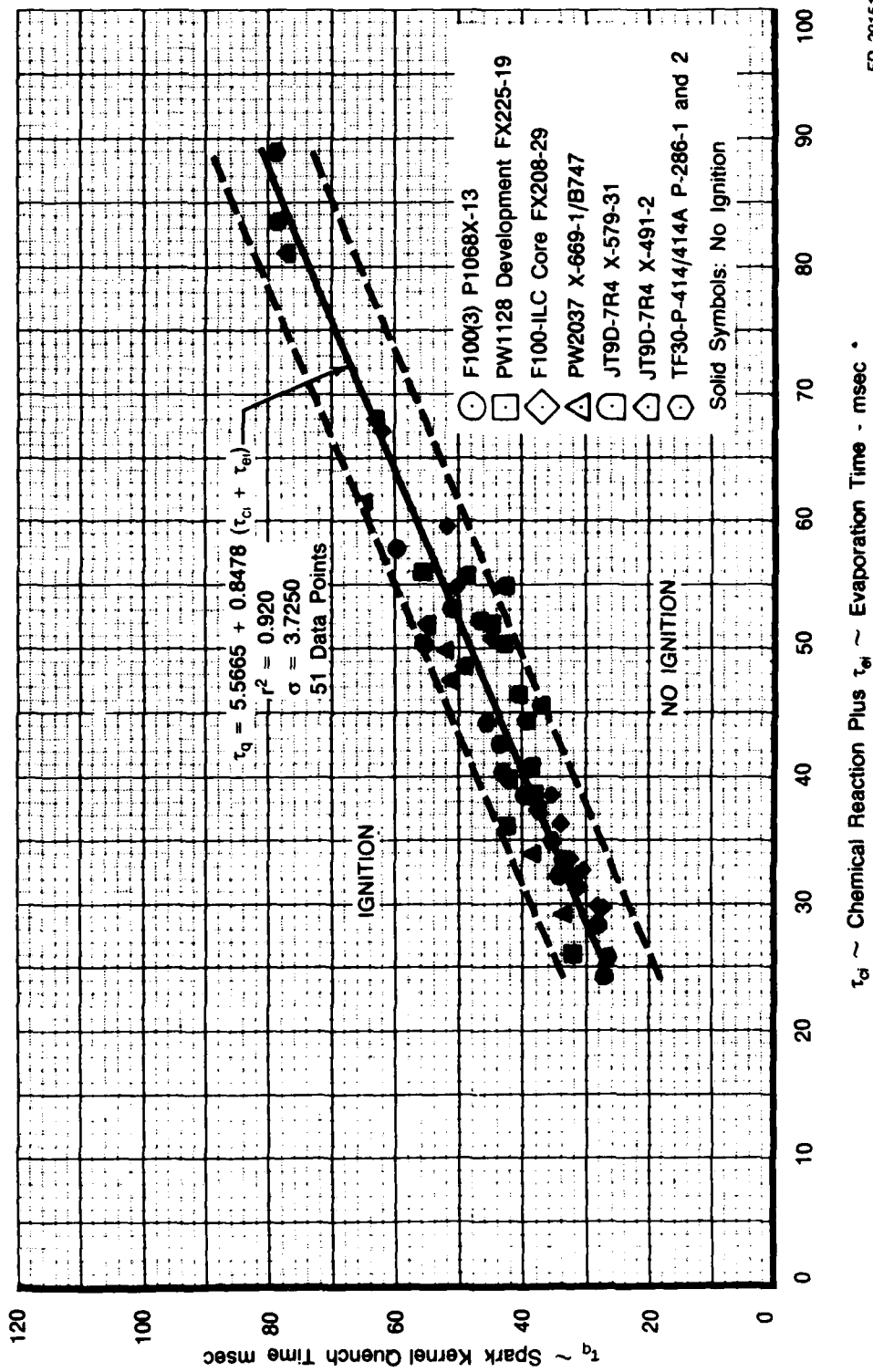
The correlation models are valid over a wide range of combustor operating conditions which include pressures from 0.2 to 1.0 atm, primary zone velocity of 5 to 40 ft/sec, Sauter mean diameter of 30 through 180 microns, primary zone equivalence ratio of 0.4 to 2.8.

The evaporation and chemical reaction effects on windmill spark ignition limit are shown in Figures 5 and 6, respectively. Evaporation time is longer than chemical reaction time. However, both physical processes are necessary to achieve a higher degree of correlation for the spark ignition model. While Figures 7 and 8 present the evaporation and chemical reaction effects on primary zone stability limit, comparison of these physical processes indicates longer chemical reaction time with little improvement in the degree of correlation for the primary zone flame stabilization model.

The effects of flow parameter ($Wa_{pz} \sqrt{T_3/P_3}$) and primary zone velocity on spark kernel quench and volumetric hot residence times are shown in Figures 9, 10, 11, and 12, respectively. The figures imply that spark ignition and primary zone flame stabilization are impeded by increases in flow parameter and velocity in the primary zone. A significant finding is that advanced engines with increased air flow and reduced volume in the primary zone exhibit the lowest available spark quench and flow residence time for a specified flow parameter. Therefore, they require shorter evaporation plus chemical reaction time for a successful engine start. The adverse effect of an increase in flow parameter or velocity on the initial phase of spark kernel development (anchored to the electrodes) can be offset by an increase in minimum ignition energy. The same adverse effect on primary zone flame stabilization can be offset by an increase in the primary zone volume and/or decrease in primary zone airflow.

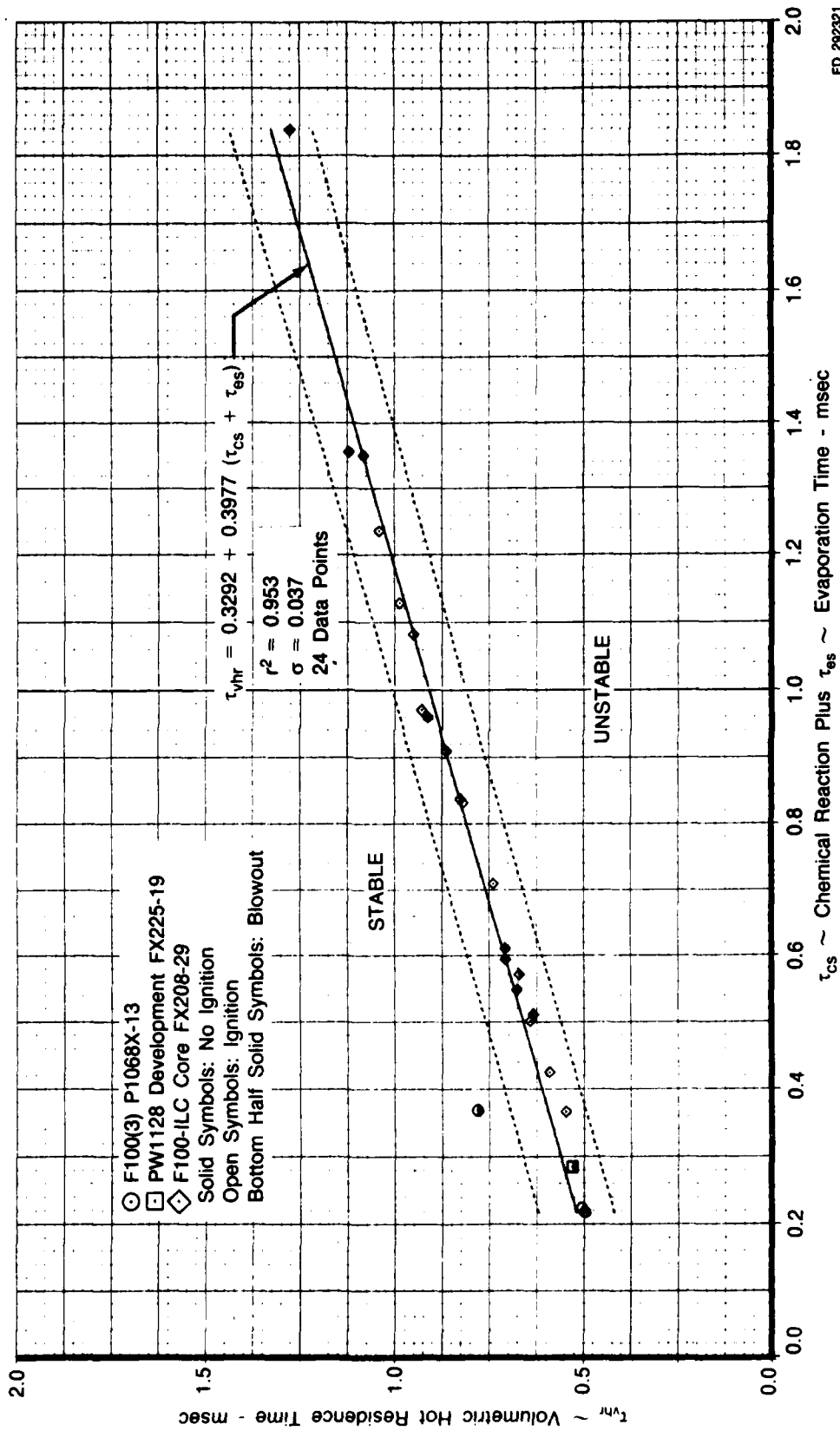
One of the most significant parameters which influence both evaporation and chemical reaction time for spark ignition, and chemical reaction time for primary zone flame stabilization is the root mean square of the fluctuating velocity component (u'). In this study, u' is proportional to the square root of the combustor pressure drop and inlet air density (see Section II). The beneficial effect of an increase in u' on spark ignition arises because evaporation plus chemical reaction time is reduced as shown in Figures 13 and 14. Thus, less spark kernel quench time is required for successful ignition. However, offsetting this advantage is the turbulent diffusion heat loss suffered by the spark kernel as it becomes detached and enters the recirculation zone, which reduces available spark kernel quench time. Figures 15 and 16 present similar beneficial effects of u' and combustor pressure drop on evaporation plus chemical reaction time for the phenomena of flame stabilization. The adverse effect of u' on primary zone stability is due to the entrainment of additional fresh material into the recirculation zone, which reduces available flow residence time for evaporation and chemical reaction.

An increase in Sauter mean diameter (SMD) adversely effects spark ignition and primary zone flame stabilization by increasing evaporation time. For higher values of SMD, the fuel is not fully evaporated. Therefore, additional fuel is required to ignite and maintain combustion as shown in Figure 17.



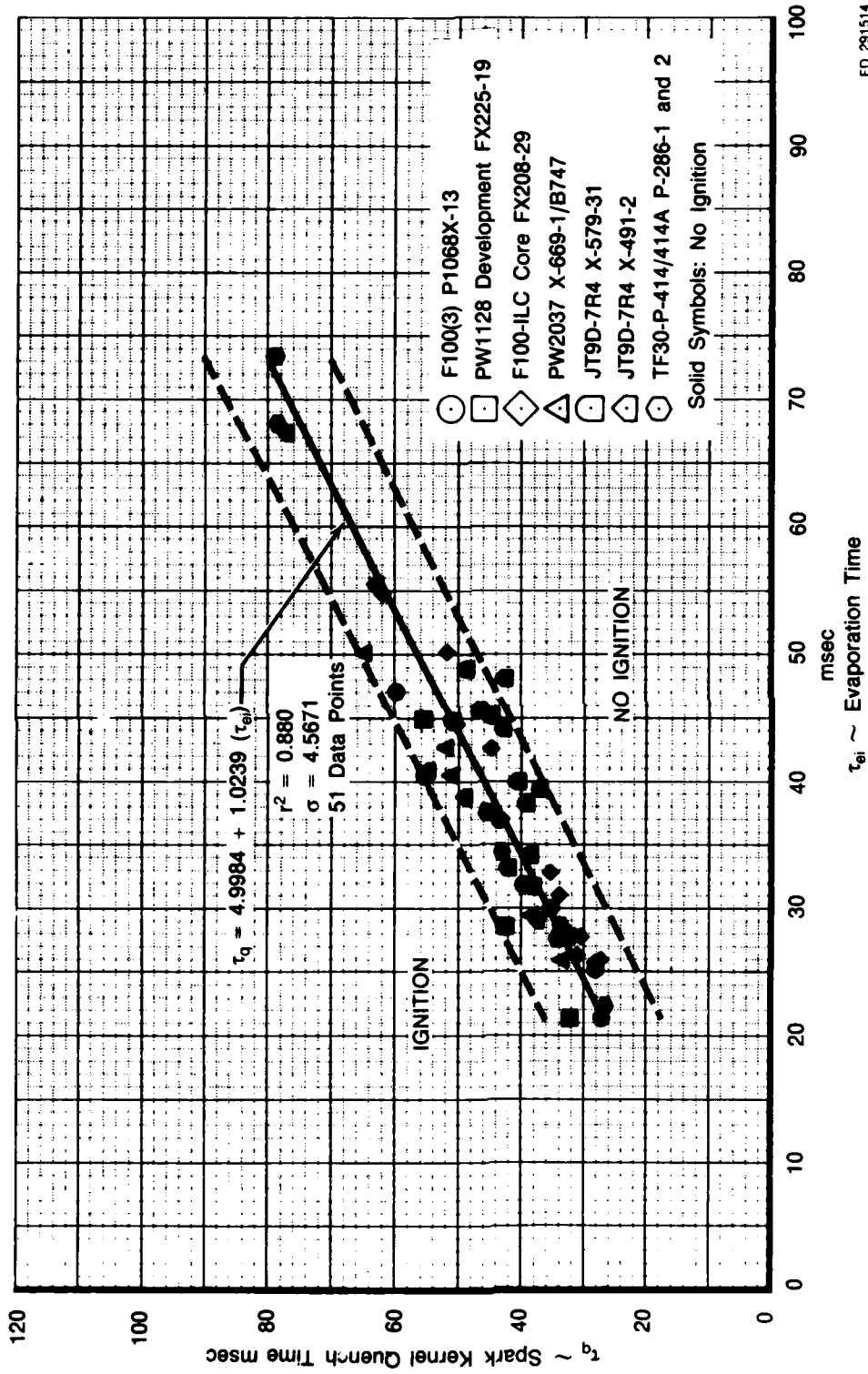
FD 291512

Figure 3. — Chemical Reaction Plus Evaporation Effects on Windmill Ignition Limit



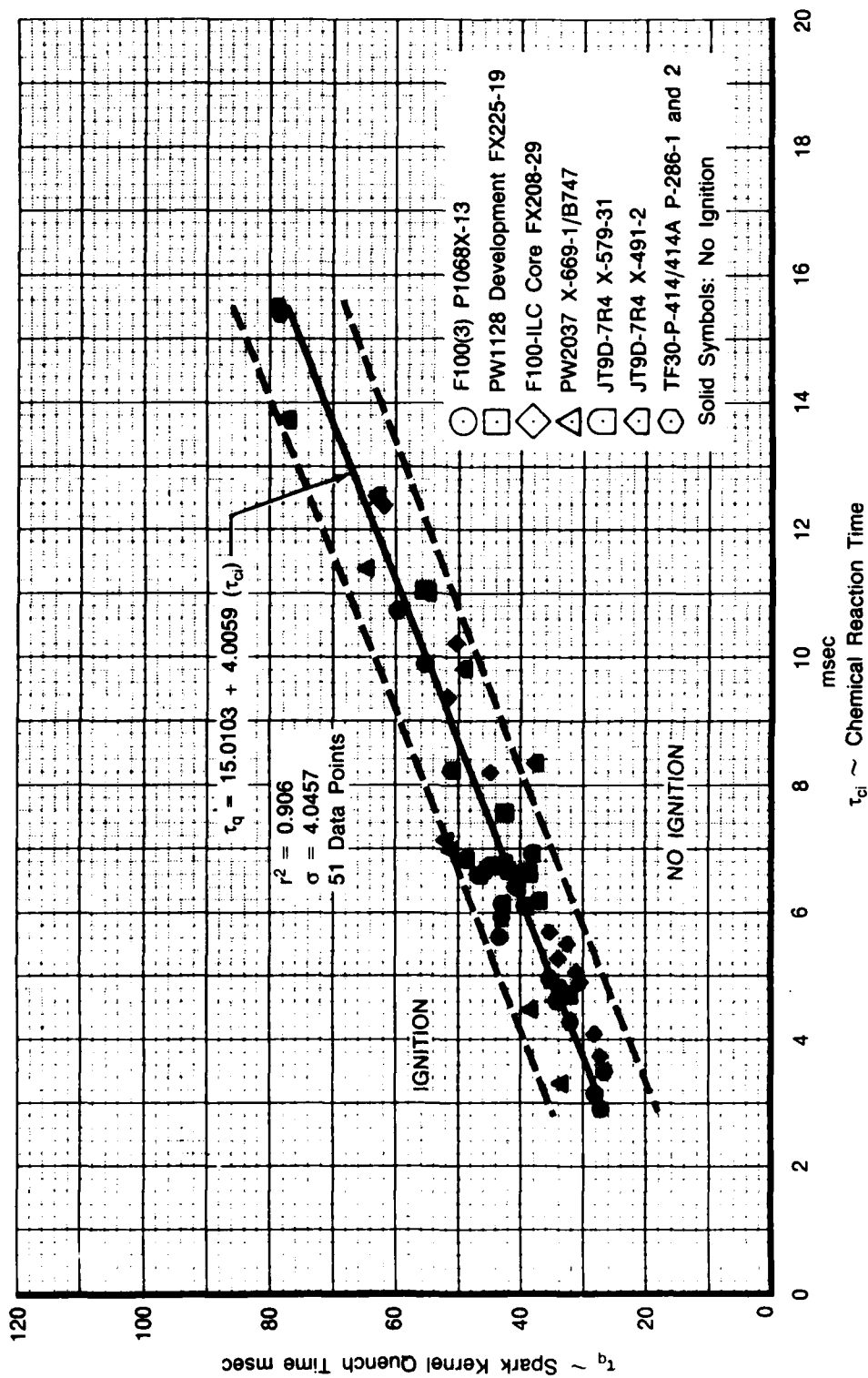
FD 202321

Figure 4. — Chemical Reaction Plus Evaporation Effects on Primary Zone Stability Limit During Windmill Ignition



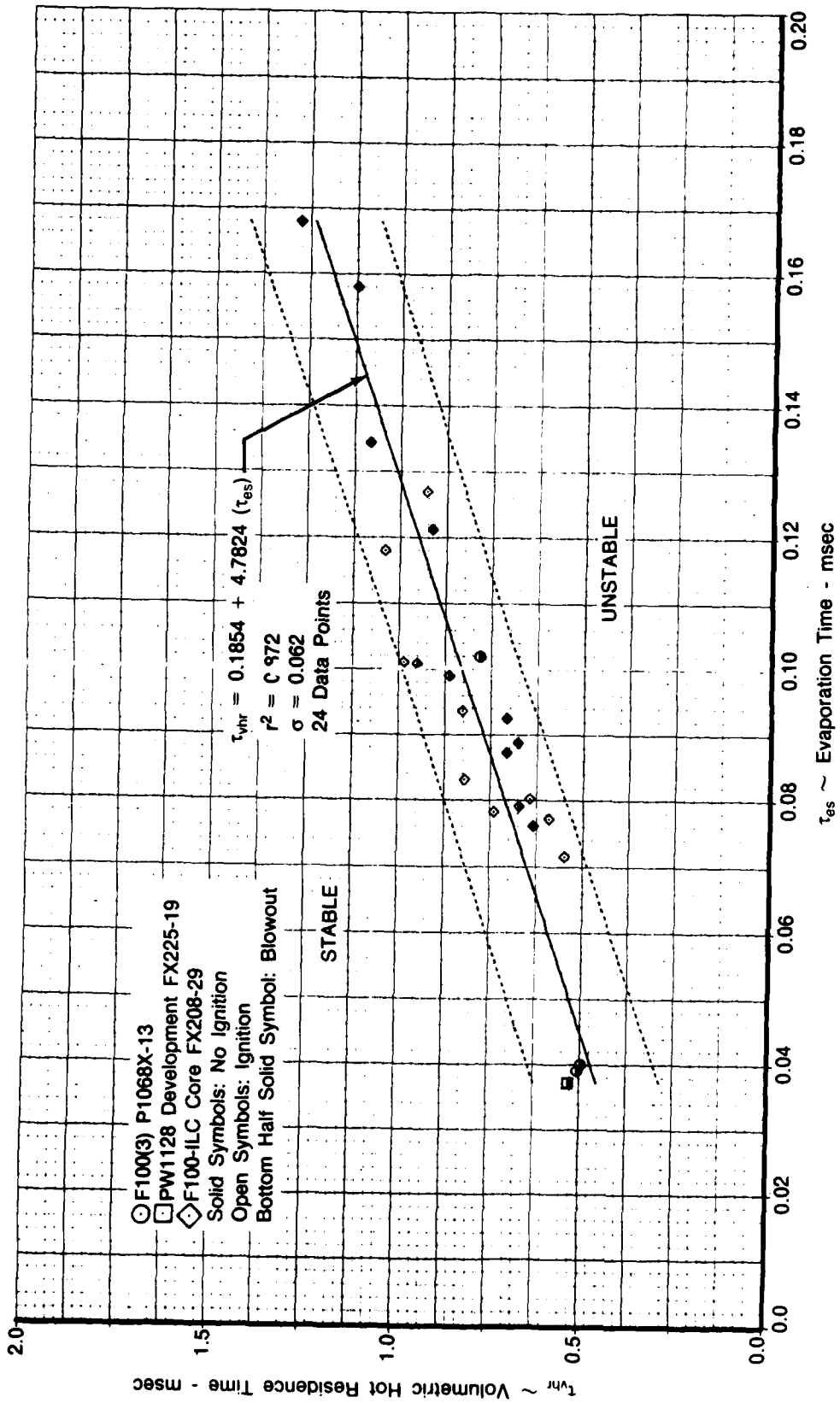
FD 291514

Figure 5. — Evaporation Effects on Windmill Ignition Limit



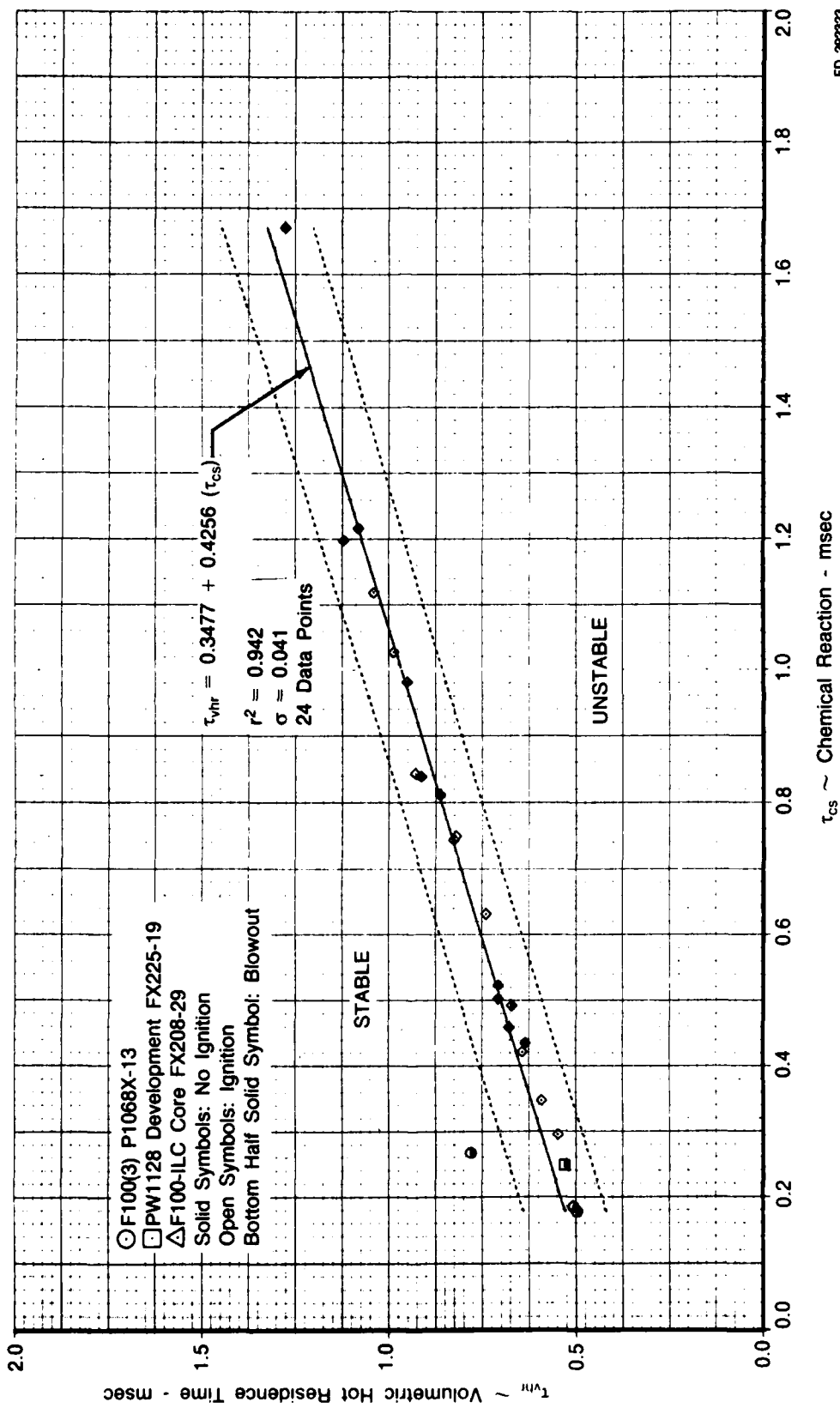
FD 291513

Figure 6. — Chemical Reaction Effects on Windmill Ignition Limit



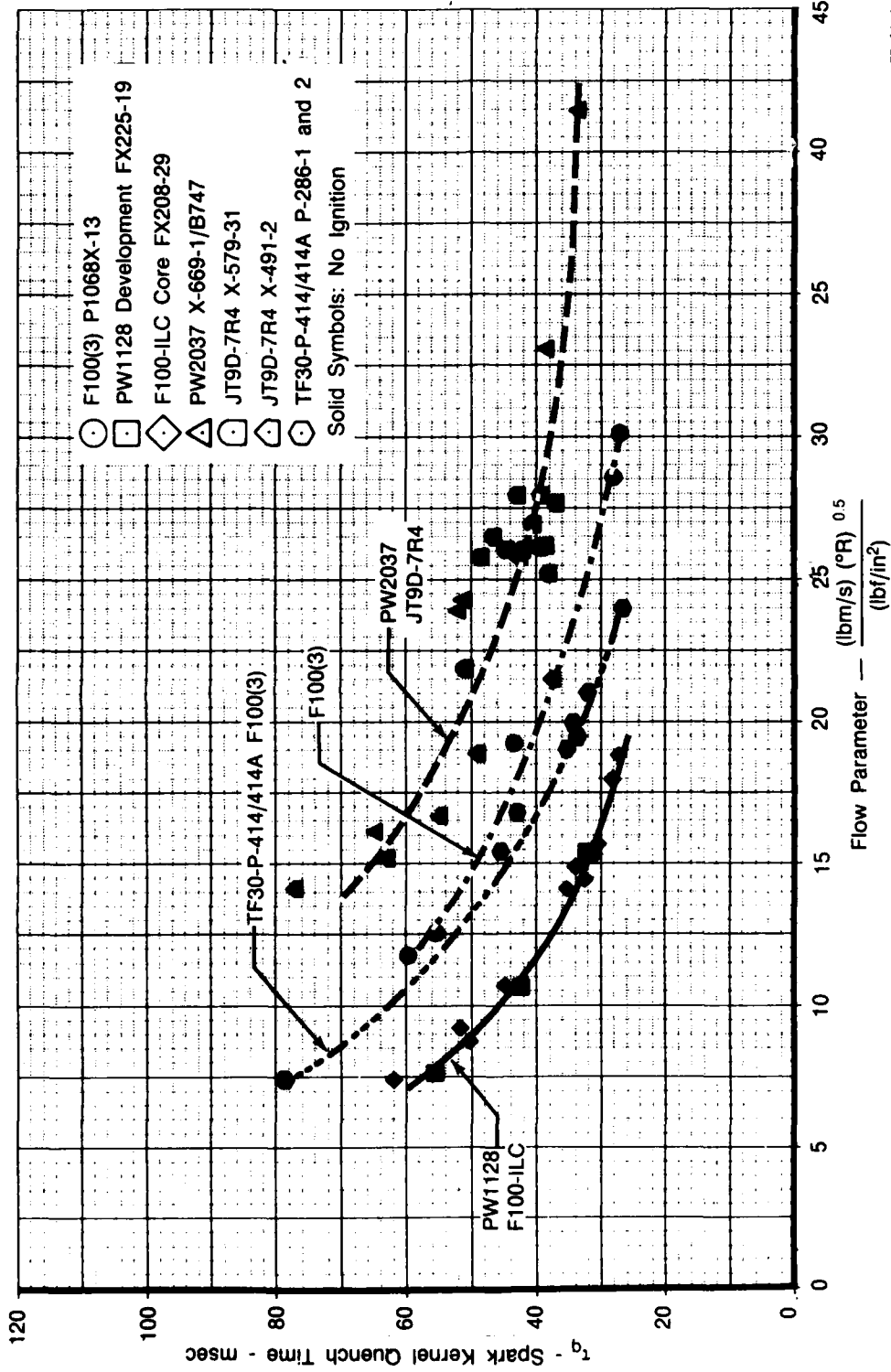
FD 282322

Figure 7. — Evaporation Effects on Primary Zone Stability Limit During Windmill Ignition



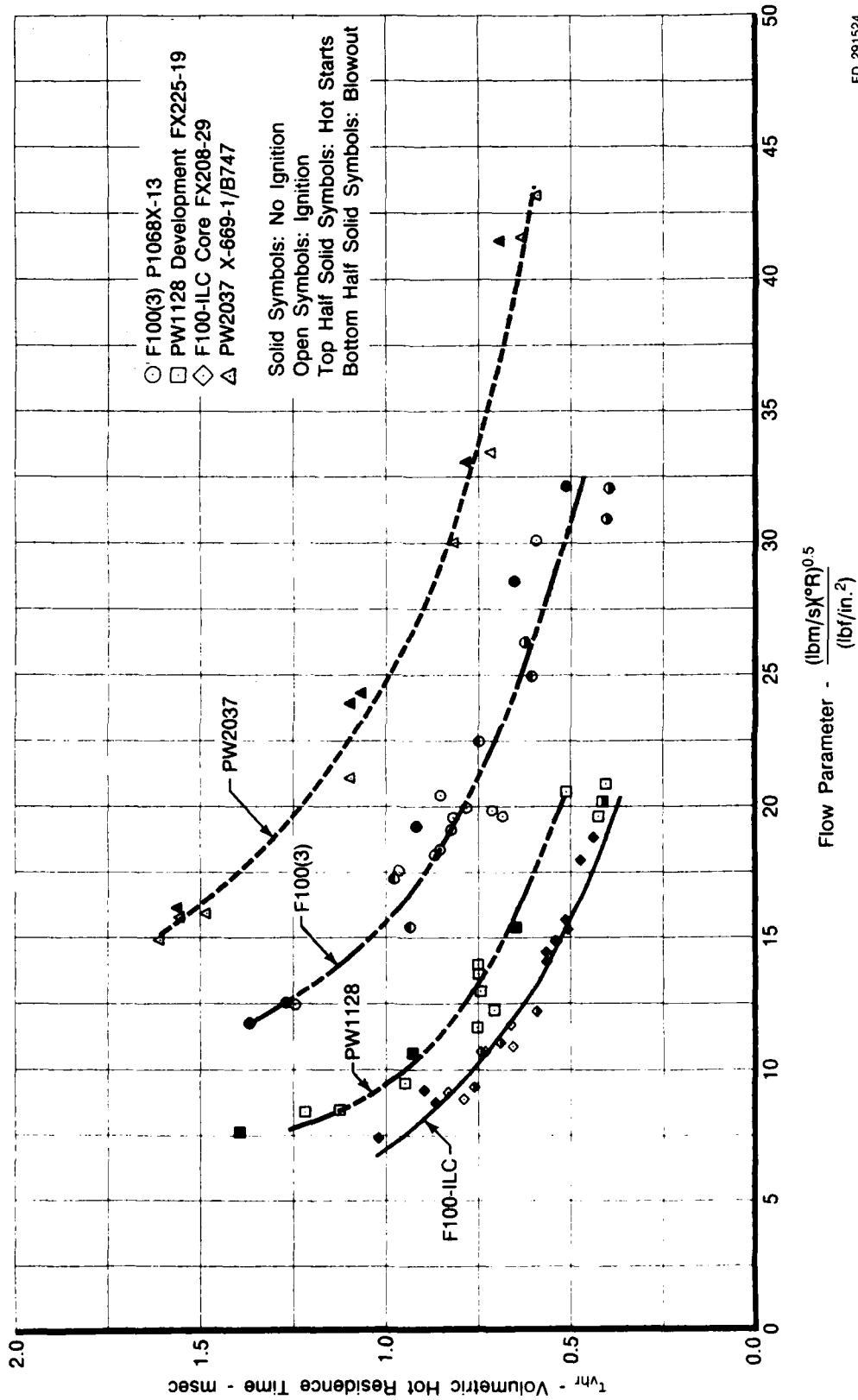
FD 262323

Figure 8. — Chemical Reaction Effects on Primary Zone Stability During Windmill Ignition



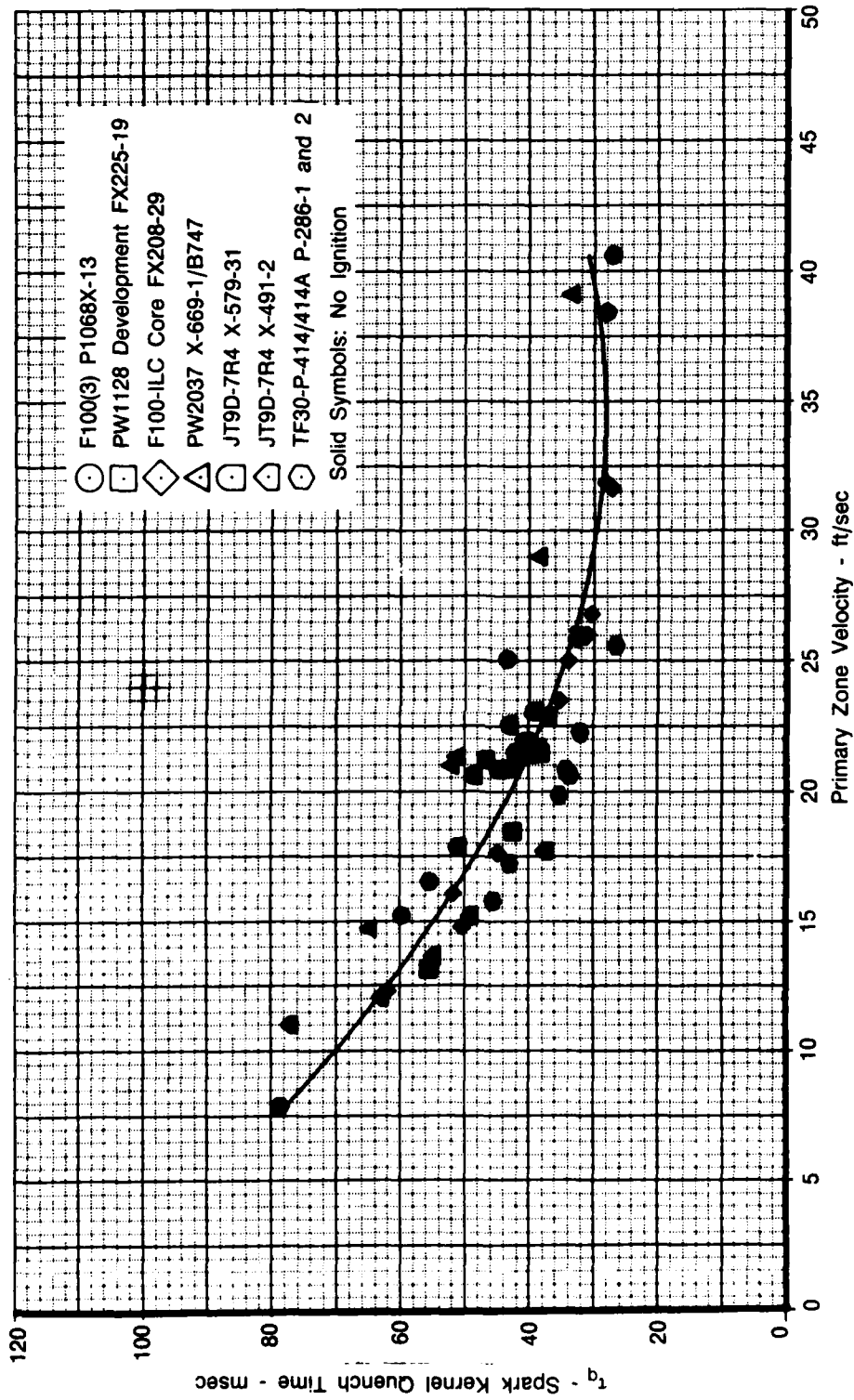
FD 291515

Figure 9. — Effect of Flow Parameter on Spark Kernel Quench Time During Windmill Ignition



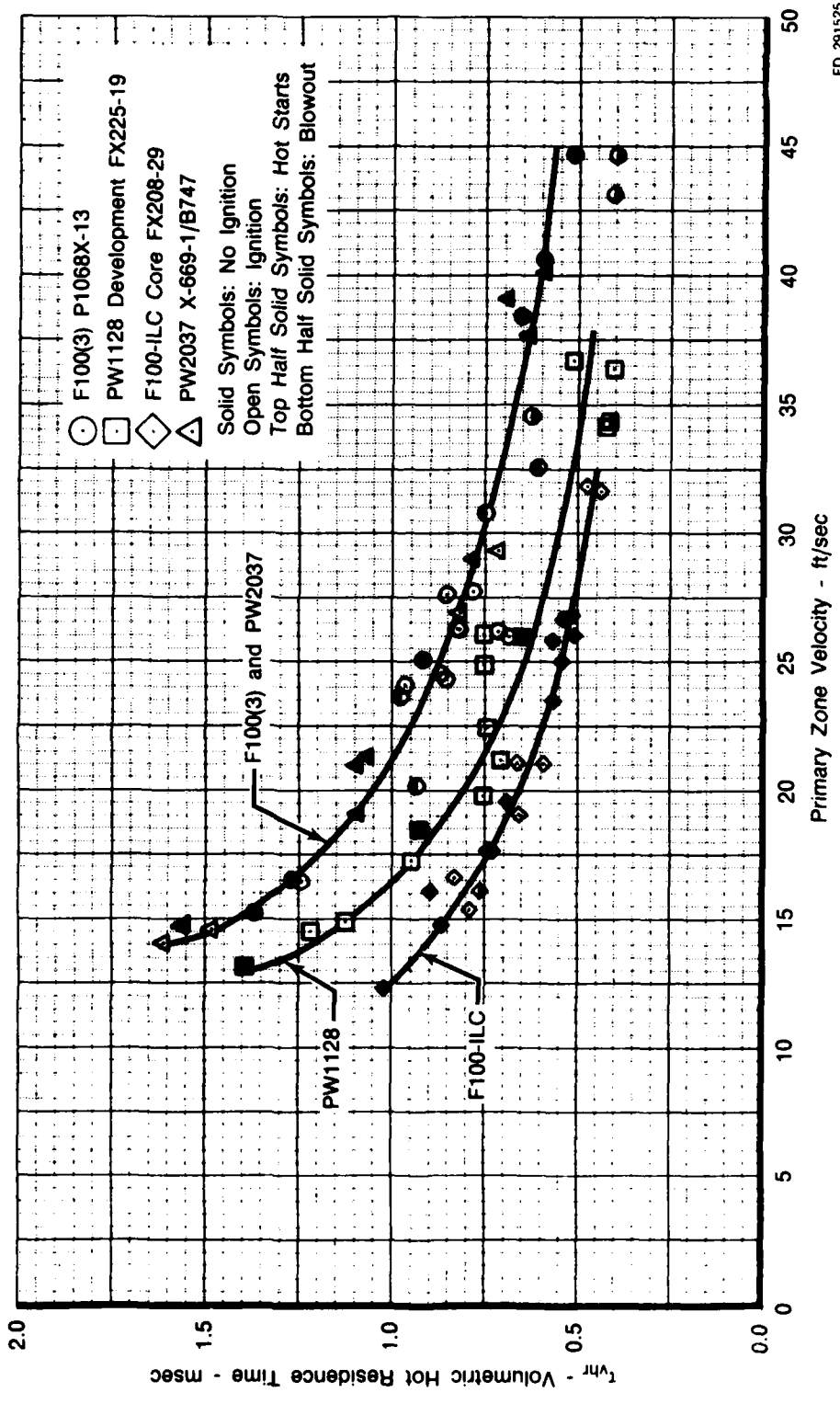
FD 291524

Figure 10. — Effect of Flow Parameter on Volumetric Hot Residence Time During Windmill Ignition



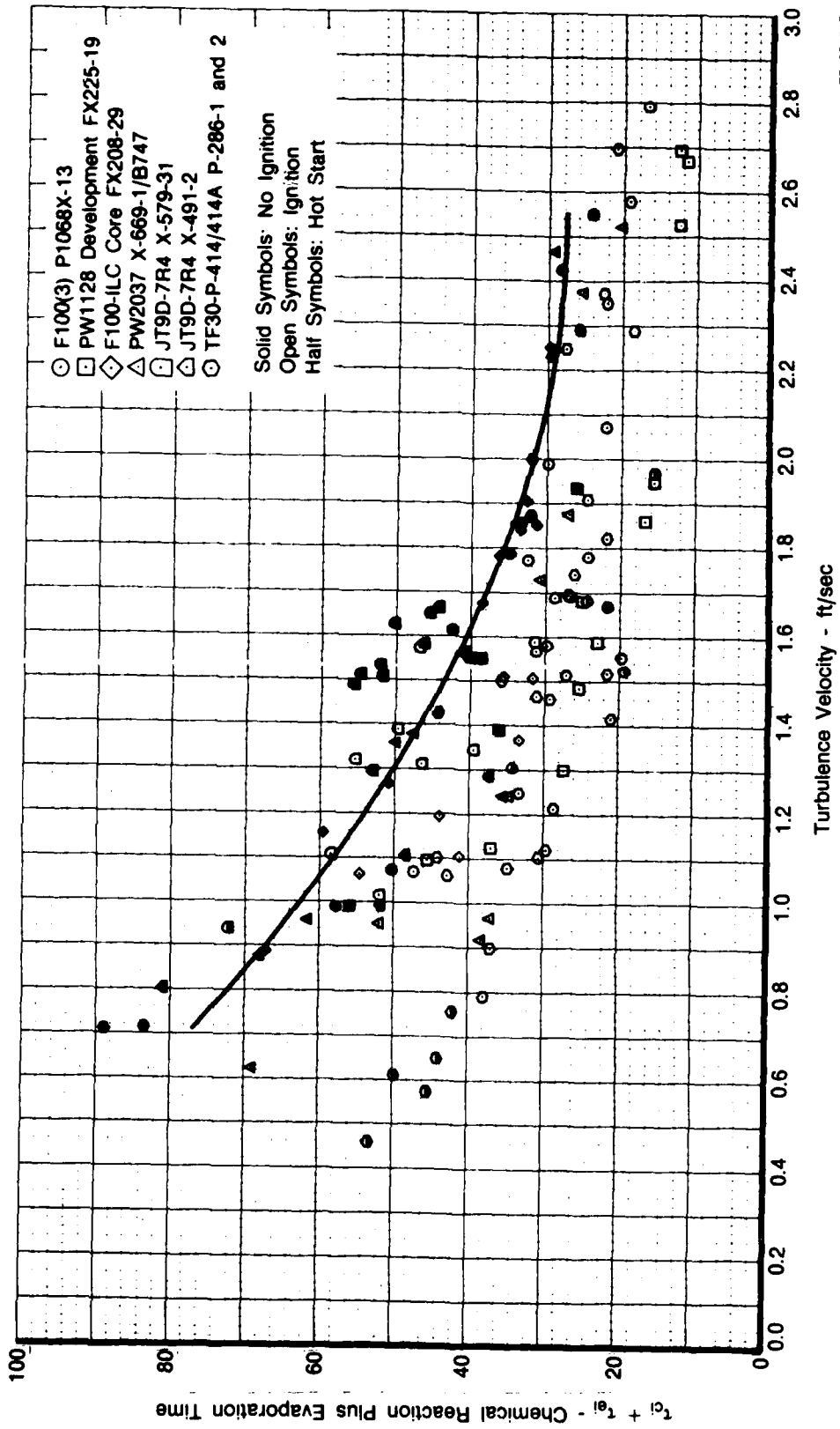
FD 291516

Figure 11. — Effect of Primary Zone Velocity on Spark Kernel Quench During Windmill Ignition



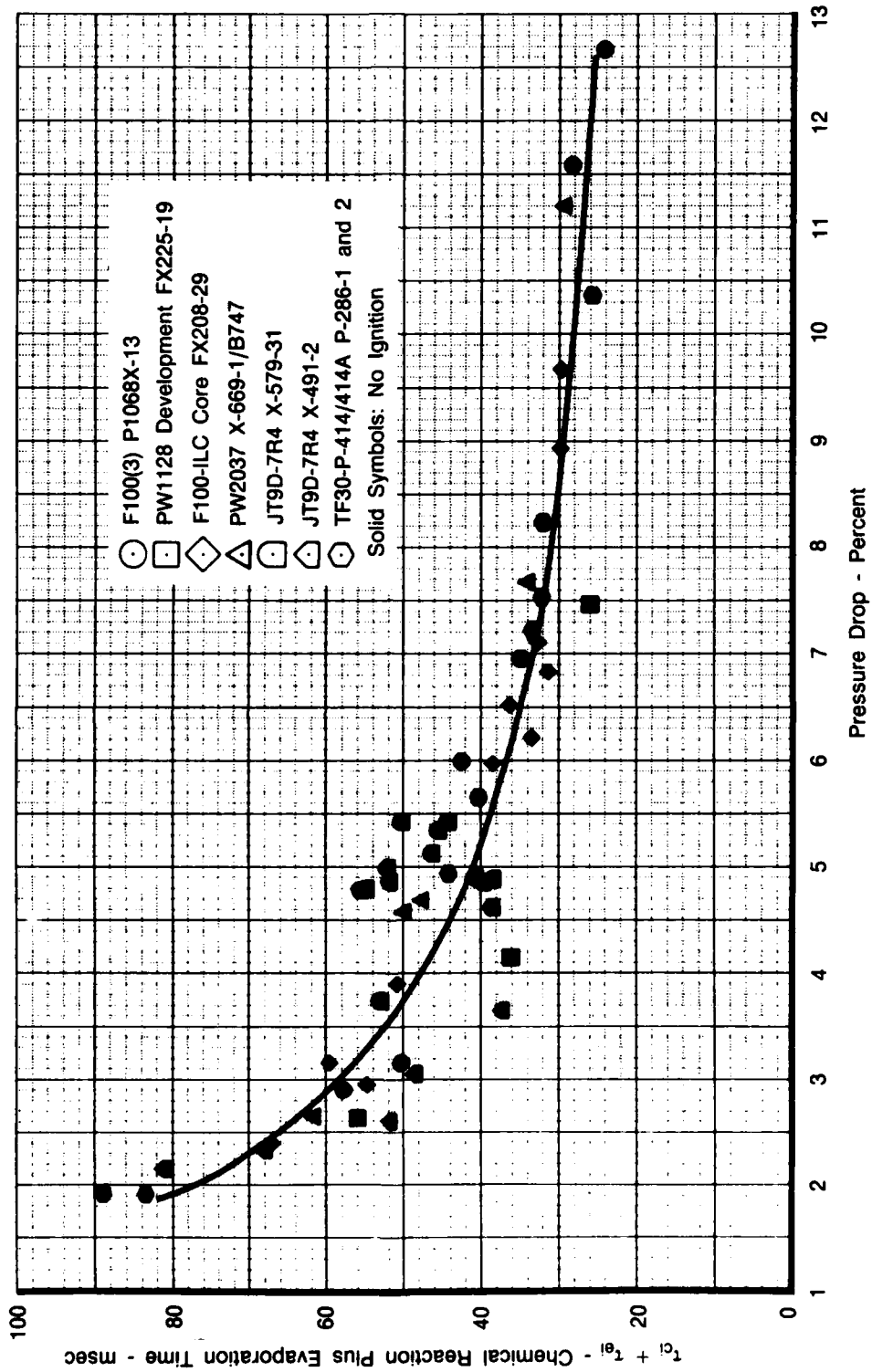
FD 291525

Figure 12. — Effect of Primary Zone Velocity on Volumetric Hot Residence Time During Windmill Ignition



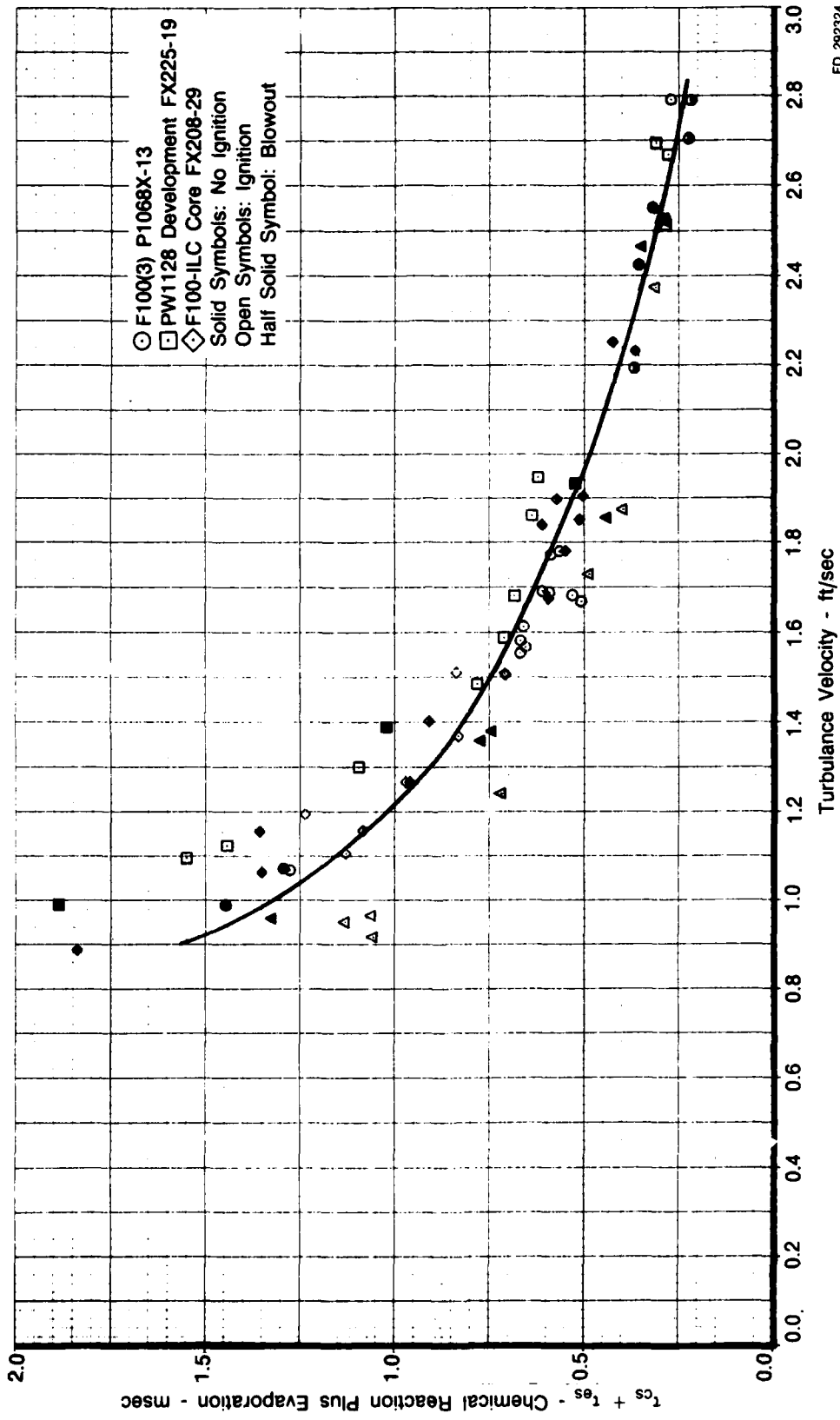
FD 291517

Figure 13. — Effect of Root Mean Square Turbulent Velocity Effect on Windmill Ignition Limit



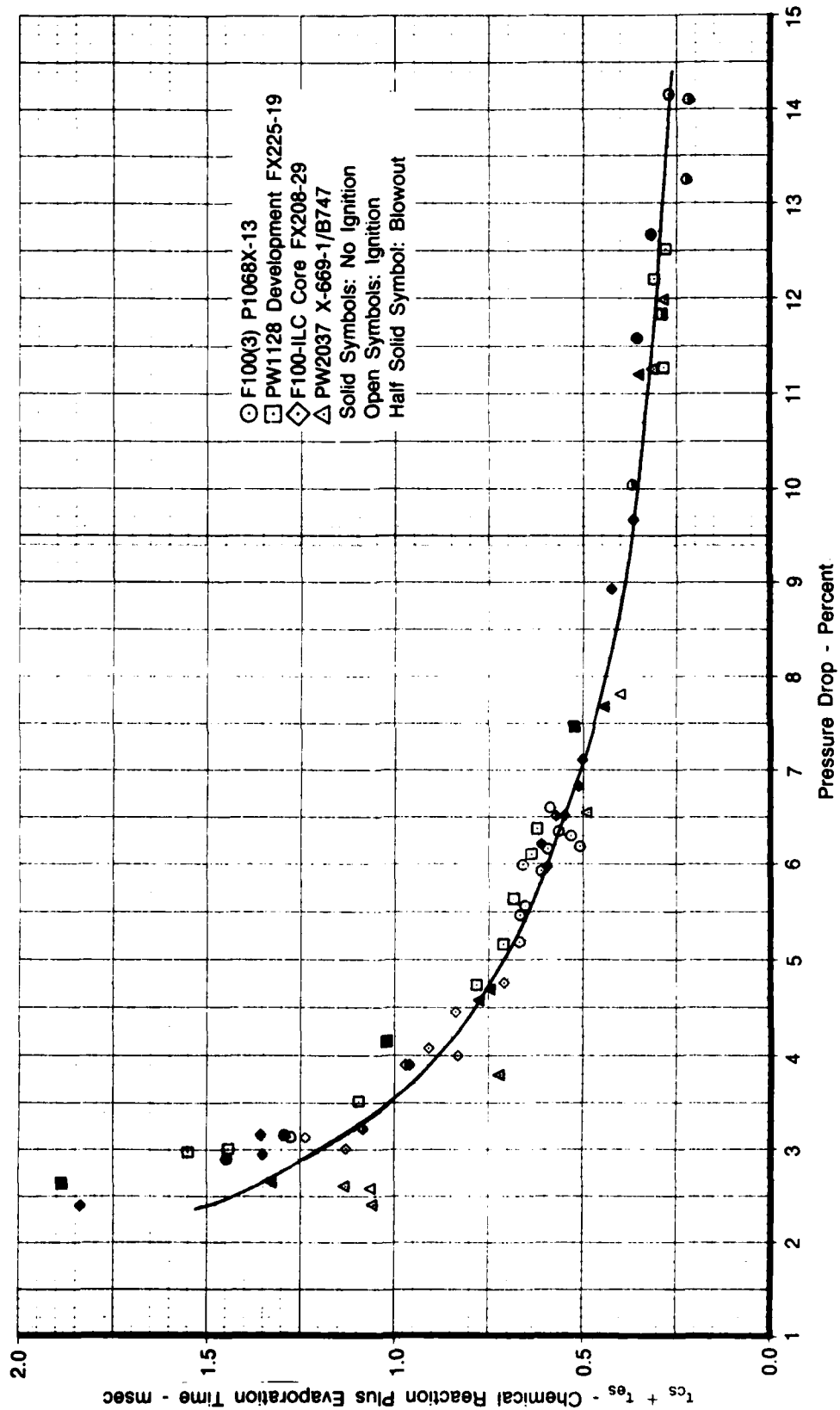
FD 291518

Figure 14. — Effect of Combustor Pressure Drop on Windmill Ignition Limit



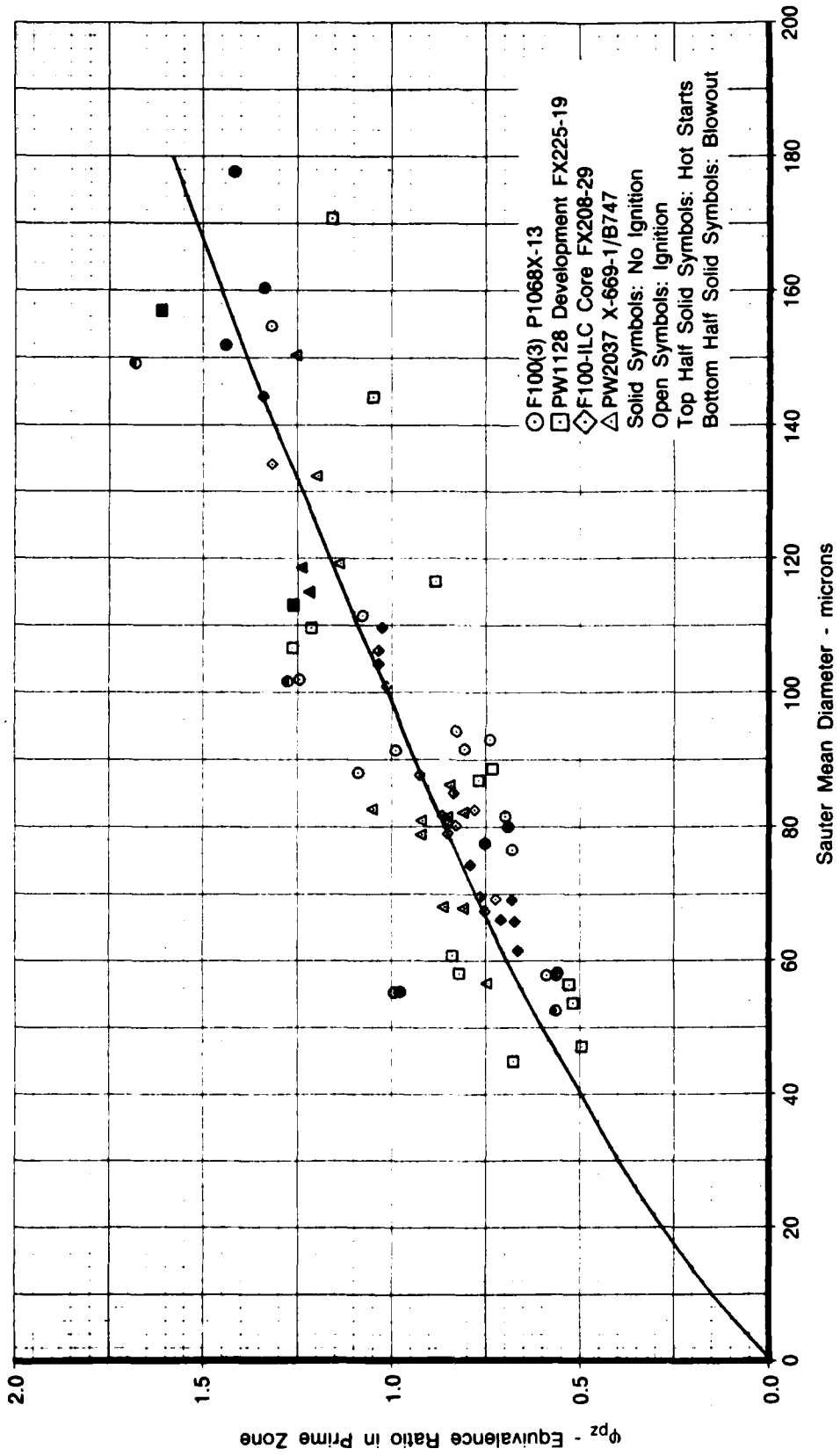
FD 292324

Figure 15. — Effect of Root Mean Square Turbulent Velocity Effect on Stability Limit During Windmill Ignition



FD 292325

Figure 16. — Effect of Combustor Pressure Drop Effect on Stability Limit During Windmill Ignition



FD 292326

Figure 17. — Effect of Sauter Mean Diameter on Windmill Ignition Limit

2. SPOOLDOWN IGNITION AND PRIMARY ZONE FLAME STABILIZATION

Although spooldown and windmill are different modes of ignition, the formulation of the characteristic time models for spark ignition and primary zone flame stabilization developed for windmill ignition were also applicable to spooldown ignition. In both cases, ignition must occur at low levels of combustor pressure with slightly higher inlet temperature during spooldown ignition. The most significant difference between windmill and spooldown modes is the engine operation prior to ignition. During windmill ignition, constant airflow is provided to the combustor, while during spooldown ignition, the air flow is continuously decreasing until ignition followed by engine acceleration occurs. Therefore, the spooldown ignition data must cross the stability and ignition limit at the time of ignition while the windmill ignition data can exist on either side of the limits.

The spooldown spark ignition and primary zone flame stabilization models were developed using F100(3) and PW1128 Development engine data (40 percent and 25 percent spooldown). Linear correlation models of spooldown spark ignition and primary zone stability limits were obtained. For the phenomena of spark ignition, the available spark kernel quench time has been correlated against the evaporation plus chemical reaction time with a coefficient of determination of 0.904 and standard deviation of 3.775 as shown in Figure 18. Also, for the phenomena of flame stabilization, the available volumetric hot residence time has been correlated against evaporation plus chemical reaction time with a coefficient of determination of 0.946 and standard deviation of 0.187 as shown in Figure 19. The models are valid over the entire range of conditions for which data were available.

Separate plots illustrating the effects of evaporation and chemical reaction time on spark kernel quench time and volumetric hot residence time, are shown in Figures 20 through 23. Both physical processes are necessary to achieve a higher degree of correlation for the phenomena of ignition and stabilization. However, evaporation time is longer for the spark ignition model while chemical reaction time is longer for the primary zone flame stabilization model.

The adverse effects of flow parameter and primary zone velocity on spark kernel quench time and volumetric hot residence time are shown in Figures 24 through 27. Similar results were also obtained with the windmill ignition data. Future engines show trends of decreasing spark ignition and stability limit with increasing flow parameter and primary zone velocity (increasing airflow and/or decreasing primary zone volume).

The adverse and beneficial effects of an increase in u' (increase pressure drop or inlet temperature) on spark ignition and flame stabilization limits were also observed with the spooldown data as shown in Figures 28 through 31. Similarly, for the results obtained with the windmill data, an increase in SMD requires higher equivalence ratio for successful ignition as shown in Figure 32.

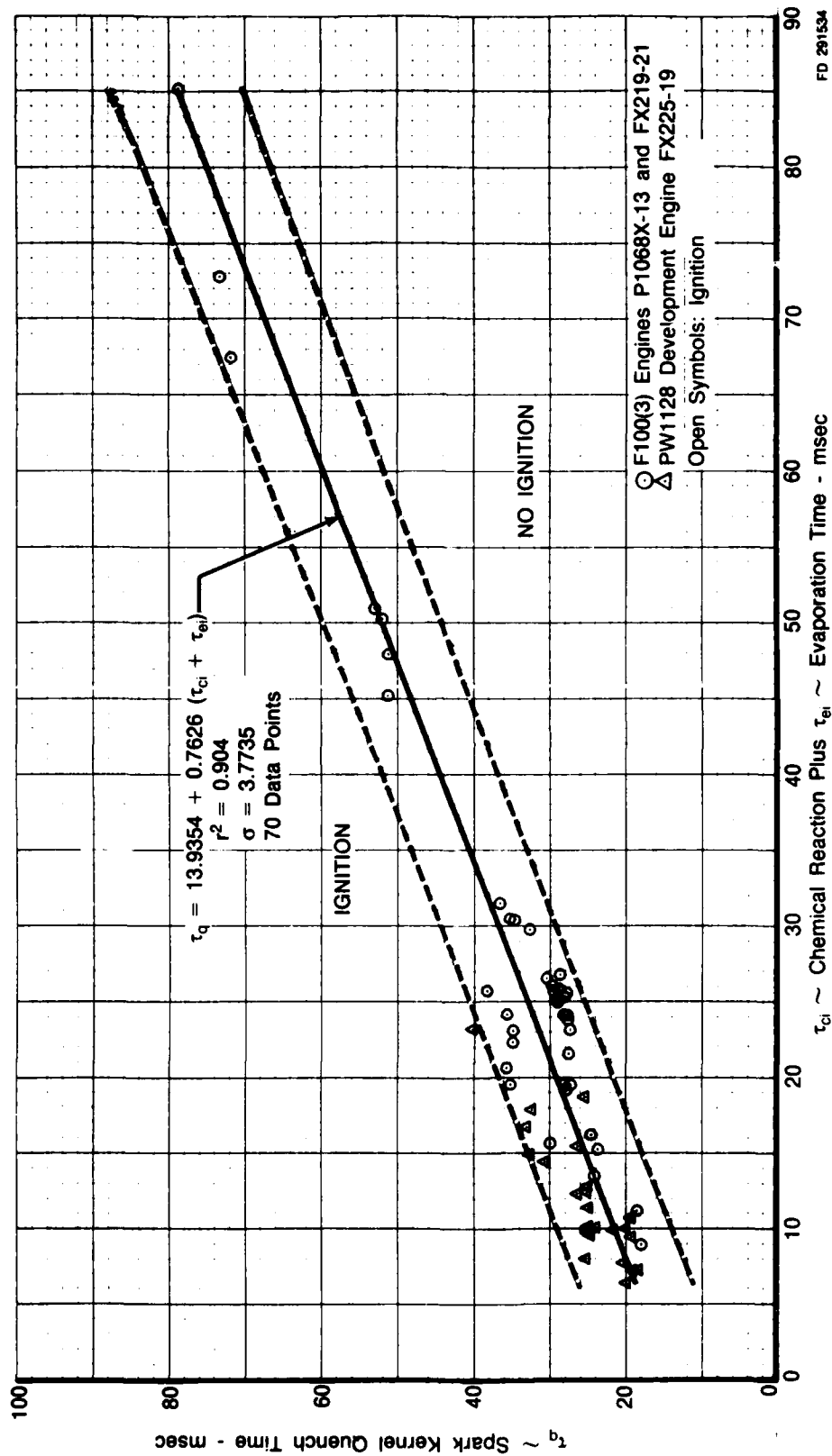


Figure 18. — Chemical Reaction Plus Evaporation Effects on Spooldown Ignition Limits

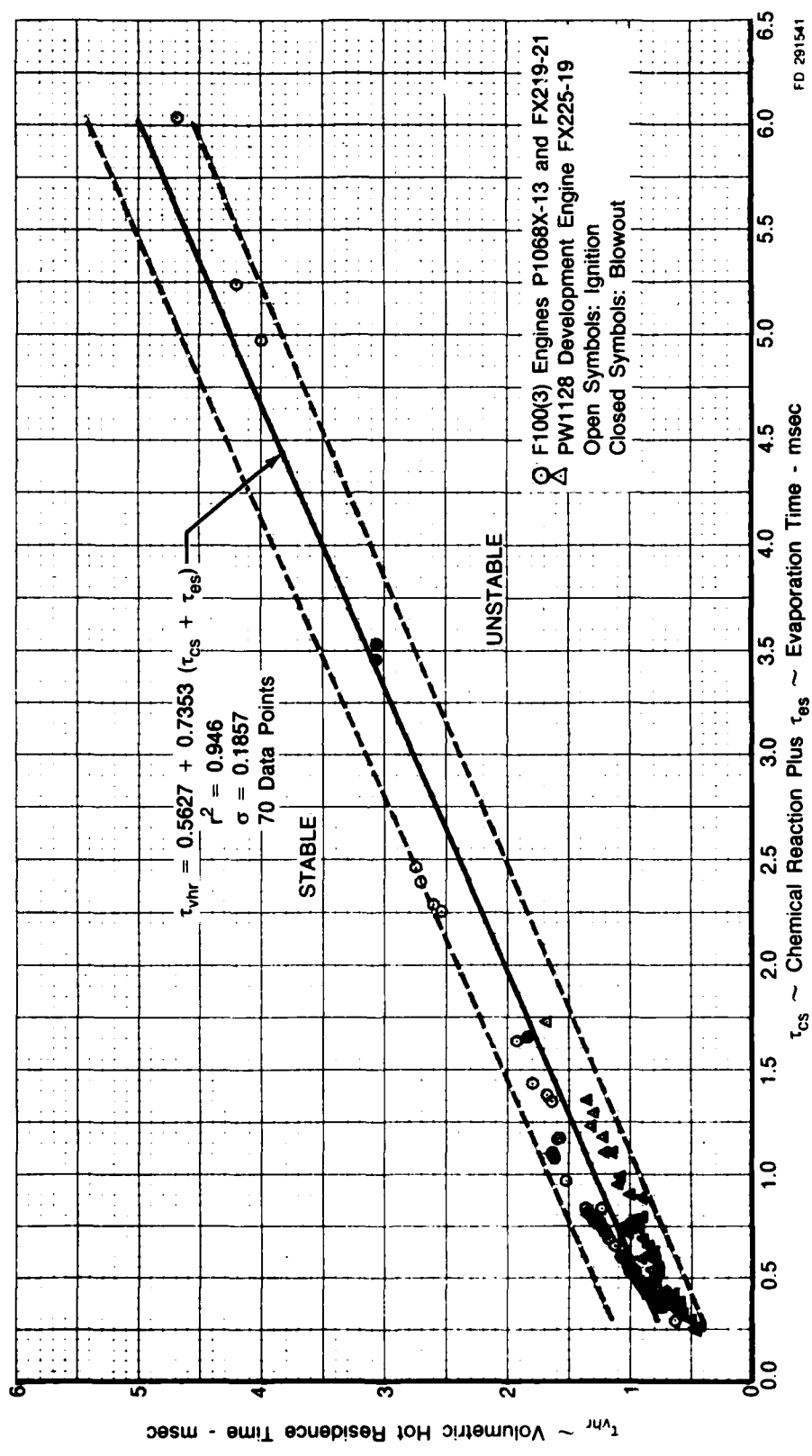
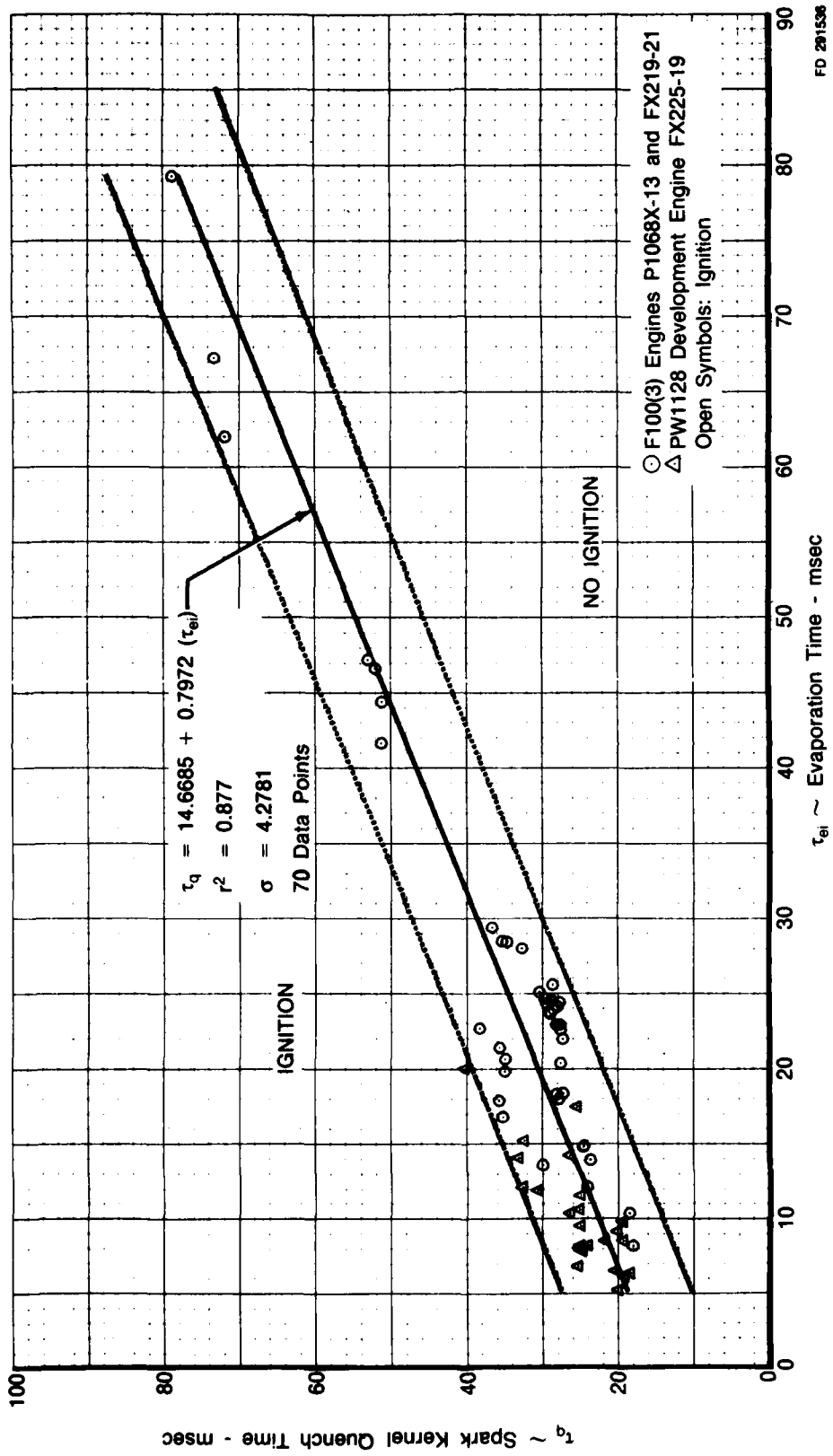


Figure 19. — Chemical Reaction Plus Evaporation Effects on Primary Zone Stability Limit During Spooldown Ignition



FD 291536

Figure 20. — Evaporation Effect on Spooldown Ignition Limit

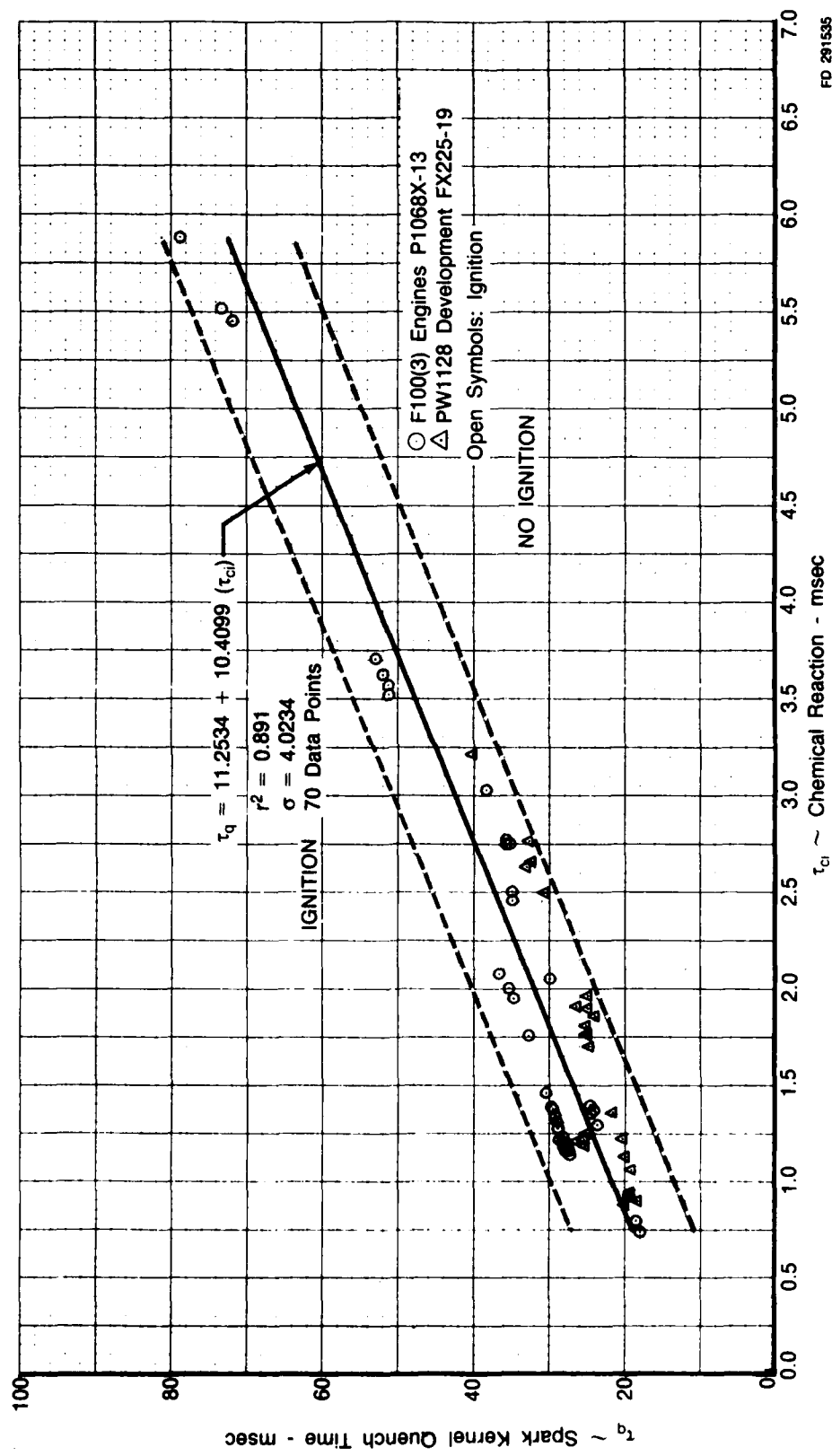


Figure 21. — Chemical Reaction Effect on Spooldown Ignition Limit

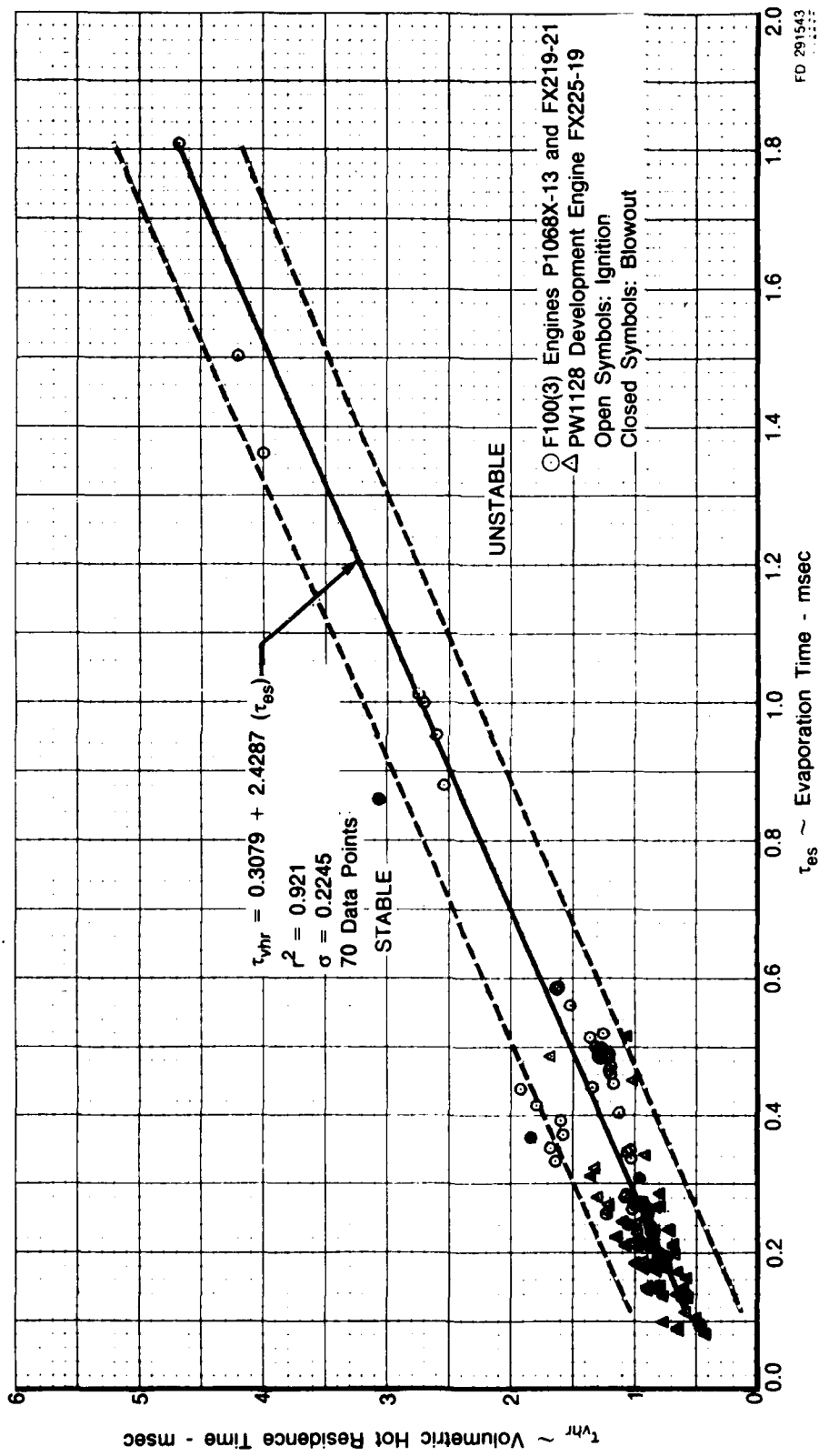


Figure 22. — Evaporation Effects on Primary Zone Stability Limit During Spooldown Ignition

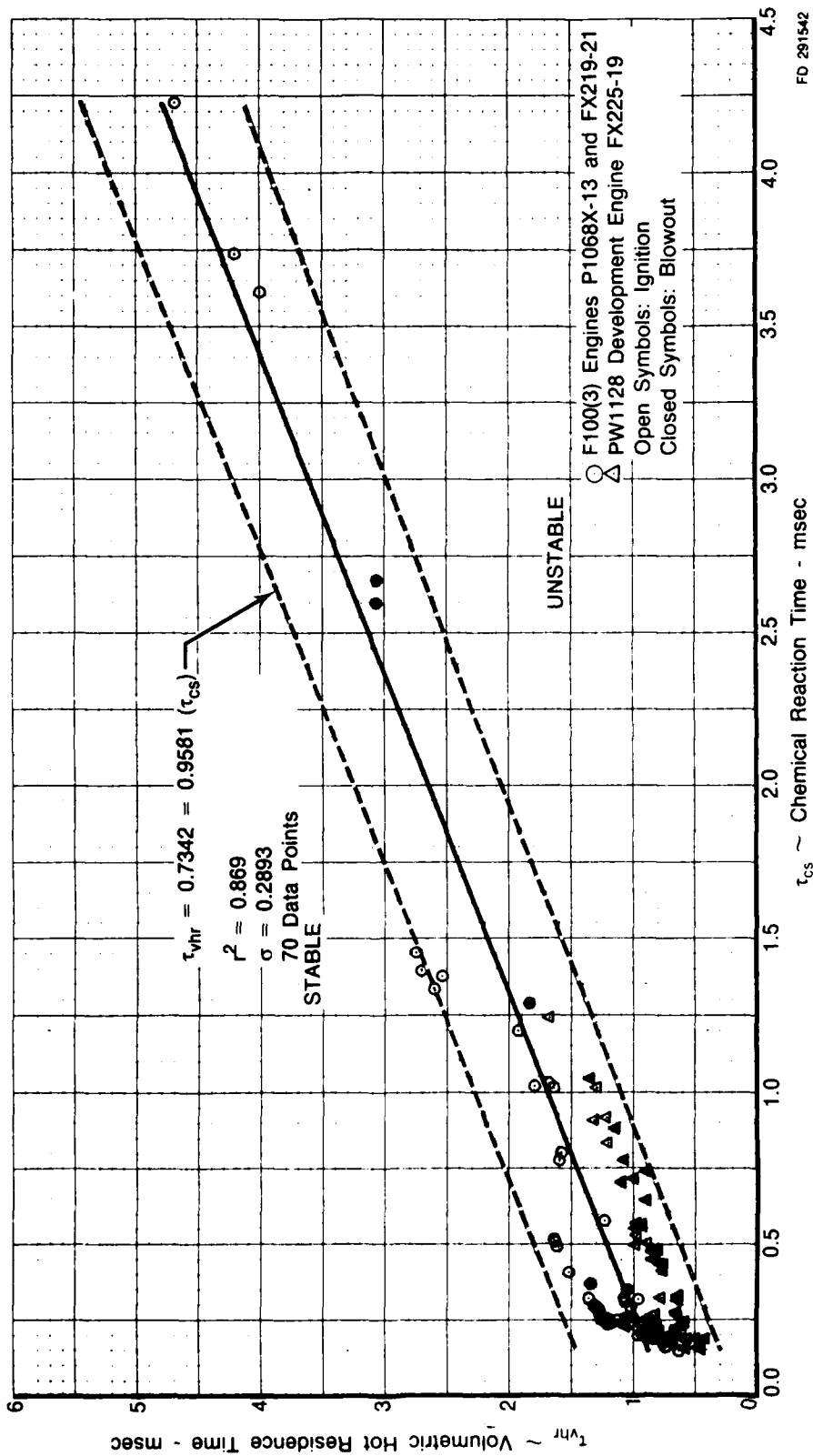
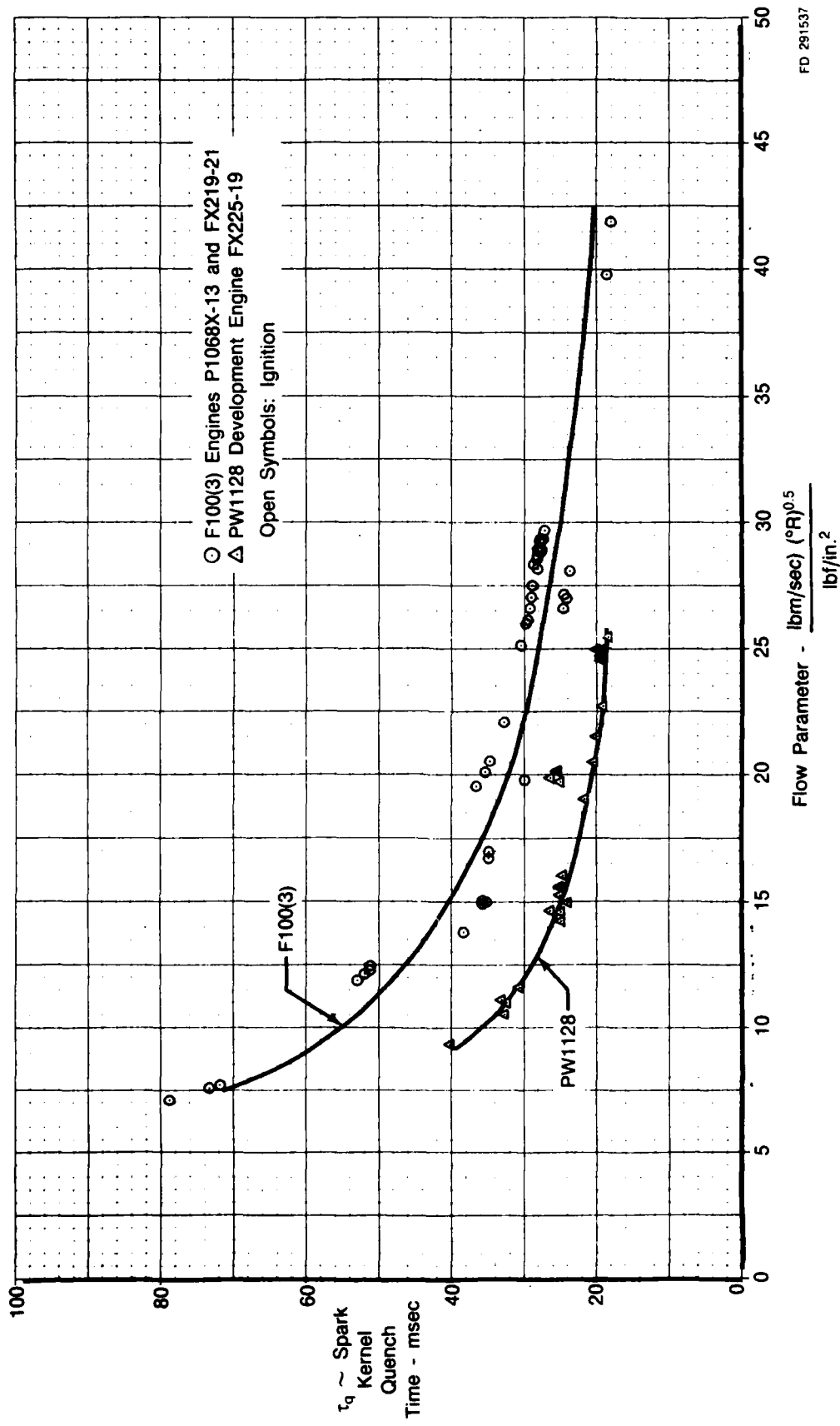
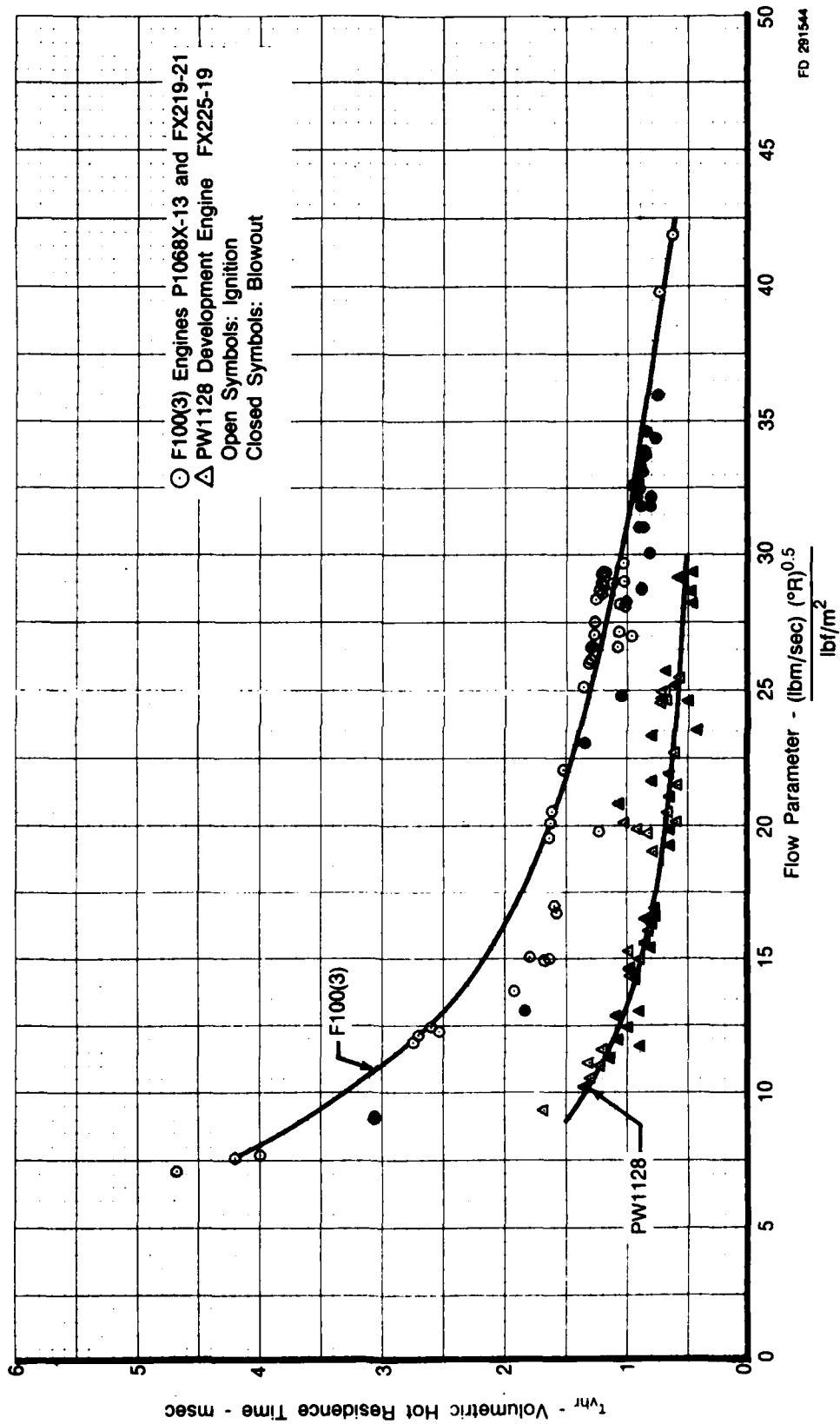


Figure 23. — Chemical Reaction Effects on Primary Zone Stability Limit During Spooldown Ignition



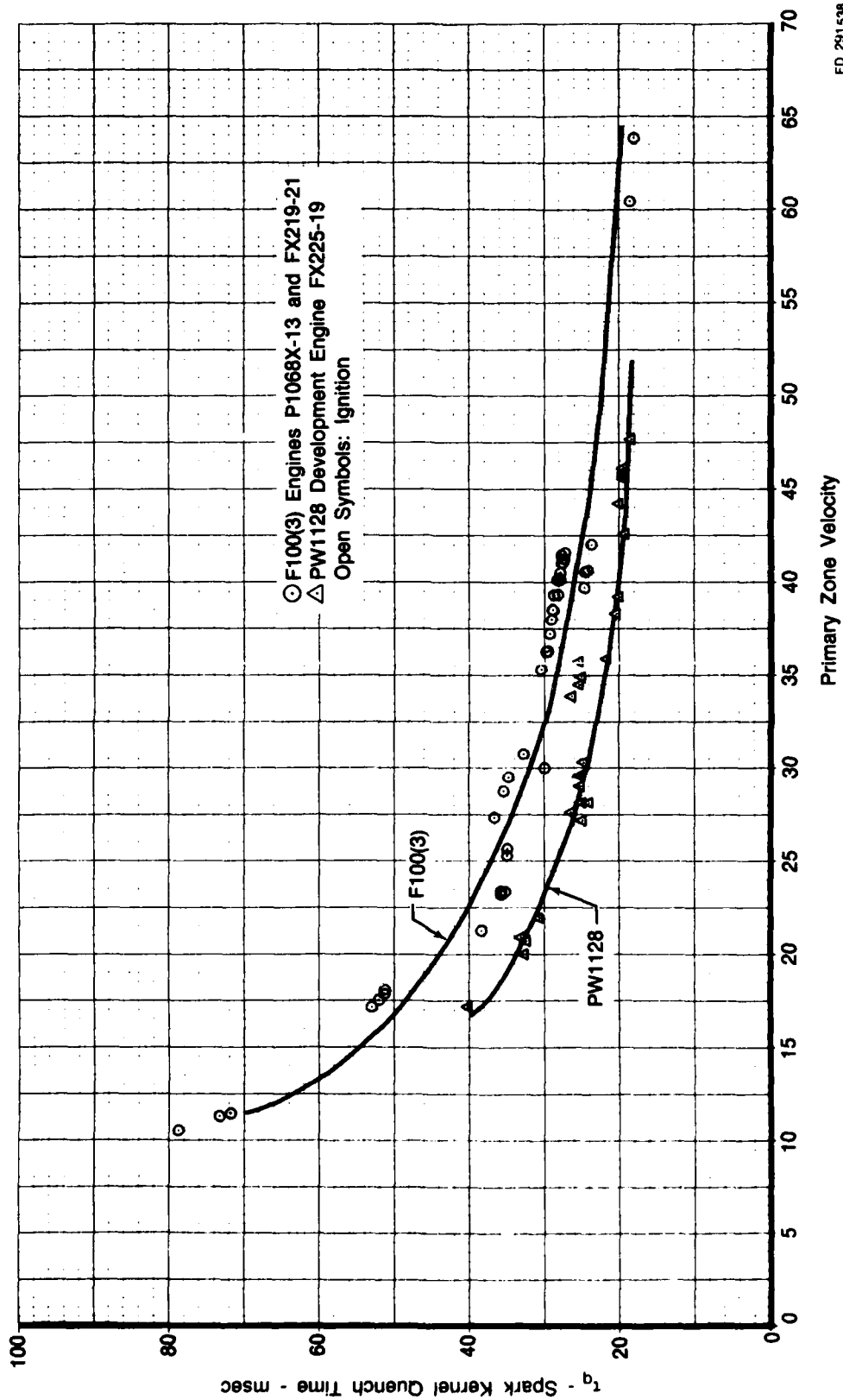
FD 291537

Figure 24. — Effect of Flow Parameter on Spark Kernel Quench During Spooldown Ignition



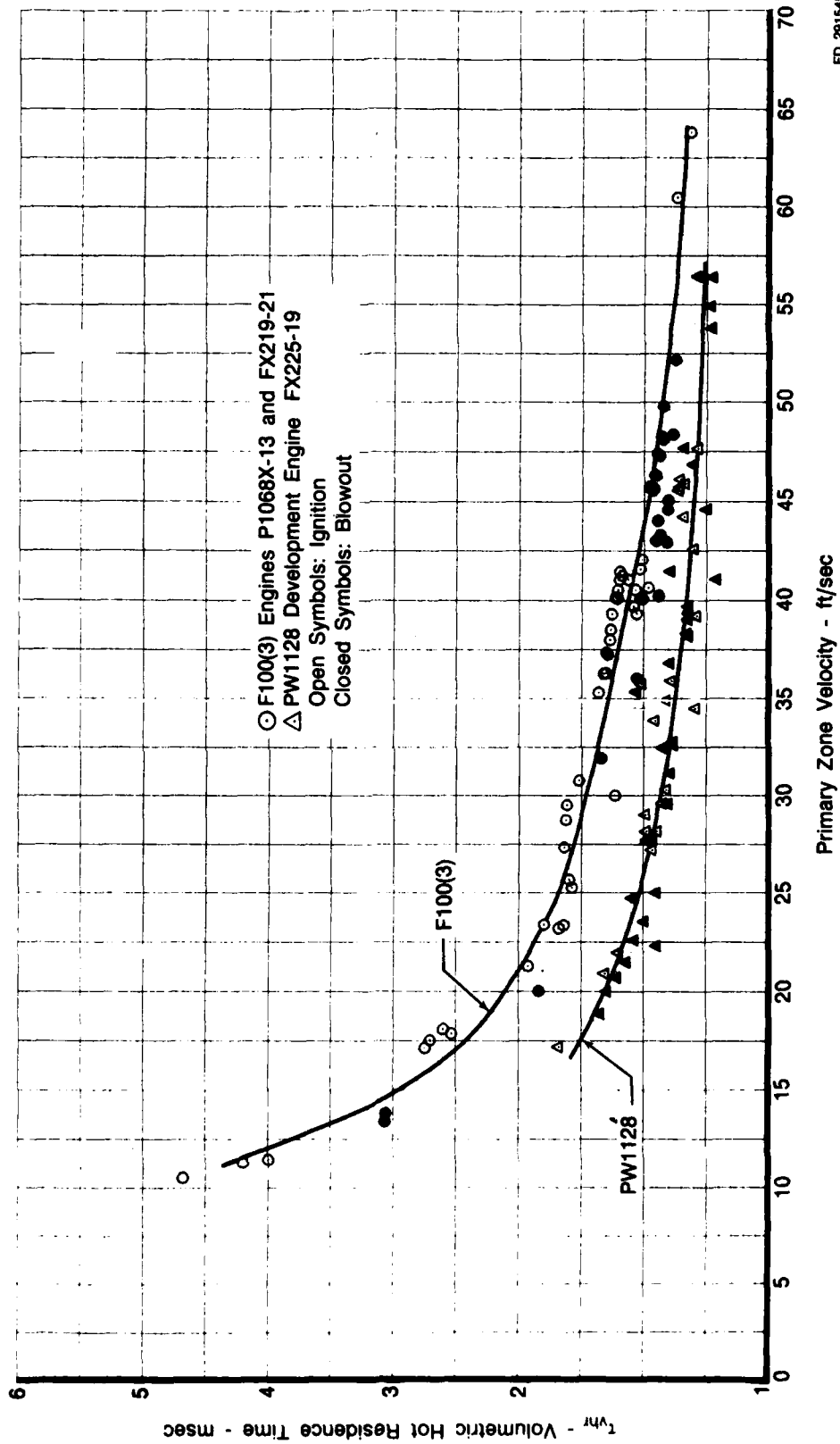
FD 281544

Figure 25. — Effect of Flow Parameter on Volumetric Hot Residence During Spooldown Ignition



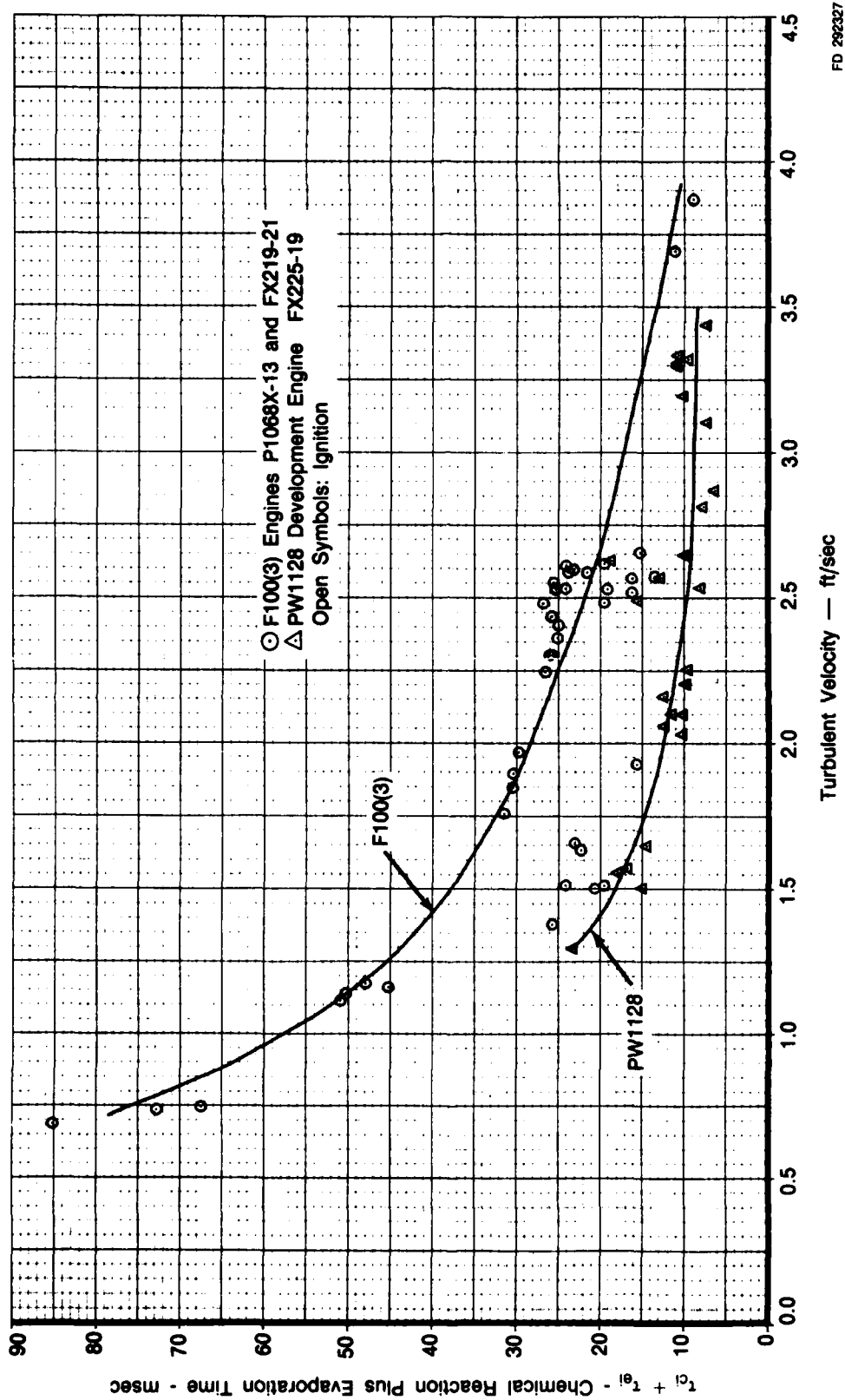
FD 291538

Figure 26. — Effect of Primary Zone Velocity on Spark Kernel Quench During Spooldown Ignition



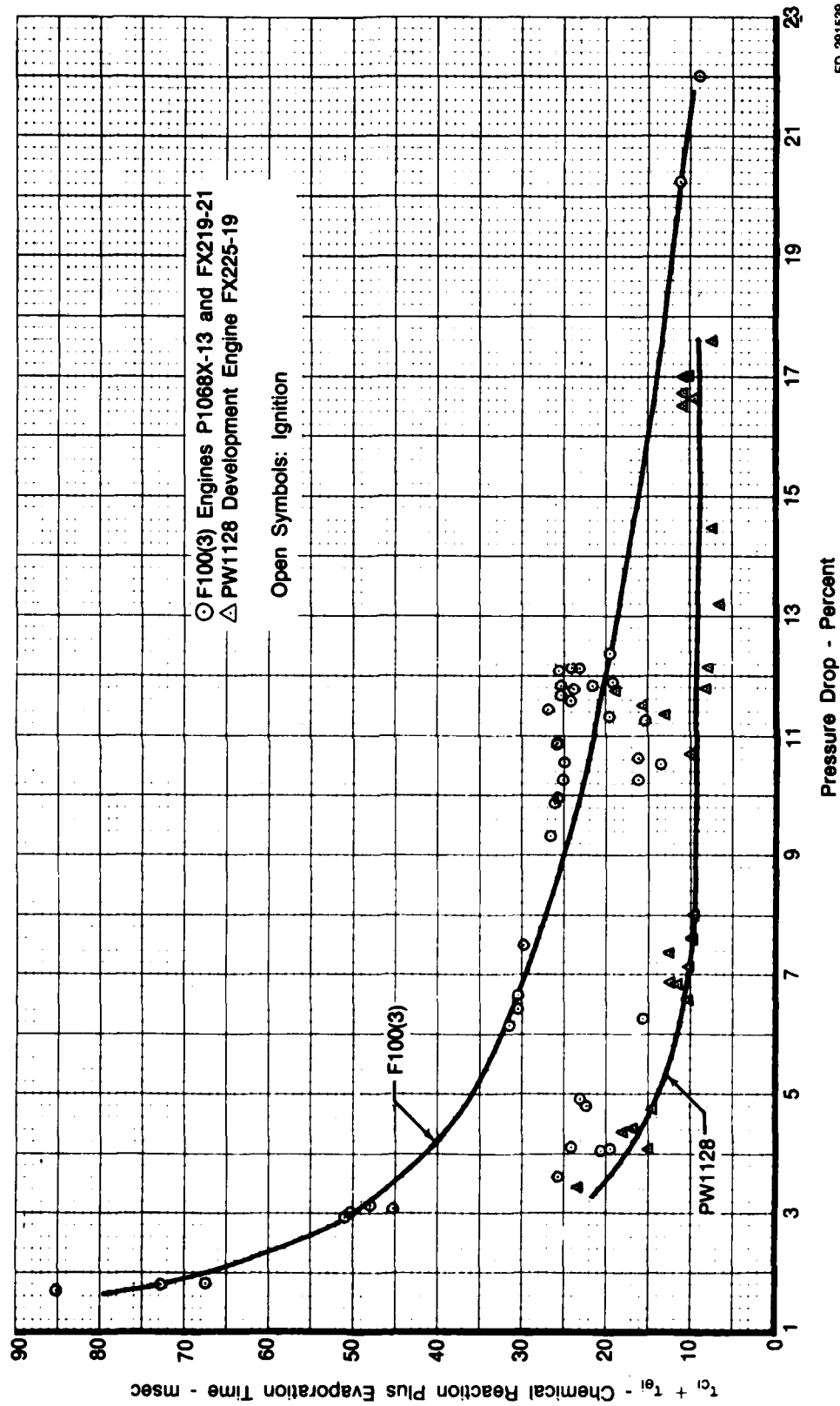
FD 291545

Figure 27. — Effect of Primary Zone Velocity on Volumetric Hot Residence Time During Spooldown Ignition



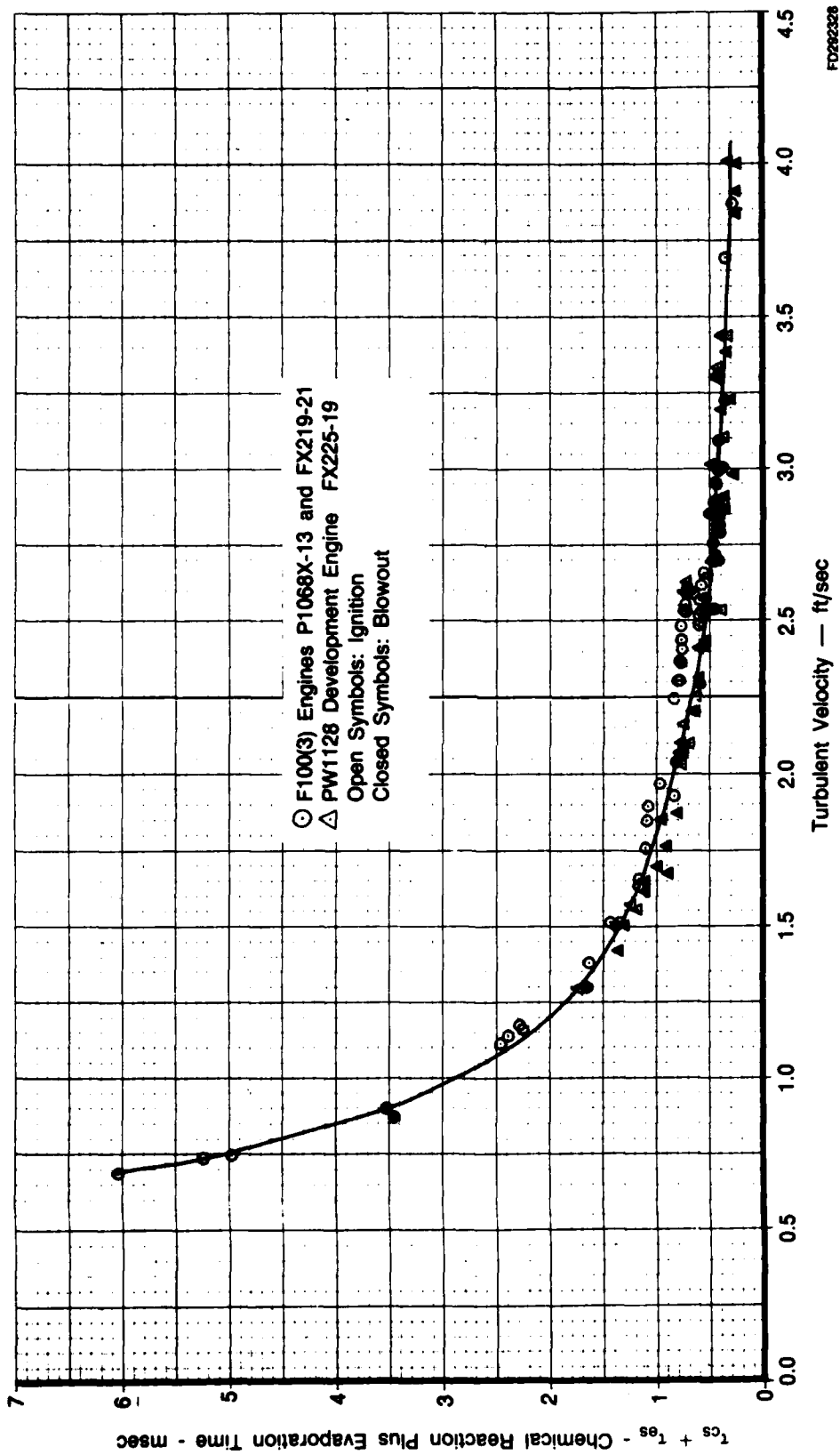
FD 292327

Figure 28. — Effect of Root Mean Square Turbulent Velocity on Spool-down Ignition



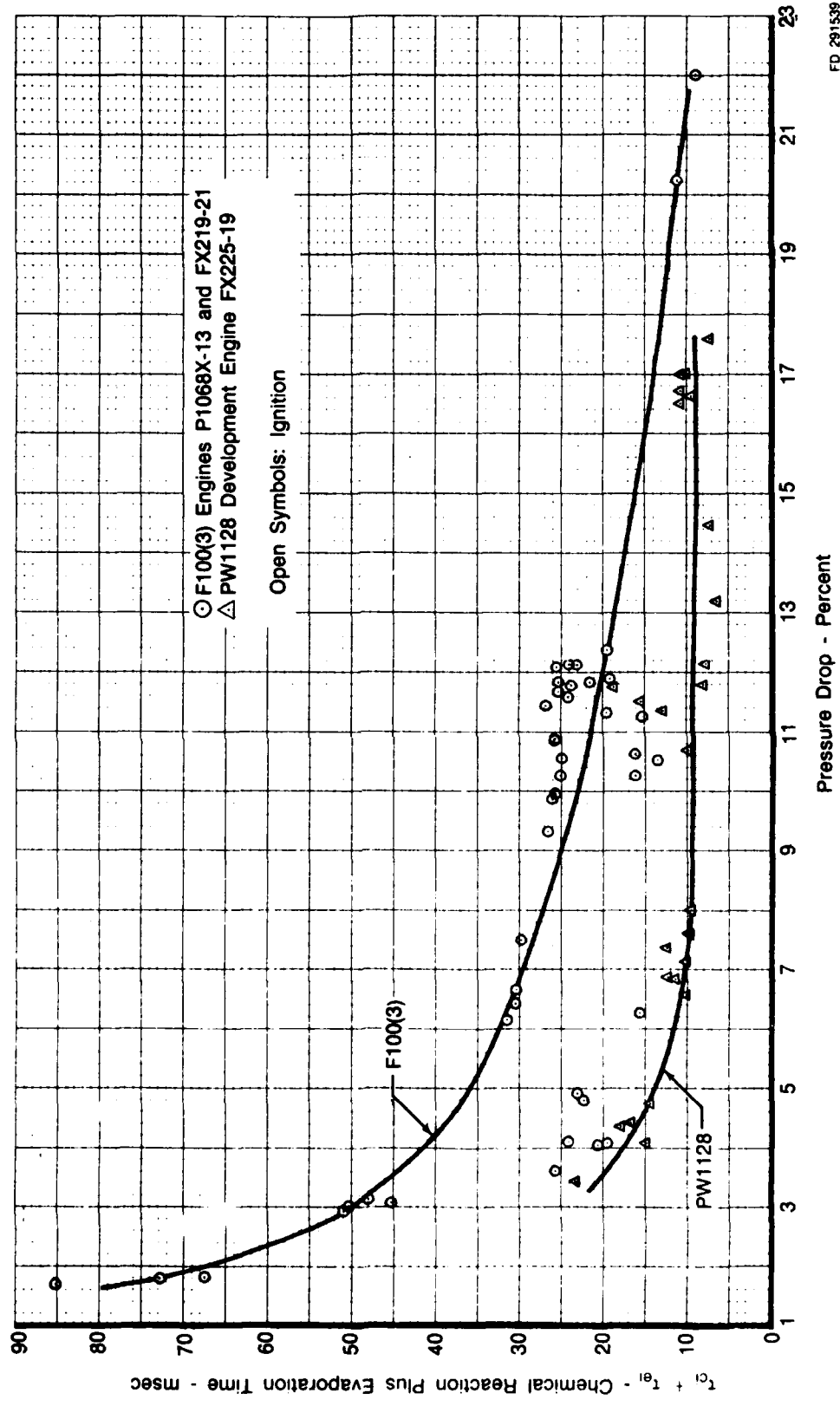
FD 291539

Figure 29. — Effect of Combustor Pressure Drop on Spooldown Ignition



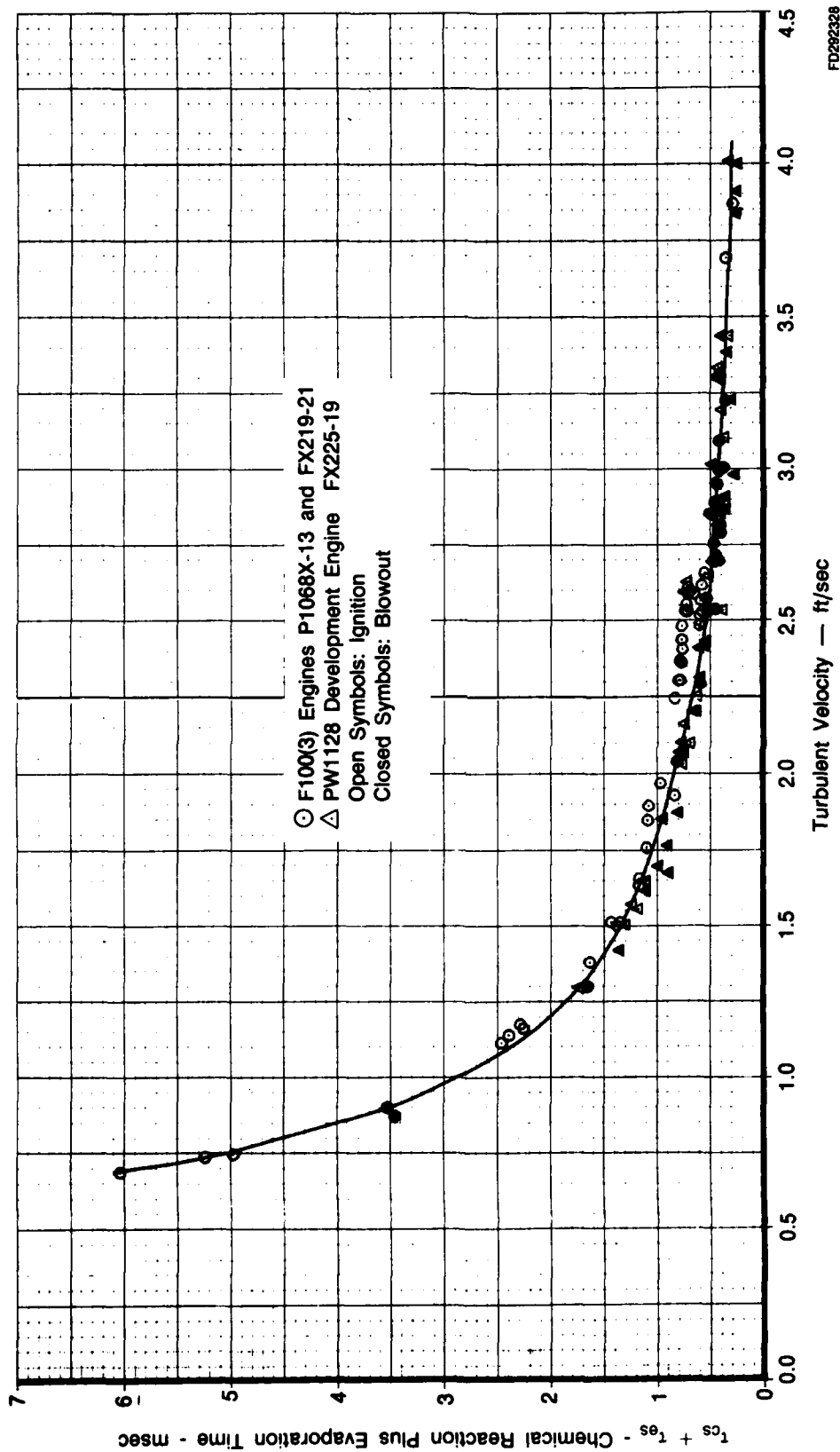
FD262328

Figure 30. — Effect of Root Mean Square Turbulent Velocity on Primary Zone Stability Limit During Spooldown Ignition



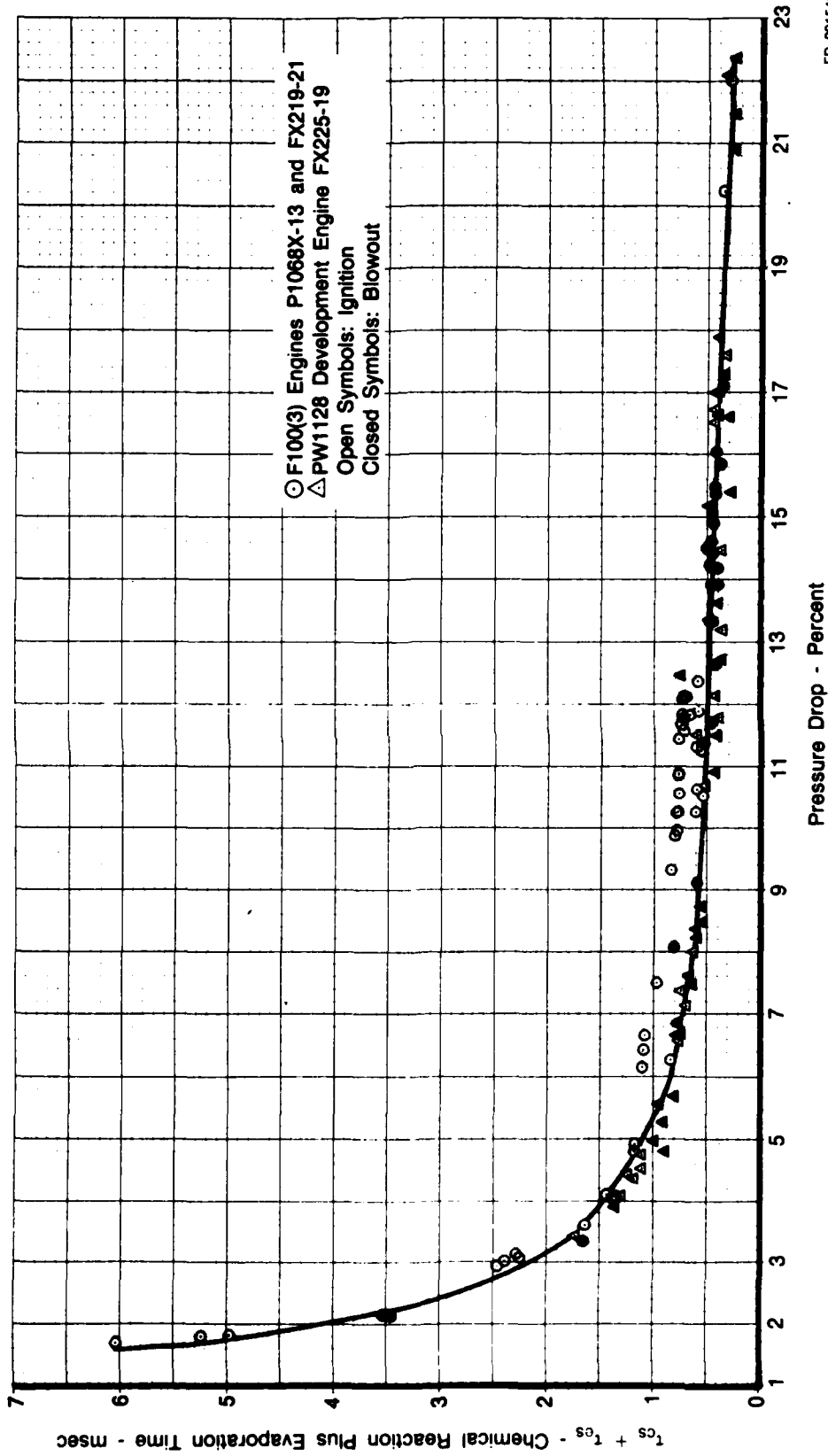
FD 291539

Figure 29. — Effect of Combustor Pressure Drop on Spool-down Ignition



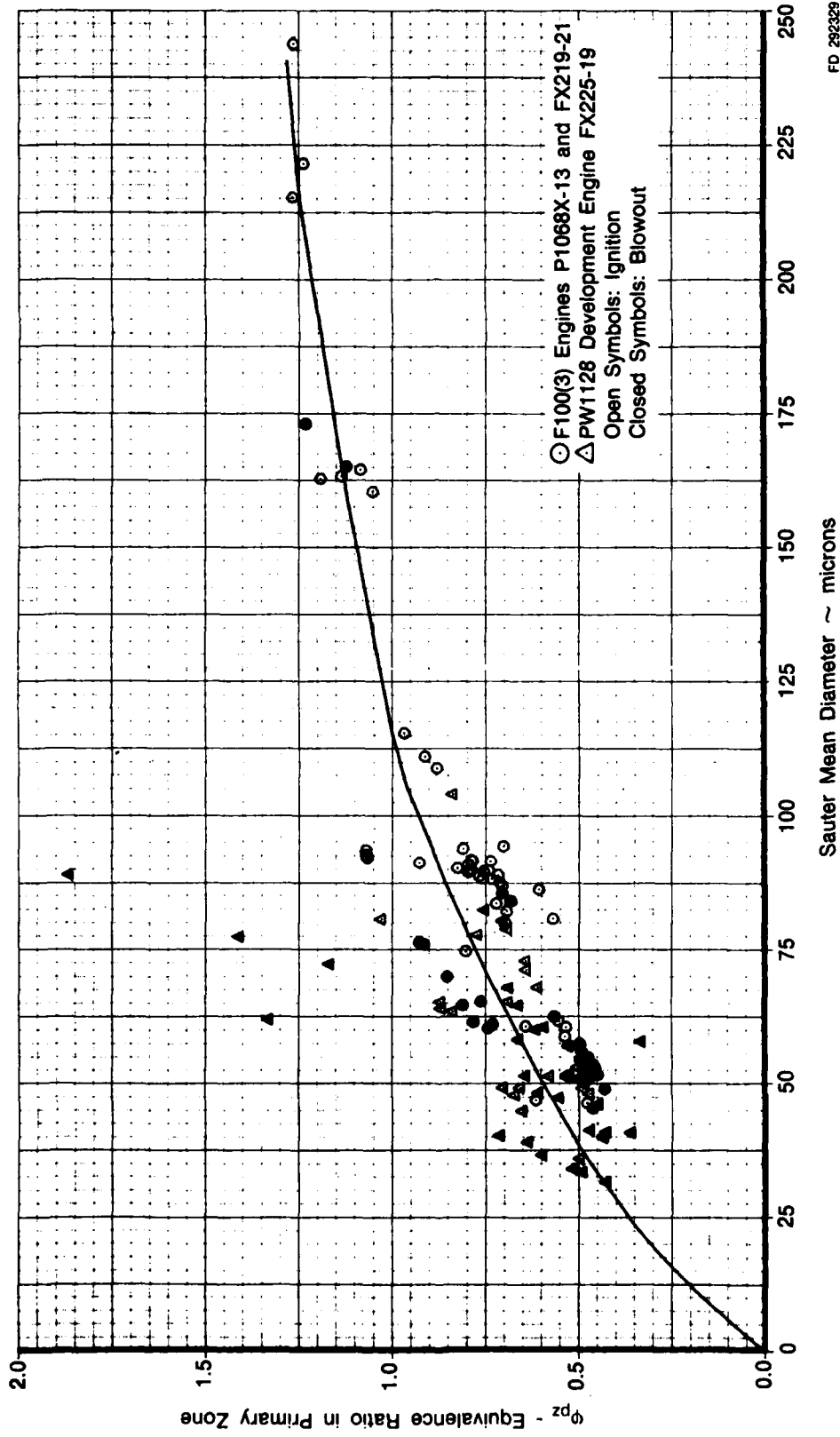
FD292328

Figure 30. — Effect of Root Mean Square Turbulent Velocity on Primary Zone Stability Limit During Spooldown Ignition



FD 291546

Figure 31. — Effect of Combustor Pressure Drop on Primary Zone Stability Limit During Spool-down Ignition



FD 292329

Figure 32. — Effect of Sauter Mean Diameter on Spooldown Ignition

SECTION IV

LEAN DECELERATION BLOWOUT MODEL

A lean deceleration blowout model was developed using F100-PW-200, F100-ILC Development and PW2037 engine data. The blowout operating conditions were encountered by decreasing deceleration fuel flow schedules (i.e., decrease engine deceleration time) and consequently allowing lower fuel-air ratios and combustor pressures to occur (all limits were deactivated). The igniters were turned off such that a full combustor blowout would not relight thereby clouding the results. In order to determine the combustor operating conditions during blowout, the derivative of the combustor pressure, with respect to time was plotted as a function of the combustor pressure as shown in Figure 33. As can be seen, the blowout conditions were encountered at a decel schedule of 3RU evidenced by the drastic change in the derivative of the combustor pressure, while the combustor operated successfully at a decel schedule of 5RU. The corresponding successful operating conditions were determined based on an average time interval from the start of the decel to the time the blowout points occurred. The corresponding successful operating conditions were determined based on an average time interval from the start of the decel to the time the blowout points occurred.

The essential feature of a gas turbine combustor, as far as the lean deceleration model is concerned, is the recirculation zone which is created in the combustor primary zone flow field and imposed by (1) the air entering through the swirl vanes; (2) the air jets from the primary combustion holes; and (3) swirler purge air, and deflector cooling air. One of the important functions of the primary zone is to recirculate combustion products to mix and burn with the incoming air and fuel. By this means a mechanism of continuous ignition is established, and combustion can be sustained over a wide range of operating conditions.

The key to developing a successful model for lean deceleration blowout is the identification of the physical processes occurring in the flow field of the primary zone. The model is based on the characteristic time approach and considers the effects of three processes fundamental to flame stabilization: flow residence, chemical reaction and droplet evaporation. The region of interest is the shear layer between the fresh air and the recirculating fuel and burned gas mixture. The turbulent eddies present in the shear-layer region must ignite and react before they are quenched by the relatively cold free stream; if they cannot ignite, the shear-layer flame blows off. The stabilization models with their corresponding characteristic times presented in Section II were considered as candidates for the lean deceleration blowout model. Comparison of the degree of correlation for these models indicated the selection of the following characteristic times for the lean deceleration.

- For volumetric hot residence time

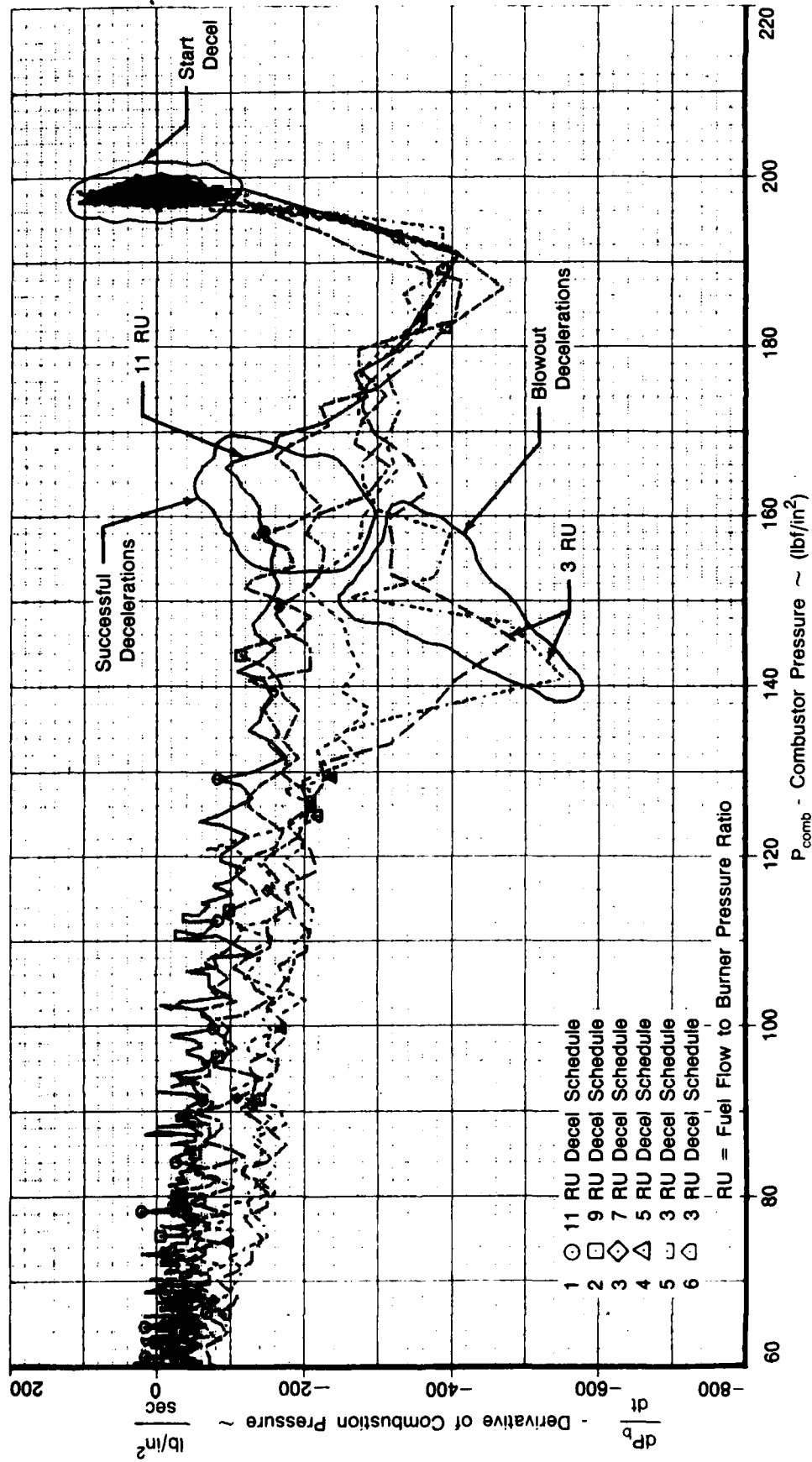
$$\tau_{vhr} = \frac{V_{pz} \rho_k}{W a_{pz}} \text{ (msec)} \quad (33)$$

- For evaporation time

$$\tau_{es} = \frac{C_3^3 \rho_f C_{p,k} (\text{SMD})^2 (1-\Omega)}{8 C_1 k_r \phi_{pz} \ln(1+B) (1+25 C_2^{0.25} Re_1^{0.5})} \text{ (msec)} \quad (34)$$

- For chemical reaction time

$$\tau_{cs} = \frac{15.6a}{u' (S_T - 0.63 u')} \text{ (msec)} \quad (35)$$



FD 292330

Figure 33. — Identification of Lean Decel Blowout Points for F100-ILC Development Engine FX217-21

An excellent correlation model of the lean deceleration blowout limit was obtained with the aforementioned engine data. As shown in Figures 34 and 35, the volumetric hot residence time in the primary zone has been correlated with the characteristic times of chemical reaction and evaporation. The relationship defines regions of stable and unstable combustion. The solid line represents the lean deceleration blowout limit over the entire range of conditions for which data were available. The coefficient of determination, r^2 was 0.985.

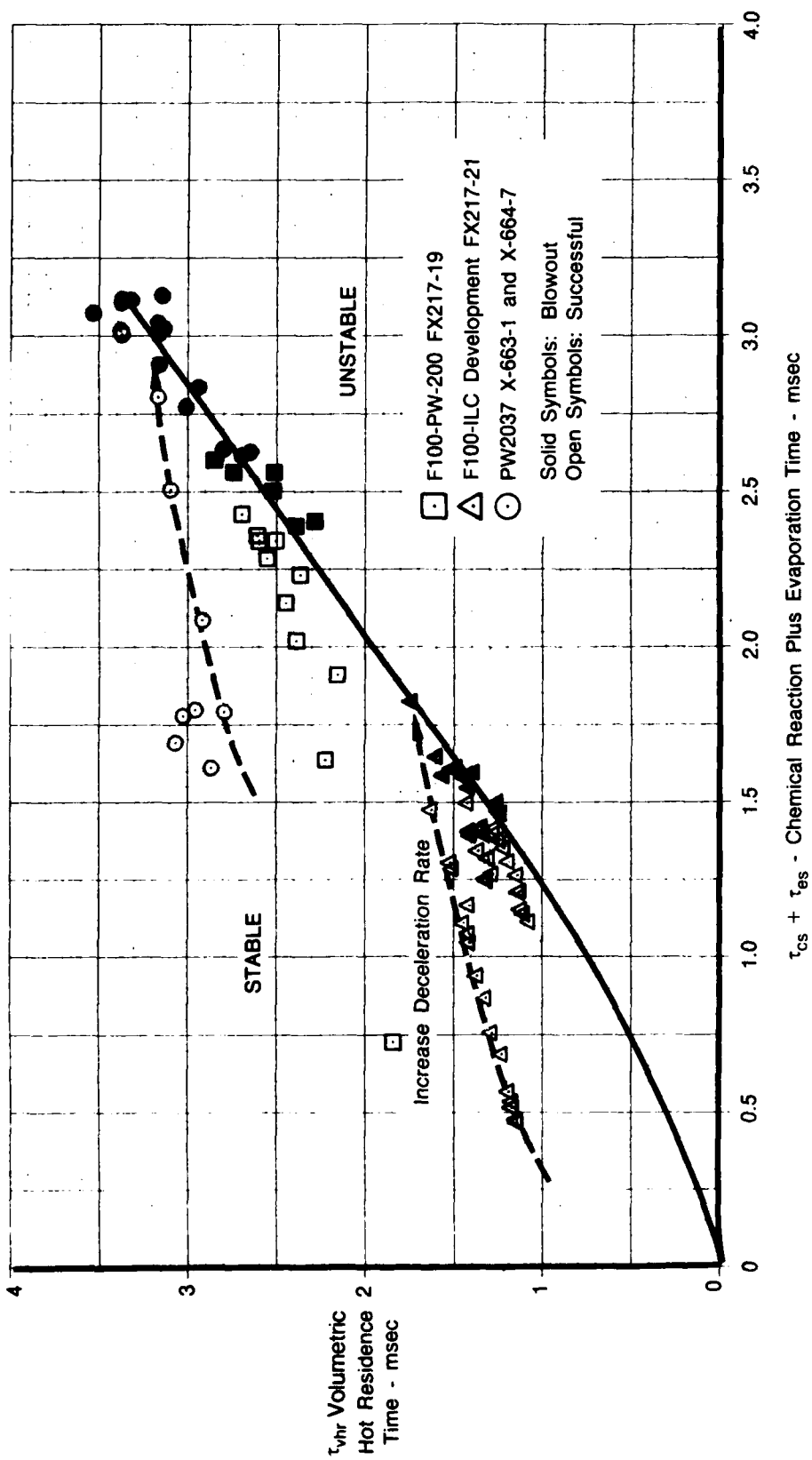
The successful deceleration data points lie in the region of stable combustion and approach the lean decel blowout limit as the deceleration rate is increased (i.e., decreased engine deceleration time) as shown on the dashed lines in Figure 34. For a specified combustor geometry and operating condition (fixed volumetric hot residence time), the blowout equivalence ratio is uniquely related to the sum of chemical reaction and evaporation time. Alternately, an increase in the volumetric hot residence time of the primary zone, by reducing airflow (decreasing primary zone velocity) or increasing primary zone volume, will permit use of lower equivalence ratio.

Plots illustrating separately the effects of evaporation and chemical reaction time on lean deceleration limit are shown in Figures 36, 37, and 38. The chemical reaction rates are significantly longer than the evaporation rates for well atomized fuel and low equivalence ratio. Therefore, chemical reaction time was concluded to be the controlling process of lean deceleration blowout. Also, as shown by the dashed line in Figure 36, an increase in the deceleration rate has no significant effect on the evaporation time, while a decrease in the volumetric hot residence time increases evaporation time slightly.

Figures 39 and 40 present the effect of the pressure drop and overall fuel air ratio on chemical reaction time, respectively. With increased pressure drop from one engine to another, the chemical reaction time is reduced, since pressure drop induces mixing between hot gases and fresh reactants. However, for a given engine, chemical reaction time increases with increasing deceleration rate (i.e., decreased engine deceleration time) until blowout occurs as shown in Figure 39. The slight increase in pressure drop is overcome by the decrease in flame speed associated with the decrease in fuel air ratio. Also, as shown in Figure 40, a decrease in combustor pressure results in lean decel blowout at higher overall fuel air ratio with a longer engine deceleration time. Similar results were also observed with the other engines.

The volumetric hot residence time is shown as a function of fuel flow to burner pressure ratio at blowout in Figure 41. Reduction in fuel flow to burner pressure ratio (i.e., decreased engine deceleration time) increases volumetric hot residence time. The effect is less pronounced with engines of lower flow residence time (increased front end air flow or reduced primary zone length). Also, as shown in Figure 42, increasing deceleration rate along a constant pressure line with engines of longer volumetric hot residence time results in a blowout at lower primary zone equivalence ratio and shorter engine deceleration times.

The effects of combustor inlet temperature and pressure on lean deceleration blowout limits are shown in Figures 43 and 44, respectively. Increases in inlet temperature lead to higher temperature combustion products and a decrease in chemical reaction time. An increase in combustor pressure results in an increase in flame speed and therefore a reduction in chemical reaction. Hence, this leads to a widening of the stability limits with successful lean deceleration at lower fuel air ratio.



FD 291548

Figure 34. — Chemical Reaction and Evaporation Effects on Lean Decel Blowout Limit

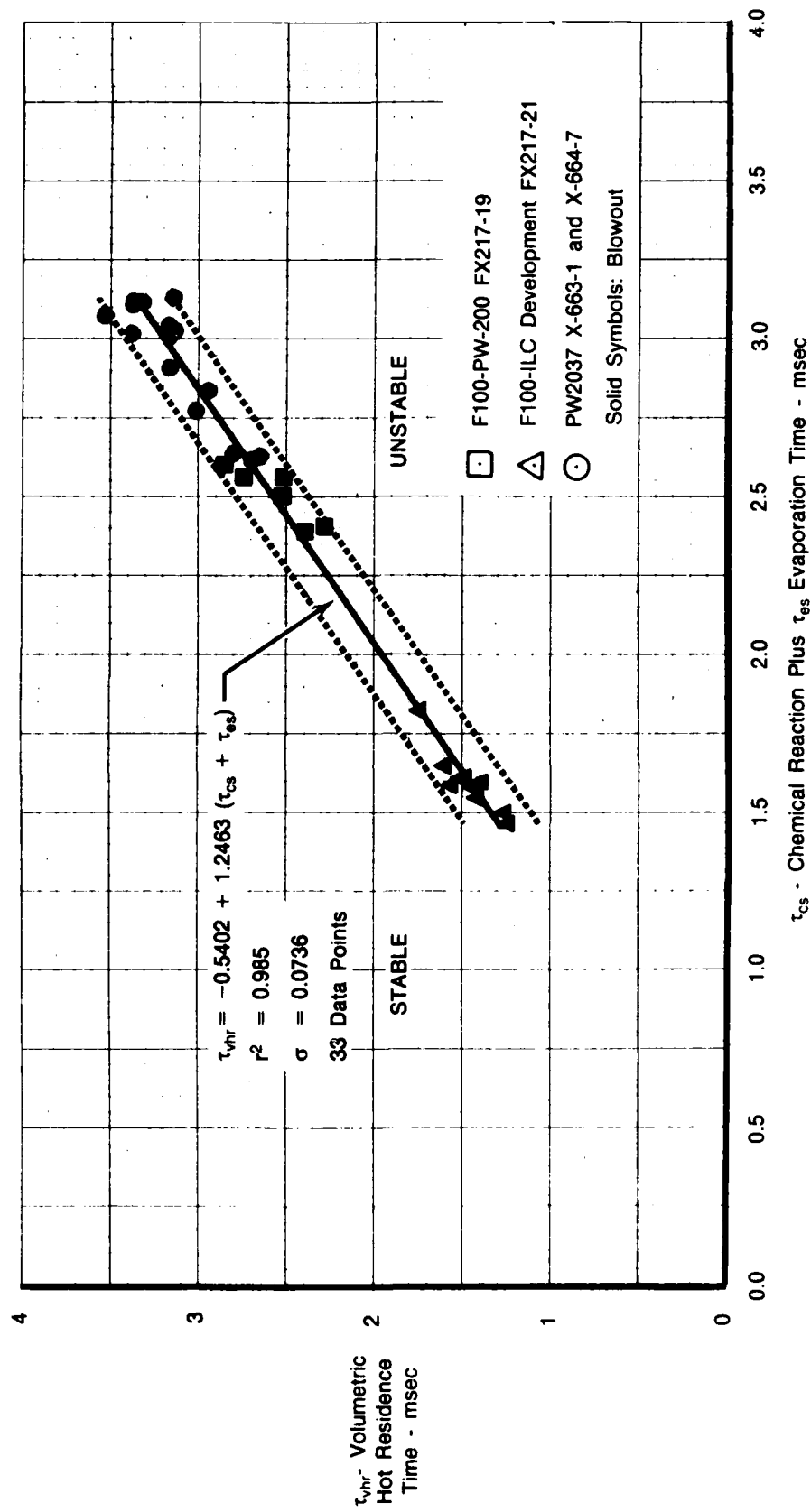
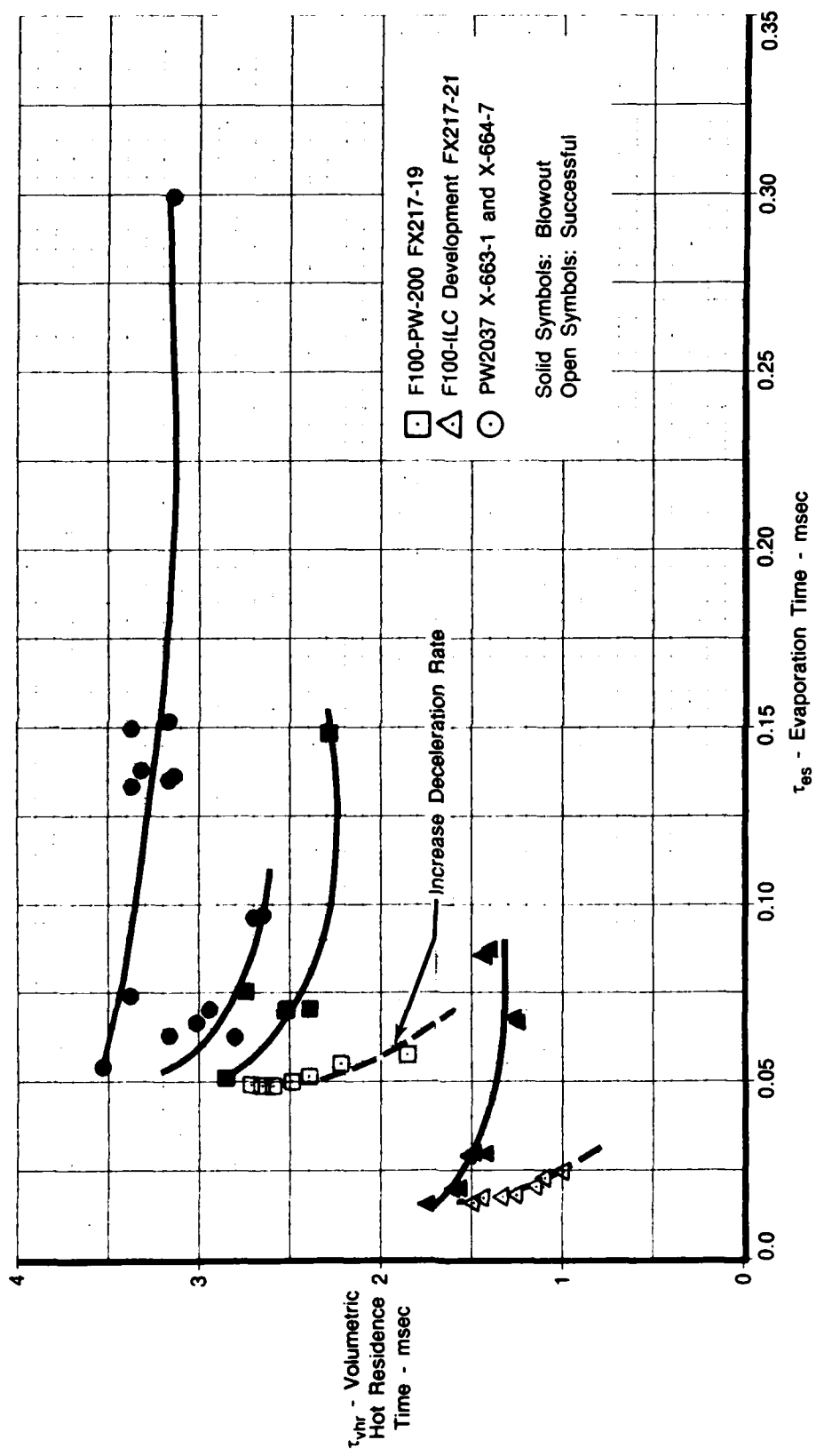
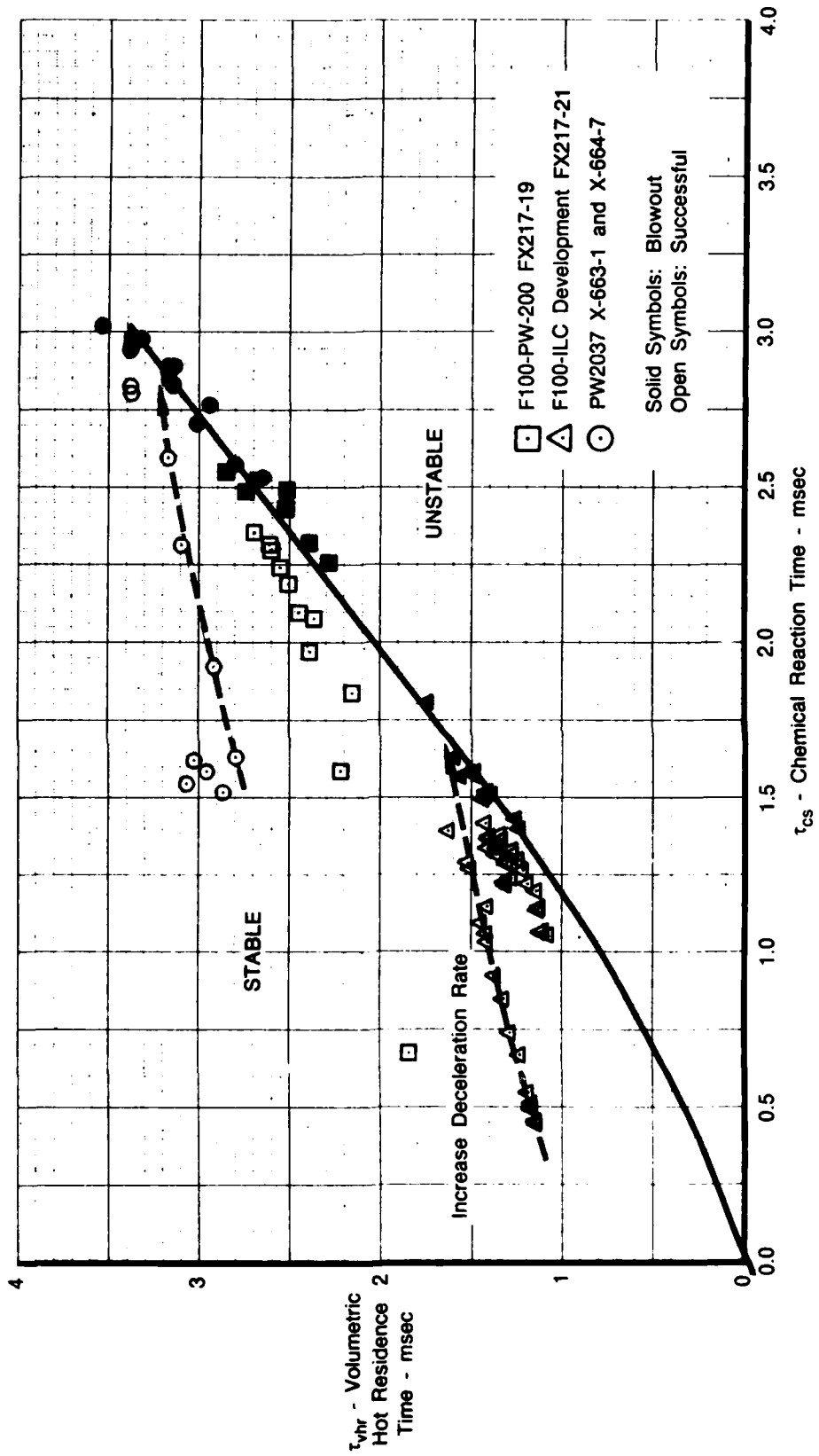


Figure 35. — Chemical Reaction and Evaporation Effects on Lean Decel Blowout Limit



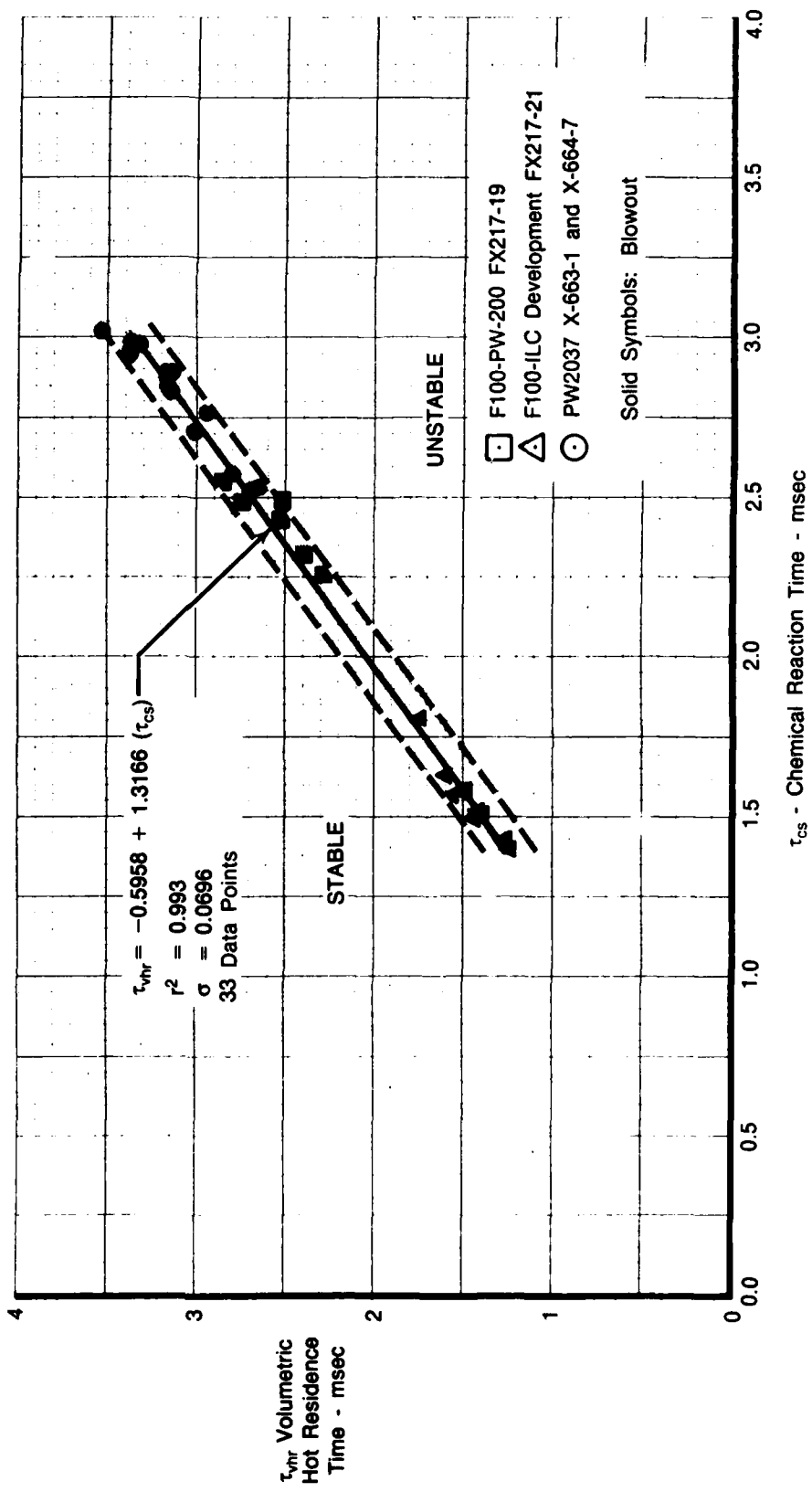
FD 291602

Figure 36. — Evaporation Effect on Lean Decel Blowout Limit



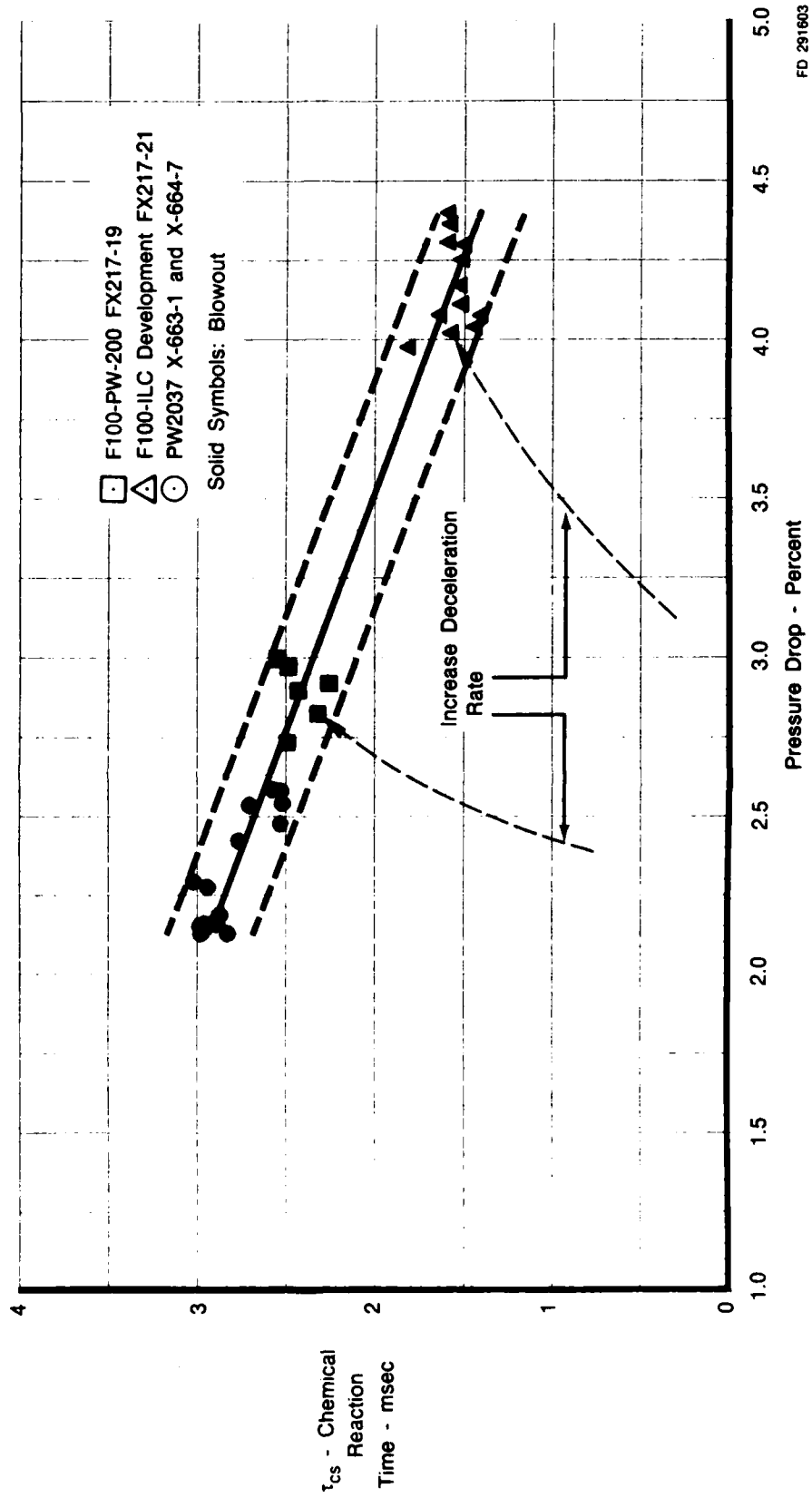
FD 291550

Figure 37. — Chemical Reaction Effects on Lean Decel Blowout Limit



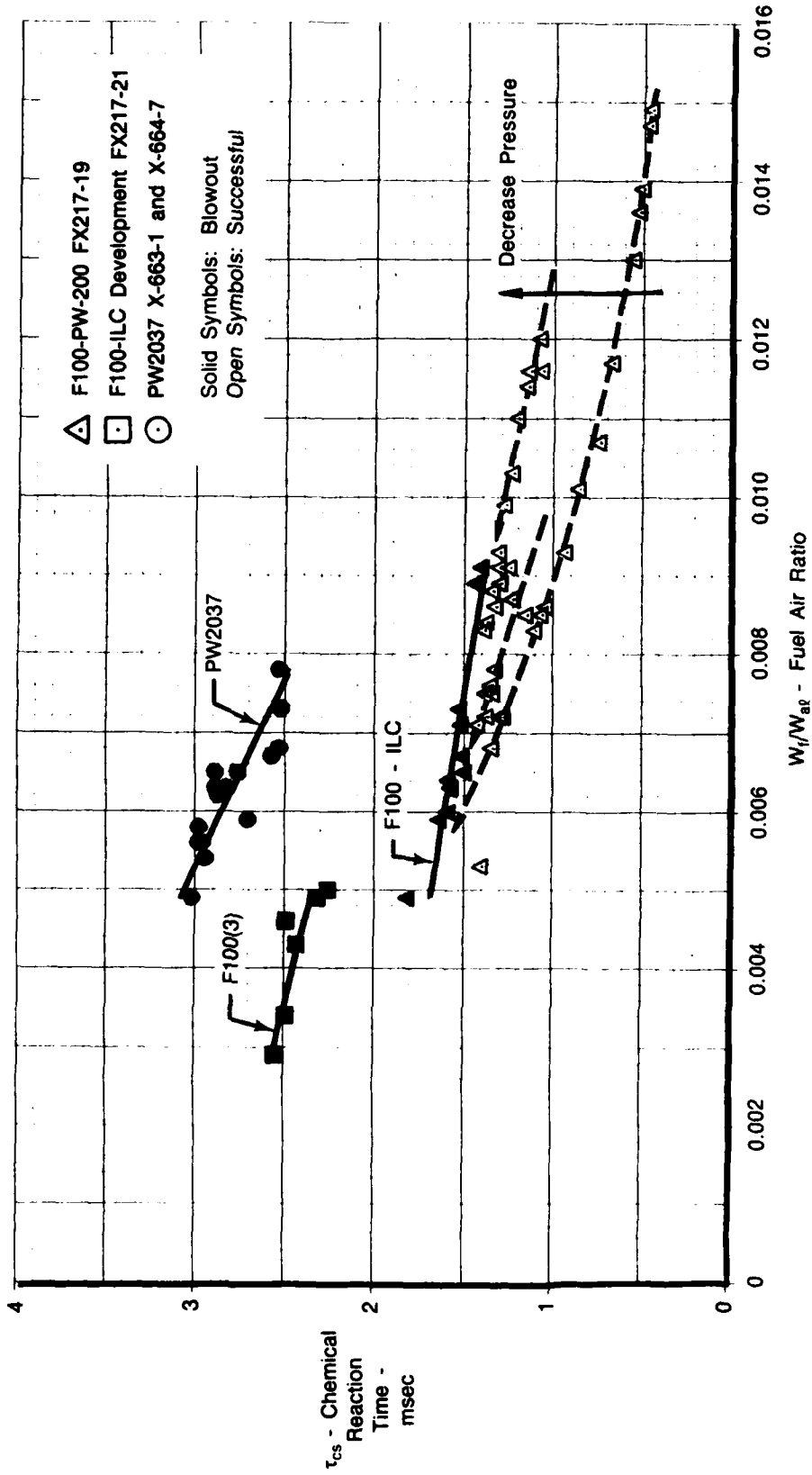
FD 291601

Figure 38. — Chemical Reaction Effect on Lean Decel Blowout Limit



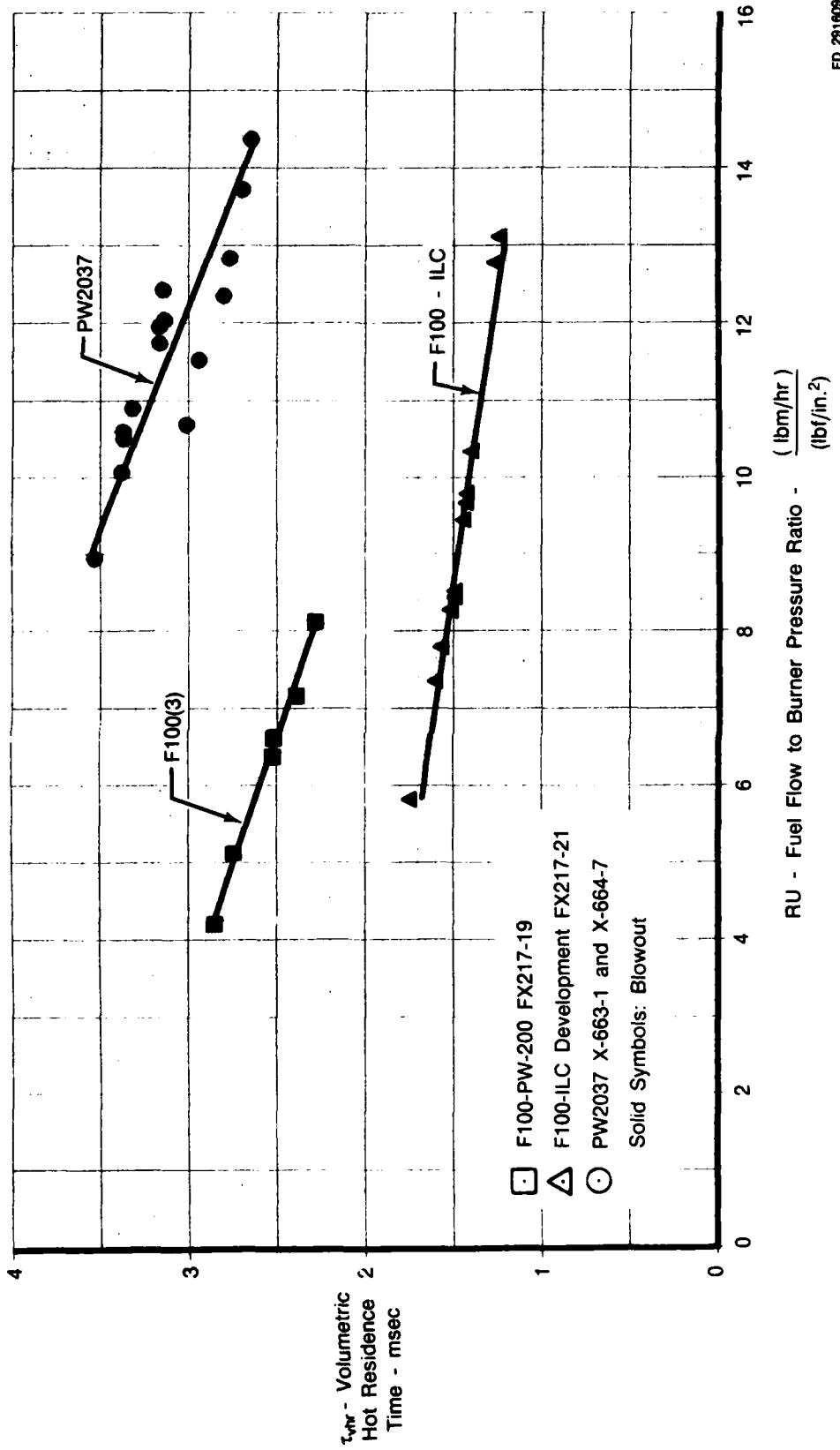
FD 291603

Figure 39. — Effect of Pressure Drop on Chemical Reaction Time During Lean Decel Blowout



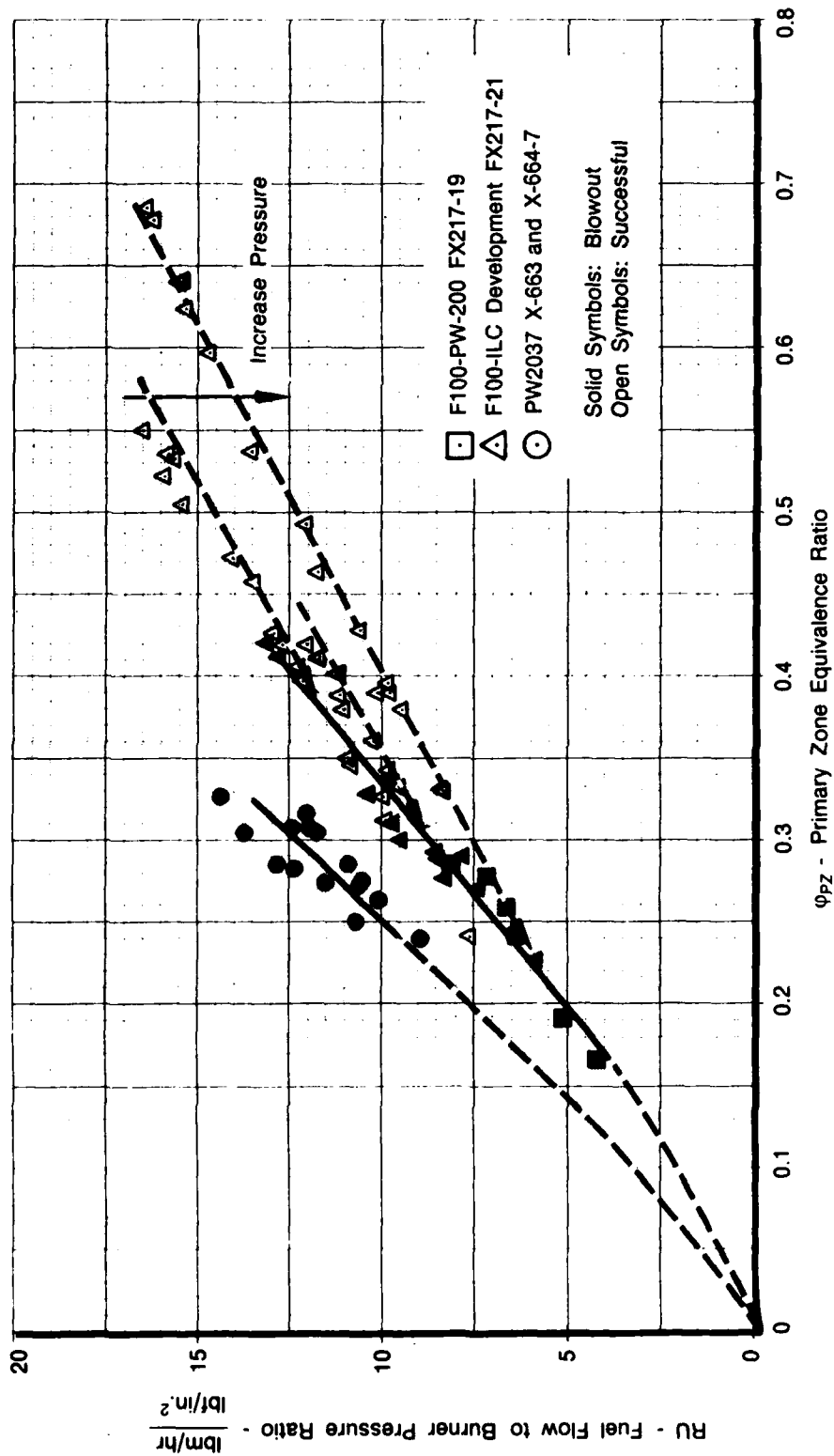
FD 291605

Figure 40. — Chemical Reaction Versus Combustor Fuel Air Ratio Overall During Lean Decel Blowout



FD 291609

Figure 41. — Effect of Fuel Flow to Burner Pressure Ratio on Volumetric Hot Residence Time During Lean Decel Blowout



FD 291611

Figure 42. — Fuel Flow to Burner Pressure Ratio Versus Primary Zone Equivalence Ratio

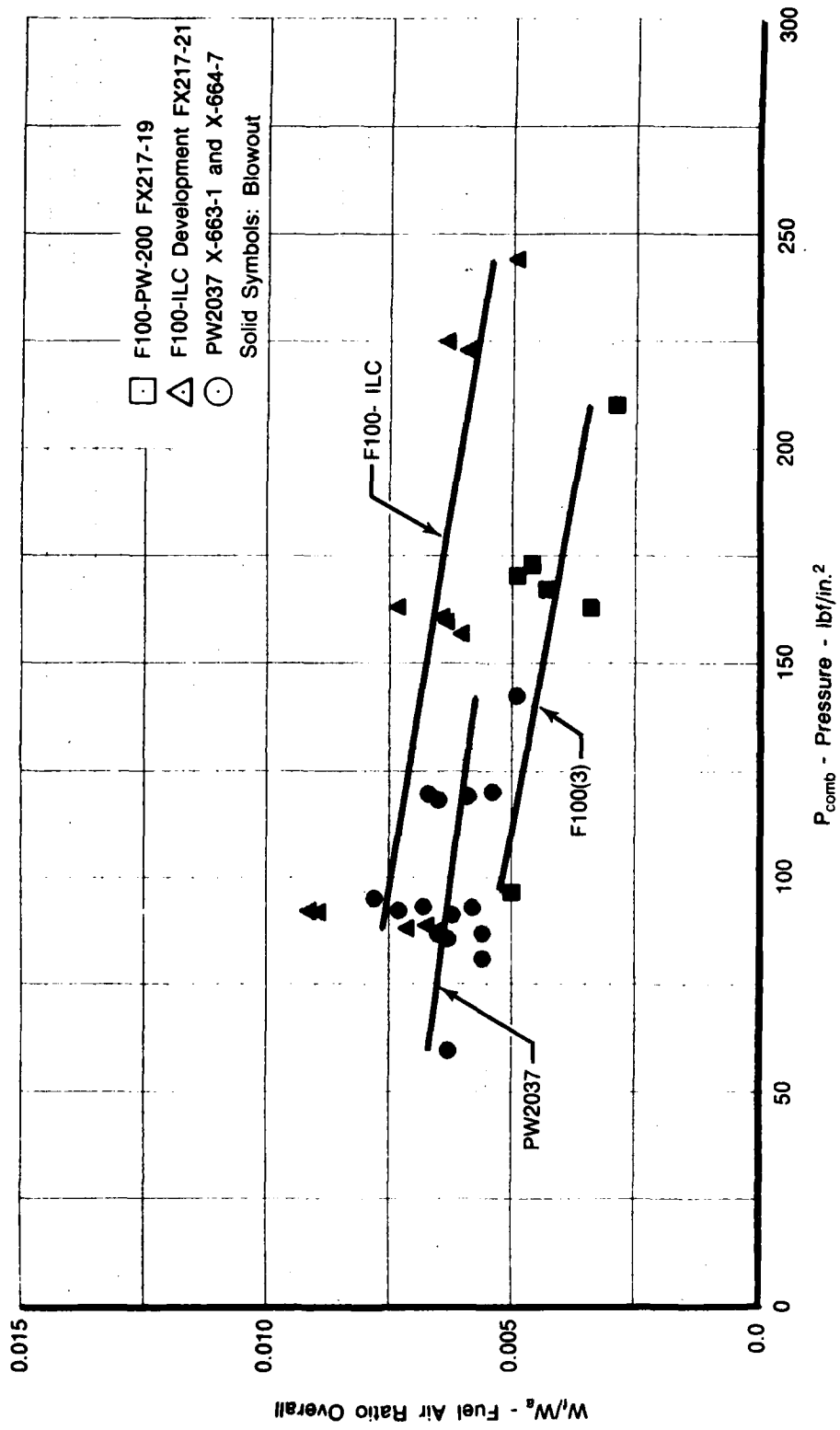
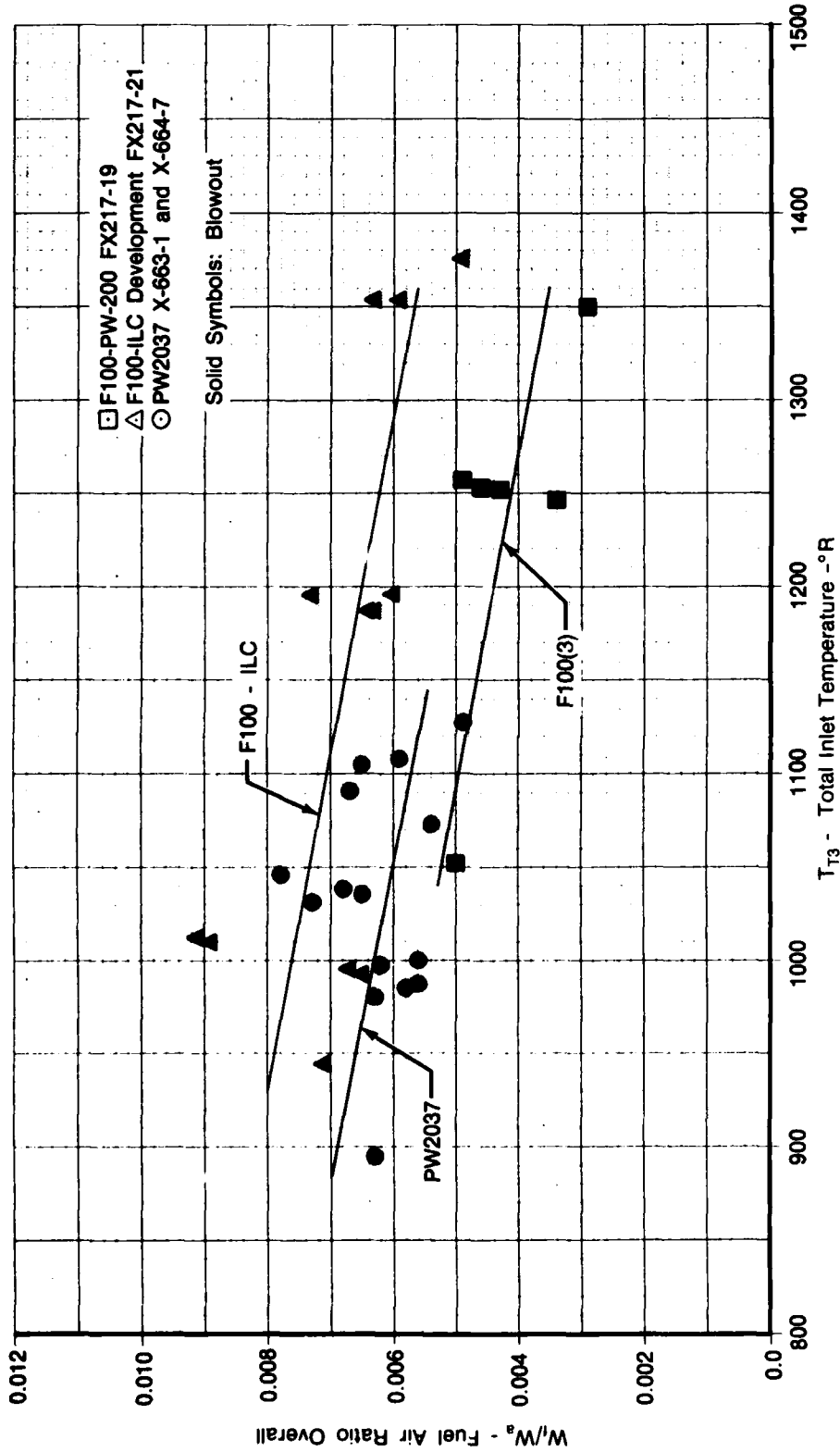


Figure 43. — Effect of Combustor Pressure on Fuel Air Ratio During Lean Decel Blowout



FD 291606

Figure 44. — Effect of Combustor Total Inlet Temperature on Fuel Air Ratio Overall During Decel Blowout

SECTION V

CONCLUSIONS

Based upon the results of the analyses conducted in this study, a number of conclusions have been drawn relative to the effect of the important physical processes in the combustor on altitude ignition and lean deceleration blowout performance, and the relationship of these processes to combustor operation conditions and design variables.

1. The characteristic time models for spark ignition and flame stabilization were used to correlate windmill altitude ignition and lean deceleration blowout limits of current and advanced military and commercial engine data. The correlations had near zero intercepts with good statistical significance.
2. Although the evaporation time is longer than the chemical reaction time for the phenomena of windmill altitude ignition, consideration of both physical processes provides a higher degree of correlation.
3. Increased flow parameter adversely affects spark ignition since it reduces available spark kernel quench time. Advanced military engines with increased air flow and reduced volume in the primary zone for specified flow parameter exhibit the lowest available spark quench time.
4. Windmill altitude ignition is impeded by increased airflow and reduced primary zone volume (i.e., increased velocity in the primary zone) for current and advanced gas turbine combustors. The increased primary zone velocity reduces available spark kernel quench time. Similar results were also observed with increased turbulence intensity or the fluctuating component of velocity. The spark quench time is reduced due to the turbulent diffusion heat loss suffered by the spark kernel as it enters the recirculation zone.
5. The adverse effect of increased turbulence intensity (i.e., decreased available spark kernel quench time) is offset by the decreased evaporation plus chemical reaction time for successful ignition and acceleration to occur.
6. Increased SMD requires higher fuel air ratio to ignite and maintain combustion.
7. The lean deceleration blowout limit for the engine data used in this study is controlled by chemical reaction.
8. Longer engine deceleration time is required to avoid lean deceleration blowout with decreased primary zone volume or increased combustion zone airflow.
9. Increased pressure drop has a beneficial effect on lean deceleration blowout limit by decreasing chemical reaction time. However, offsetting this advantage is the reduction in the primary zone flow residence time.

10. Decreased combustor pressure and temperature adversely effect stability limits with lean deceleration blowout at higher fuel air ratio.
11. The critical parameters of applying the windmill altitude ignition and lean deceleration blowout models are: (1) the empirical estimates of SMD, (2) the equivalence ratio in the primary zone and near the ignitor based on fuel spray distribution, and (3) the turbulence intensity in the combustion zone.

REFERENCES

1. Ballal, D. R., Lefebvre, A. H., "General Model of Spark Ignition for Gaseous and Liquid Fuel-Air Mixtures," Symp Int Combustion 18th, Waterloo, Can., Aug 17-22 1980 by Combust Inst, Pittsburgh Pa, USA 1981 p 1737-1746.
2. Peters, J. E. and Mellor, A. M., "A Spark Ignition Model for Liquid Fuels Sprays Applied to Gas Turbine Engines," *Journal of Energy*, Vol 6, July-Aug 1982 p. 272-274.
3. Peters, J. E., and Mellor, A. M., "An Ignition Model for Quiescent Fuel Sprays," *Combustion and Flame* 38: 65-74 (1980).
4. Mellor, A. M., "Semi-Empirical Correlations for Gas Turbine Emissions, Ignition and Flame Stabilization," *Prog Energy Combust Sci*, Vol. 6, pp. 347-358, 1980.
5. Ballal, D. R. and A. H. Lefebvre, "Weak Extinction Limits of Turbulent Heterogeneous Fuel/Air Mixtures," *Trans. ASME, J. Eng. Power*, Vol. 102, No. 2, pp. 416-421 (1980).
6. Ballal, D. R. and A. H. Lefebvre, "Weak Extinction Limits of Turbulent Flowing Mixtures," *Trans. ASME, J. Eng. Power*, Vol. 101, No. 3, pp. 343-348, (1979).
7. Lefebvre, A. H., Mellor, A. M., and Peters, J. E., Ignition/Stabilization/Atomization: Alternate Fuels in Gas Turbine Combustors," AIAA 1978, p. 137-158; Discussion, p. 158-159/ Combustion and Chemical Kinetics, SQUID Workshop, Columbia, Md., September 7-9, 1977.
8. Ballal, D. R., and A. H. Lefebvre, "Ignition and Flame Quenching of Flowing Heterogeneous Fuel-Air Mixtures," *Combustion and Flame* 35: 155-168 (1979).
9. Ballal, D. R., A. H. Lefebvre, "Ignition and Flame Quenching of Quiescent Fuel Mists," *Proc. Roy. Soc. Land. A. 364*, 277-294 (1978).
10. Ballal, D. R., Lefebvre, A. H., "Some Fundamental Aspects of Flame Stabilization," International Symposium on Air Breathing Engines, 5th, Bangalore, India, February 16-22, 1981, Proceedings, Bangalore, National Aeronautical Laboratory, 1981, p. 48-1 to 48-8.
11. Ballal, D. R., Lefebvre, A. H., "Basic Ignition Research Related to Altitude Relight Problems," *Gas Turbine Combustor Design Problems*, Washington, D. C., Hemisphere Publishing Corp., 1980, p. 180-200; Discussion p. 200-201.
12. Plee, S. L., and Mellor, A. M., "Characteristic Time Correlation for Lean Blowoff of Bluff-Body Stabilized Flames," *Combustion and Flame* 35: 61-80 (1979).
13. Leonard, P. A., and Mellor, A. M., "Lean Blowoff in High Intensity Combustion with Dominant Fuel Spray Effects," *Combustion and Flame* 42: 93-100 (1981).
14. Ballal, D. R., and Lefebvre, A. H., "Ignition of Liquid Fuel Sprays at Subatmospheric Pressures," *Combustion and Flame* 31, 115-126 (1978).
15. Rao, K. V. L., and Lefebvre A. H., "Minimum Ignition Energies in Flowing Kerosene - Air Mixtures" *Combustion and Flame* 27, 1-20 (1976).
16. Ballal, D. R., and Lefebvre A. H., "Ignition and Flame Quenching in Flowing Gaseous Mixtures," *Proc. R. Soc. Land. A. 357*, 163-181 (1977).

17. Subba Rao, H. N., and Lefebvre, A. H., "Ignition and Kerosene Fuel Sprays in a Flowing Air Stream," *Combustion Science and Technology* 1973, Vol 8, pp 95-100.
18. Greenhough, V. W., and Lefebvre, A. H., "*Some Applications of Combustion Theory to Gas Turbine Development.*"
19. Plee, S. L., and Mellor, A. M., "Flame Stabilization in Simplified Pre vaporizing, Partially Vaporizing and Conventional Gas Turbine Combustors," AIAA/SAE 14th Joint Propulsion Conference, Las Vegas, Nev, July 25-27, 1978.
20. Odgers J. and Carrier C., "Modeling of Gas Turbine Combustors Considerations of Combustion Efficiency and Stability" ASME paper No. 72-NA/GT-1 September 1973.
21. Ballal, D. R., and Lefebvre, A. H., "The Influence of Spark Discharge Characteristics on Minimum Ignition Energy in Flowing Gases," *Combustion and Flame* 24, pp. 99-108 1975.
22. Ballal, D. R., "Spark Ignition of Turbulent Flowing Gases," AIAA 77-185, Presented at AIAA Fifteenth Aerospace Science Meeting, Los Angeles, 1977.
23. J. B. Fenn, "Lean Flammability Limit and Minimum Spark Ignition Energy," *Ind. Eng Chem.*, Vol. 43, No. 12, pp. 2865-2869, 1951.
24. J. Odgers, "Combustion Modeling Within Gas Turbine Engines," AIAA 77-152, Presented at AIAA Fifteenth Aerospace Science Meeting, Los Angeles, 1977.
25. Ballal D. R. and Lefebvre A. H., "Flame Quenching in Turbulent Flowing Gaseous Mixtures" Sixteenth Symposium (International) on Combustion, pp. 1689-1698, The Combustion Institute, Pittsburgh 1977.
26. Moses C. A. and Naegeli D. W., "Fuel Property Effects on Combustor Performance," ASME 79-GT-178, Presented at the Gas Turbine Conference and Exhibit and Solar Energy Conference, San Diego, Calif., March 1979.
27. Moses C. A., "Studies of Fuel Volatility Effects on Turbine Combustor Performance, Combustion Institute, Central and Western States Section" Meeting, San Antonio, Texas, April 21-22, 1975.
28. Al Dabbagh, N. A., and Andrews, G. E., "Weak Extinction and Turbulent Burning Velocity for Grid Plate Stabilized Premixed Flames," *Combustion and Flames* 55:31-52 (1984).
29. Naegeli, D. W., Moses, C. A. and Mellor, A. M., "Preliminary Correlation of Fuel Effects on Ignitability for Gas Turbine Engines," ASME Paper No. 83-JPGC-GT-8.
30. Lefebvre, A. H., "Airblast Atomization," *Energy Combustion Science*, Vol 6, pp 233-261, Great Britain, 1980.
31. Lefebvre, A. H., "Fuel Effects on Gas Turbine Combustion-Ignition, Stability and Combustion Efficiency," *Trans. ASME*, October 1, 1984.

APPENDIX A

LITERATURE SURVEY OF ALTITUDE IGNITION AND LEAN DECEL PROGRAM

Title	Author	Source	Synopsis
1. General Model of Spark Ignition for Gaseous and Liquid Fuel-Air Mixtures Reference No. 1	D. R. Ballal and A. H. Lefebvre	Symp Int. Combustion 13th, Waterloo, Can., Aug 17-22 1980.	<p>• In a previous publication a model for the spark ignition of heterogeneous fuel-air mixtures is described which assumes that chemical reaction rates are infinitely fast, and that the sole criterion for successful ignition is an adequate concentration of fuel vapor in the ignition zone. In this work the model is extended to include (1) the effects of finite chemical reaction rates, which are known to be significant for well-atomized fuels at low pressures and low equivalence ratios, and (2) the presence of fuel vapor in the mixture flowing into the ignition zone. It has general application to both quiescent and flowing mixtures of air with either gaseous, liquid or evaporated fuel, or any combination of these fuels. The general validity of the new model is demonstrated by a close level of agreement between theoretical predictions of minimum ignition energy and the corresponding experimental values obtained over wide ranges of pressure, velocity, equivalence ratio, mean fuel drop size and fuel volatility.</p>
2. A Spark Ignition Model for Liquid Fuels Sprays Applied to Gas Turbine Engines Reference No. 2	J. E. Peters and A. M. Mellor	Journal of Energy Vol 6, July-Aug 1982, p. 272-274	<p>• The characteristic time model for ignition is used to describe the spark ignition of liquid fuel sprays in gas turbine combustors. The model states that for ignition to occur, the energy of a spark must heat up an initial volume such that the heat release rate within that volume is greater than the loss rate. Heat generation is limited first by a droplet evaporation time and then a kinetic time; heat loss (for gas turbine applications) is due to turbulent diffusion and, hence, is controlled by a mixing time. Data from two can type combustors and seventeen fuels are correlated by a single ignition limit curve. The key to applying the model to engine data is the estimation of drop sizes and equivalence ratios at the spark gap.</p>
3. Semi Empirical Correlations for Gas Turbine Emissions, Ignition and Flame Stabilization Reference No. 4	A. M. Mellor	Prog. Energy Combust. Sci., Vol. 6, pp. 347-358, 1980	<p>• For operating conditions where the fuel evaporation rate is fast compared to the fuel vapor/air mixing rate, a characteristic time model has been formulated to predict gaseous emissions and efficiency in terms of combustor inlet conditions and geometry. The model, which involves kinetic and fluid mechanic times, has been used to design low NO_x burners, and study of several different conventional engine combustors suggests that the correlation may be universal. A related model, which includes a fuel droplet evaporation time, is being validated with data from laboratory combustors for spark ignition and lean flame stabilization. The preliminary application of this latter model to engine situations is described.</p>

LITERATURE SURVEY OF ALTITUDE IGNITION AND LEAN DECEL PROGRAM (Continued)

Title	Author	Source	Synopsis
4. Weak Extinction Limits of Turbulent Heterogeneous Fuel/Air Mixtures Reference No. 5	D. R. Ballal and A. H. Lefebvre	Trans. ASME, J. Eng. Power, Vol. 102, No. 2, pp. 416-421, 1980	• Experimental and theoretical studies are made of the factors governing the weak extinction limits of stabilized flames supplied with flowing mixtures of liquid fuel drops of and air. The test program includes wide variations in inlet air pressure, velocity and turbulence level, and also covers wide ranges of fuel volatility and mean drop size. The influence of flameholder size and blockage is also examined. An equation is derived for predicting weak extinction limits which shows good agreement with the corresponding experimental values. Paper No. 79-GT-157.
5. Ignition/Stabilization/Atomization: Alternative Fuels in Gas Turbine Combustor Reference No. 7	A. H. Lefebvre, A. M. Mellor, and J. E. Peters	Progress in Astronautics and Aeronautics 62, 1973, pp. 137-159.	• It is pointed out that fuel preparation, ignition, flame spreading, and flame stabilization are important considerations in the design of gas turbine engines. It is discussed how changes in the major properties of alternative fuels will affect atomization, ignition, flame spread and lean blowoff in gas turbine burners. It is found that it is primarily the physical properties of the fuel which influence the performance parameters. Studies have shown that ignition is strongly dependent on fuel volatility and viscosity. A graph showing the influence of atomization quality on ignition limits is presented. For all fuels considered the atomization quality is found to be markedly inferior to that of normal kerosene, indicating that problems of ignition and lean blowoff will be more severe. The correlations predict that jet fuels derived from shale oils, tar sands, and coal syncrudes will pose more serious problems of atomization than similar petroleum-based fuels.
6. Characteristic Time Correlation for Lean Blowoff of Bluff-Body Stabilized Flames Reference No. 12	S. L. Plee and A. M. Mellor	Combustion and Flame 35: 61-80 (1979)	• Characteristic times associated with turbulent mixing homogeneous chemical kinetics, liquid-droplet evaporation, and fuel injection are quantified for lean blowoff. The model linearly correlates variations in combustor pressure, inlet temperature, air velocity, flameholder geometry, fuel type, and injector size using data obtained from three different bluff-body stabilizers that simulate the same fundamental combustion process of both conventional and advanced pre vaporizing-premixing gas-turbine combustors. The characteristic time model does not attempt to solve for the entire combustor flow field but rather considers only key regions of the flow that are important to the flame-stabilization process. Lean blowoff is viewed as the competition between a fluid mechanic and chemical time evaluated in the shear-layer region between the hot recirculation zone and the free stream. Heterogeneous effects associated with fuel evaporation and injection representation perturbations on this process that are correlated using a droplet-evaporation time and fuel-injection mixing time, respectively.

LITERATURE SURVEY OF ALTITUDE IGNITION AND LEAN DECEL PROGRAM (Continued)

Title	Author	Source	Synopsis
7. Ignition and Flame Quenching of Flowing Heterogeneous Fuel-Air Mixtures Reference No. 8	D. R. Ballal and A. H. Lefebvre	Combustion and Flame 35: 155-168 (1979)	<p>• A model is described for the ignition of heterogeneous fuel-air mixtures that assumes that mixing rates and chemical kinetics are infinitely fast and that sole criterion for successful ignition is an adequate concentration of fuel vapor in the ignition zone. From analysis of the relevant heat and mass-transfer processes involved, expressions for quenching distance and minimum ignition energy are derived that have general application to both quiescent and flowing mixtures.</p> <p>In the present investigation attention is focused on flowing mixtures, and minimum ignition energies are measured over wide ranges of pressure, velocity, turbulence intensity, equivalence ratio, mean drop size, and fuel volatility. The results obtained show very satisfactory agreement with corresponding predicted values, thus confirming the basic premise of the model.</p>
8. Basic Ignition Research Related to Altitude Relight Problems Reference No. 11	D. R. Ballal and A. H. Lefebvre	Gas Turbine Combustor Design Problems, Washington D. C., Hemisphere Publishing Corp., 1980, pp. 189-201.	<p>• A problem of major importance to aircraft gas turbines is that of reestablishing combustion after a flameout at high altitudes. The problem is aggravated by the fact that almost all of the accepted means of improving relight performance usually incur penalties in other important aspects of combustion performance.</p> <p>A question that often arises is why the ignition energy requirements of gas turbine combustors are so much higher than the corresponding values obtained from more basic studies of minimum ignition energy in gaseous and heterogeneous fuel/air mixtures, as reported in the literature.</p> <p>In order to shed more light on this question, a series of experiments have been conducted on the influence on minimum energy of various relevant parameters such as air pressure, temperature, velocity, turbulence, fuel/air ratio and, in the case of liquid fuels, meandrop size. The results show that, in addition to the adverse effects on ignition of low air pressure and temperature, the main reason for the large ignition energies associated with turbojet combustors is the high level of turbulence in the primary combustion zone. Another important consideration is the mean drop size of the fuel spray. It is found that quite modest improvements to atomization quality can reduce appreciably the amount of spark energy needed to effect ignition.</p>

LITERATURE SURVEY OF ALTITUDE IGNITION AND LEAN DECEL PROGRAM (Continued)

Title	Author	Source	Synopsis
9. Fuel Effects on Gas Turbine Engine Combustion	R. C. Ernst and D. Andreadis	AFWAL-TR-83-2048, June 1983 F33615-79-C-2092	This study was undertaken with the objective of preparing a correlative model of the effect of fuel properties on the performance and life of United States Air Force gas turbine engine hot sections. The data base used in constructing the model consisted primarily of fuel effect data which has been obtained over the past few years under a number of Department of Defense contracts. The approach taken in the study was to first develop fuel effect correlations for altitude and groundstart ignition, lean blowout, combustion efficiency, pattern factor, smoke and peak combustor wall temperature then tie together these correlations using engine design parameters, thereby allowing prediction of fuel effects in any current or future aircraft gas turbine combustion system. Combustors modeled included the F100, F101, TF30, J79, TF33, and TF41.
10. Fuel Effects on Gas Turbine Combustion	A. H. Lefebvre	AFWAL, USAF AFSC WPAPB, Ohio 45433 January 1983 F33615-81-C-2067	is analytical study was to develop appropriate relationships and correlations between combustion performance (efficiency, lean blowout, ignition, liner metal temperature, emissions and pattern factor) and the relevant fuel properties, combustor design features, and combustor operating conditions. The method followed was to study each aspect of combustion performance from as fundamental a viewpoint as possible, making full use of existing knowledge on the basic chemical and physical processes involved. Combustors modeled included the F100, F101, TF33, TF39, TF41, J85, and J79.
11. Weak Extinction and Turbulent Velocity for Grid Plate Stabilized Premixed Flames	N. A. Al Dabbagh and G. E. Andrews	Combustion and Flame 55:31-52 (1984)	The use of premixed prevaporized combustor designs, as a means of achieving low NO _x emissions for gas turbines, is limited by the problems of flame stability. Grid plate flame stabilizers offer a technique for burning weak mixtures efficiently with low NO _x . Weak stability data is presented for a wide range of grid plate geometries at simulated gas turbine conditions. The influence of stabilizer geometry, pressure loss, mean velocity, and inlet temperature is investigated for premixed propane-air flames. Weak extinction is postulated to occur when the mean flow velocity exceeds the turbulent burning velocity. The weak extinction data are shown to correlate with the same parameters as conventional turbulent burning velocity data.
Reference No. 28			

LITERATURE SURVEY OF ALTITUDE IGNITION AND LEAN DECEL PROGRAM (Continued)

<i>Title</i>	<i>Author</i>	<i>Source</i>	<i>Synopsis</i>
12. Preliminary Correlation of Fuel Effects on Ignitability for Gas Turbine Engines Reference No. 29	D. W. Naegeli, C. A. Moses and A. M. Mellor	Trans ASME No. 83-JPGC-GT-8	The characteristic time model for ignition is used to correlate the spark ignition limits of fuel sprays in gas turbine combustors. The correlations are based on ignition data from several fuels in the JP-4 to JP-8 specification range and six gas turbine combustors. In the model, the criterion for ignition is that the spark energy must heat up an initial volume such that the heat release rate within that volume is greater than the loss rate. Heat generation is limited first by droplet evaporation and then the rate of hydrocarbon oxidation; heat loss is controlled by the rate of mixing (eddy diffusion). Conceptually, the rates are expressed as characteristic times in order to illustrate the relative importance of each process in the ignition event. Ignition limit correlations are given for each combustor as well as a single correlation of 322 data for four engines combined.

DISTRIBUTION LIST FOR AFWAL TR-85-2054

ALLISON GAS TURBINE DIVISION Division of GMC ATTN: Hukam Mongia, MS T14 P.O. Box 420 Indianapolis IN 46206-0420	1 Copy
ALLISON GAS TURBINE DIVISION Division of GMC ATTN: Sam Reider, MS T01 P.O. Box 420 Indianapolis IN 46206-0420	1 Copy
ALLISON GAS TURBINE DIVISION Division of GMC ATTN: Technical Library, MS S5 P.O. Box 420 Indianapolis IN 46206-0420	1 Copy
WILLIAMS INTERNATIONAL ATTN: Mike Bak, MS 5-16 P.O. Box 200 Walled Lake MI 48088	1 Copy
WILLIAMS INTERNATIONAL ATTN: Technical Library P.O. Box 200 Walled Lake MI 48088	1 Copy
PRATT & WHITNEY AIRCRAFT ATTN: Tom Dubell, MS 713-13 P.O. Box 2691 West Palm Beach FL 33402	1 Copy
PRATT & WHITNEY AIRCRAFT ATTN: Technical Library, MS 706-50 P.O. Box 2691 West Palm Beach FL 33402	1 Copy
US ARMY RESEARCH & TECHNOLOGY LAB Director Applied Technology Lab ATTN: SAVDL-ATL-ATP (Mr Robert Bolton) Ft Eustis VA 23604	1 Copy
AVCO LYCOMING ATTN: George Opdyke 550 S. Main Street Stratford CT 06497	1 Copy

DISTRIBUTION LIST FOR AFWAL TR-85-2054 (Concluded)

NASA LEWIS RESEARCH CENTER ATTN: Jim Bigalow, MS 6-12 21000 Brookpark Road Cleveland OH 44135	2 Copies
GENERAL ELECTRIC COMPANY Aircraft Engine Business Group ATTN: D. W. Bahr, Mail Drop K64 1 Neumann Way Cincinnati OH 45215	4 Copies
Commanding Officer NAVAL AIR PROPULSION CENTER ATTN: A. Cifone, PE 42 P.O. Box 7176 Trenton NJ 08628	3 Copies
AFWAL/POTC ATTN: Ken Hopkins WPAFB OH 45433-6563	5 Copies
AFWAL/GLIST WPAFB OH 45433-6563	2 Copies
AFWAL/PS WPAFB OH 45433-6563	1 Copy
AIR UNIVERSITY LIBRARY/LSE Maxwell AFB AL 36112	1 Copy
DEFENSE TECHNICAL INFO CENTER ATTN: DDA Cameron Station Alexandria VA 22304-6145	2 Copies
TELEDYNE CAE ATTN: Dick Trauth 1330 Laskey Road P.O. Box 6971 Toledo OH 43612-0971	1 Copy
TELEDYNE CAE ATTN: Technical Library 1330 Laskey Road P.O. Box 6971 Toledo OH 43612-0971	2 Copies
GARRETT TURBINE ENGINE COMPANY ATTN: John Sanborn, 93-352-503-4R 111 South 34th Street P.O. Box 5217 Phoenix AZ 85034	1 Copy

END

FILMED

2-86

DTIC